Advances in Applied Energy 11 (2023) 100150

Contents lists available at ScienceDirect

Advances in Applied Energy

journal homepage: www.elsevier.com/locate/adapen

Advances in solar forecasting: Computer vision with deep learning

Quentin Paletta [a,b,c,d,*], Guillermo Terrén-Serrano [e,f], Yuhao Nie [g], Binghui Li [h], Jacob Bieker [i], Wenqi Zhang [j], Laurent Dubus [k,l], Soumyabrata Dev [m], Cong Feng [n,**]

[a] Department of Engineering, University of Cambridge, UK
[b] European Space Research Institute, European Space Agency, Italy
[c] European Centre for Space Applications and Telecommunications, European Space Agency, UK
[d] ENGIE Lab CRIGEN, France
[e] Environmental Studies Department, University of California Santa Barbara, USA
[f] Environmental Markets Lab (emLab), University of California Santa Barbara, USA
[g] Department of Energy Science and Engineering, Stanford University, USA
[h] Power & Energy Systems, Idaho National Laboratory, USA
[i] Open Climate Fix, UK
[j] Grid Planning & Analysis Center, National Renewable Energy Laboratory, USA
[k] Réseau de Transport d'Électricité, France
[l] World Energy & Meteorology Council, UK
[m] School of Computer Science, University College Dublin, Ireland
[n] Power Systems Engineering Center, National Renewable Energy Laboratory, USA

ARTICLE INFO

Keywords:
Solar forecasting
Computer vision
Deep learning
Satellite imagery
Sky images
Solar irradiance

ABSTRACT

Renewable energy forecasting is crucial for integrating variable energy sources into the grid. It allows power systems to address the intermittency of the energy supply at different spatiotemporal scales. To anticipate the future impact of cloud displacements on the energy generated by solar facilities, conventional modeling methods rely on numerical weather prediction or physical models, which have difficulties in assimilating cloud information and learning systematic biases. Augmenting computer vision with machine learning overcomes some of these limitations by fusing real-time cloud cover observations with surface measurements acquired from multiple sources. This Review summarizes recent progress in solar forecasting from multisensor Earth observations with a focus on deep learning, which provides the necessary theoretical framework to develop architectures capable of extracting relevant information from data generated by ground-level sky cameras, satellites, weather stations, and sensor networks. Overall, machine learning has the potential to significantly improve the accuracy and robustness of solar energy meteorology; however, more research is necessary to realize this potential and address its limitations.

1. Introduction

1.1. Solar forecasting

Solar forecasting is one of the most effective and efficient techniques to mitigate the solar power variability and uncertainty caused by atmospheric changes [1]. Most solar forecasting methods take ground- or remote-sensing information as input to infer current meteorological conditions, and predict the future global solar irradiance (GSI) or power, ranging from seconds to years ahead (Fig. 1).

Solar forecasting has been extensively used in the power and energy industry; it is also known as operational solar forecasting (Section 3.2.2). According to different lead times and horizons, solar forecasting can be roughly categorized into very short-term forecasting, short-term forecasting, medium-term forecasting, and long-term forecasting. Although there is a lack of consistency in these definitions, solar forecasts at all timescales are important to power system operations and planning. As shown in Table 1, long-term solar forecasts are usually used in long-term energy trading, system planning, and resource assessment. Short-term and very short-term solar forecasts, normally

* Corresponding author at: ϕ-Lab, European Space Research Institute, European Space Agency, Italy.
** Corresponding author at: Power Systems Engineering Center, National Renewable Energy Laboratory, USA.
E-mail addresses: quentin.paletta@esa.int (Q. Paletta), cong.feng@nrel.gov (C. Feng).

https://doi.org/10.1016/j.adapen.2023.100150
Received 11 May 2023; Received in revised form 17 July 2023; Accepted 28 July 2023
Available online 7 August 2023

Abbreviations

AI	Artificial Intelligence
ARIMA	Autoregressive Integrated Moving Average
ASI	All-Sky Imager
CNN	Convolutional Neural Network
CSP	Concentrated Solar Power
CRPS	Continuous Ranked Probability Score
CSI	Clear-Sky Index
COMS-MI	Communication Ocean and Meteorological Satellite equipped with Meteorological Imager
CVAE	Convolutional Variational Autoencoder
DNI	Direct Normal Irradiance
ECMWF	European Centre for Medium-Range Weather Forecasts
ERA5	ECMWF Reanalysis 5th
FOV	Field of View
GAN	Generative Adversarial Networks
GOES	Geostationary Operational Environmental Satellites
GHI	Global Horizontal Irradiance
GSI	Global Solar Irradiance
HDR	High Dynamic Range
HYTA	Hybrid Thresholding Algorithm
JMA	Japan Meteorological Agency
LIDAR	Laser Imaging, Detection, And Ranging
LSTM	Long Short-Term Memory
MAE	Mean Absolute Error
MBE	Mean Bias Error
MSG	Meteosat Second Generation
MTG	Meteosat Third Generation
MERRA	Modern-Era Retrospective analysis for Research and Applications
MIMO	Multi-Input Multi-Output
MOF	Methods Of Fusion
MSE	Mean Squared Error
MTL	Multitask Learning
NASA	National Aeronautics and Space Administration
NOAA	National Oceanic and Atmospheric Administration
NREL	National Renewable Energy Laboratory
NSRDB	National Solar Radiation Database
NWP	Numerical Weather Prediction
PCA	Principal Component Analysis
PIV	Particle Image Velocimetry
RGB	Red Green Blue
RMSE	Root Mean Square Error
RNN	Recurrent Neural Network
ROC	Receiver Operating Characteristic
ROI	Region Of Interest
SIMO	Single-Input Multi-Output
SEVIRI	Spinning Enhanced Visible and InfraRed Imager
SVR	Support Vector Regression
TSI	Total Sky Imager
XAI	Explainable Artificial Intelligence
WRF	Weather Research and Forecasting
PICP	Prediction Interval Coverage Probability
PINAW	Prediction Interval Normalized Averaged Width

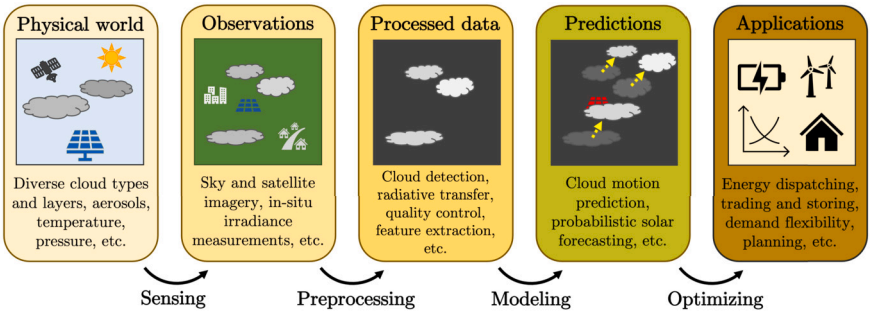

Fig. 1. Solar energy meteorology framework reviewed in the present study.

Table 1
Solar forecasting classification by timescales.

Group	Lead Time	Horizon	Application
Long-term	Months to years	Years	Capacity expansion
Medium-term	Weeks to months	Weeks to months	Capacity market
Short-term	Hours to days	Hours to one week	Day-ahead unit commitment
Very short-term	Minutes to hours	Minutes to hours	Real-time economic dispatch

defined as predictions up to a few days ahead, are used in daily power system operations and energy markets. These definitions and terminologies differ between power systems and markets. It is common practice for system operators and market participants to use medium-/short-term solar forecasts for day-ahead bidding or preliminary generator scheduling and use very short-term solar forecasts for real-time adjustments [2]; therefore, accurate solar forecasts can enhance power system reliability and resilience while reducing economic costs.

Solar forecasting techniques can be categorized into physical models [3], data-driven models [4], or hybrid models [5], depending on the involvement of physical laws. Both ground-sensing (i.e., *in situ* or mobile data) and remote-sensing data can be used as input to any type of model [6]. The most widely used remote-sensing data are satellite data, which can be processed by physical models, such as numerical weather prediction (NWP) models, to provide solar forecasts [7]. Satellite data can also be directly processed by statistical models to generate solar forecasts [8]. The most effective ground-based sensors include pyranometers and pyrheliometers, which provide local surface irradiance measurements. Compared to other target variables in energy forecasting (e.g., load forecasting, price forecasting, and wind forecasting), solar forecasting is most sensitive to cloud movement; hence, it provides unique opportunities for sensors, such as satellites and sky cameras, to play critical roles. Fig. 2 depicts the spatiotemporal resolutions and coverages of different types of sensors, where sky cameras and satellites

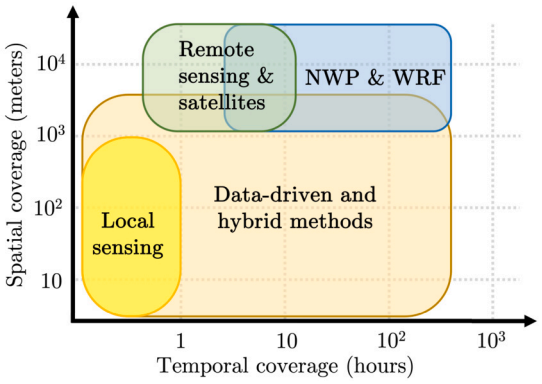

Fig. 2. Temporal and spatial coverage of different solar forecasting techniques. Adapted from [9].

cover a large spectrum of solar forecasting. One important common ground of satellites and sky cameras is that both sensors can provide data in the format of images. These observations of the cloud cover can be processed by advanced computer vision techniques to model the variability of solar power.

1.2. Computer vision in solar forecasting

The cloud cover dynamics accounts for most of the intraday irradiance variability. To better anticipate corresponding solar power fluctuations, computer vision methods based on cloud observations have been developed. Besides an inherent stochastic component in cloud modeling, the partly deterministic nature of cloud motion can be exploited to extrapolate the future cloud cover spatial configuration from past observations. The resulting ability to anticipate cloud displacement offers a significant advantage over forecasting approaches solely based on local meteorological measurements, which fail to offer reliable predictions beyond the short-term autocorrelation period of solar time series. This forecasting strategy is therefore critical to provide truly valuable solar predictions at different spatiotemporal scales [10].

Definition. A solar forecasting method is described as image-based when the covariates include sky features extracted from spatial measurements acquired by light sensing devices (e.g., ground-based imager, satellite imagery, or both). In contrast, physical approaches are based on the position of the sun, whereas statistical methods are based on an autoregressive and moving average covariate structure (i.e., time series analysis).

The principal sources of cloud observations for short-term solar forecasting are sky cameras and satellites. A sky camera equipped with a fish-eye lens is able to capture the local cloud cover spatial configuration over a few square kilometers at a subminute time period, whereas satellites provide continent-wide radiation maps of the atmosphere across a large spectrum at a lower temporal resolution of 5 to 15 minutes [11,12] (Fig. 2). Although the spatiotemporal resolution of remote sensors is expected to increase and close the gap with ground-level imagery, these two imaging technologies are currently complementarily used in solar forecasting due to their different technical characteristics and points of view on the cloud cover [13]. Regarding the forecast horizon, approaches based on sky cameras aim to provide predictions on the local solar variability up to 30 minutes ahead, depending on the local cloud velocity, whereas satellite imagery provides longer-term forecasts, up to several hours ahead, thanks to its wider field of view (FOV) [14]. Unless used in a network setup covering a larger area [15], sky cameras are best suited for locations with a high solar power density, such as a solar plant or a hybrid power plant (Fig. 3). In contrast, satellite-based techniques can provide countrywide solar output predictions benefiting applications such as grid balancing or energy trading.

Traditional computer vision approaches based on sky images or satellite images share similar methods: cloud segmentation, cloud localization, cloud properties estimation, cloud tracking, and cloud motion modeling [17]. The cloud mask in sky images is often derived from thresholding methods based on pixel value statistics [18]. In addition to similar thresholding tests [19], cloud segmentation in satellite images can be further augmented using the effective cloud albedo or cloud index (0: absence of cloud, 1: thick cloud) computed from the ground albedo, the observed albedo, and the maximum empirical albedo [20]. This continuous variable indicates the cloud transmittance, which can also be estimated with a pyrheliometer and a clear-sky model for sky camera applications [21]. Cloud geolocation is then performed using several sky cameras in stereovision mode [22,23]. Following this, cloud velocity vectors can be approximated, with block matching methods [24–26] or with optical flow [27,28], to predict the future impact of the cloud cover dynamics on solar generation in a deterministic [29,30] or probabilistic manner [31]. From the future position of clouds, it is possible to derive local or regional irradiance forecasts using the estimations of the clouds' physical properties [32,33] (Fig. 4).

Benefiting from recent advances in deep learning and the increasing accessibility of large datasets [34] (see Section 2.5), a range of data-driven approaches have been developed to address this computer vision task. The standard approach consists of training a neural network to extract spatiotemporal features from a sequence of past sky or satellite images to predict the future solar variability. Similar to traditional computer vision methods, both local values (e.g., GSI or photovoltaic power output) [35–37] and regional predictions [38] (e.g., GSI or cloud-index maps) can be obtained with this class of techniques. Despite high performance gains based on averaging metrics, including the root mean square error (RMSE) or the mean absolute error (MAE), deep learning models still face several limitations, such as difficulty in breaking the persistence barrier to predict critical events on time [39,40] or to correlate an image (especially satellite images) with its corresponding solar value (GSI or photovoltaic power output). As a result, some models rely on auxiliary data, including GSI measurements or the solar elevation.

1.3. Bibliometric analysis

Computer vision-based solar forecasting has drawn increasing attention in the solar community, as reflected in the number of publications on this topic in the recent 12 years. Fig. 5 shows the total number of journal articles, conference articles, and book chapters published each year. It is visible that the computer vision-based solar forecasting research has exponentially increased in recent years. In 2010 and 2011, satellite-based solar forecasting dominated the field. From 2012 to 2017, however, sky image-based solar forecasting played a leading role. In the past four years, satellite- and sky image-based solar forecasting have been developed in similar proportions. Fig. 6 lists the top 12 journals in terms of number of related publications (note that publication quantity does not imply quality). *Solar Energy*, the official journal of the International Solar Energy Society, is the leading journal in computer vision-based solar forecasting. Most of the well-known journals in this field are energy journals, except for *Remote Sensing* and *Atmospheric Measurement Techniques*. The former covers various aspects of remote-sensing science, where image processing is a major publishing scope. The latter is dedicated to publishing advances in remote-sensing, *in situ*, and laboratory measurement techniques for the constituents and properties of the Earth's atmosphere, including irradiance sensing and measurement research.

Although all these journals publish both ground-sensing and remote-sensing solar forecasting articles, most of them have imbalanced amounts of publications in the two areas. For example, *Solar Energy*, *Atmospheric Measurement Techniques*, *Journal of Renewable and Sustainable Energy*, and *Energy Conversion and Management* predominantly focus on ground sensing forecasting articles, whereas *Remote Sensing* and *Renewable and Sustainable Energy Reviews* specialize in remote-sensing solar

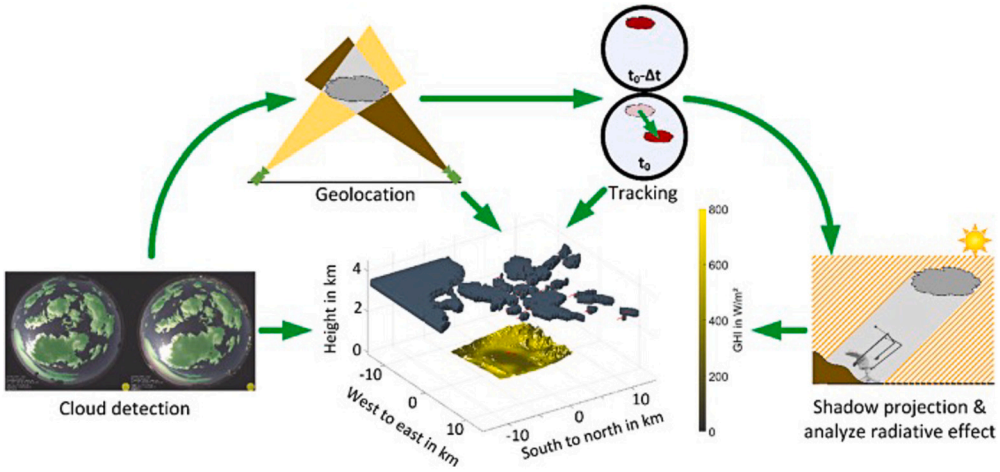

Fig. 3. Illustration of a standard physics-based solar forecasting approach using sky cameras in stereovision mode: cloud detection, geolocation, tracking, shadow projection, and analysis of radiative effect. Taken from [16].

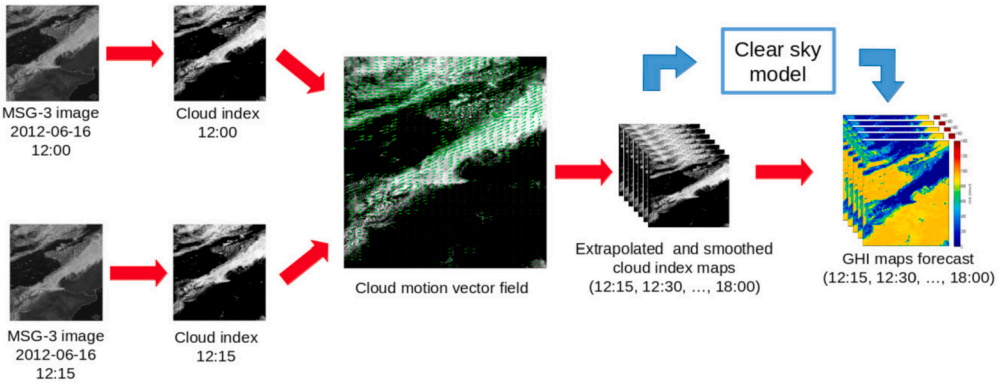

Fig. 4. Example of a physics-based solar forecasting method using satellite observations: cloud detection via cloud index mapping, cloud motion estimation, extrapolation to future time steps, and radiative transfer modeling. Taken from [33].

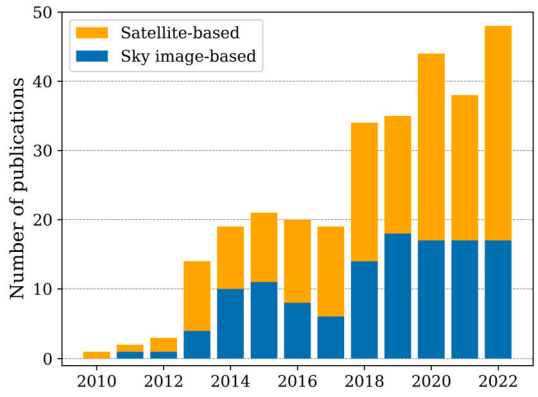

Fig. 5. Number of publications in satellite-based and sky image-based solar forecasting.

forecasting articles. This bibliometric analysis suggests the increasing research trend and top journals, which can help researchers track the state of the art in this field.

1.4. Existing review articles and motivation for the new review

Since 2010, solar forecasting has witnessed exponential growth, largely due to increasing data availability and emerging techniques, together with the rising value of solar predictions. The first wave of solar forecasting development resulted in several classic and highly cited review articles (Table 2). A comprehensive and detailed review covered clear-sky models, regressive methods, remote-sensing models, NWP models, and limited types of artificial intelligence (AI) techniques [8] for solar forecasting. The same year, a similar but briefer review focused on three types of solar forecasting techniques: statistical methods, cloud imagery and satellite-based models, and NWP models [41]. A more recent review article summarized and compared techniques for direct normal irradiance (DNI) forecasting and applications to concentrated solar power (CSP) output forecasting. Antonanzas et al. [42] reviewed specific techniques for photovoltaic power output forecasting grouped by spatial and temporal characteristics. Probabilistic solar forecasting was emphasized in the same work.

Machine learning techniques started to be applied to solar forecasting in the early 2010s and were first systematically reviewed in [4]. This work grouped machine learning methods into classification, supervised learning, unsupervised learning, and ensemble learning. The recent advances in computational power enabled deep learning methods to be widely implemented in solar forecasting. The first review article for deep learning solar forecasting methods was published in 2021, which also covered wind forecasting methods [43]. In the same year, two similar review papers were published in slightly different scopes: GSI forecasting and satellite image prediction [44,45]. The development of machine learning and deep learning has also led the advances in intra-hour solar forecasting, which could also be reflected by some recent review articles [9,46,47].

The rapid advances in the emerging field of computer vision-based solar forecasting with deep learning motivate this review. This work

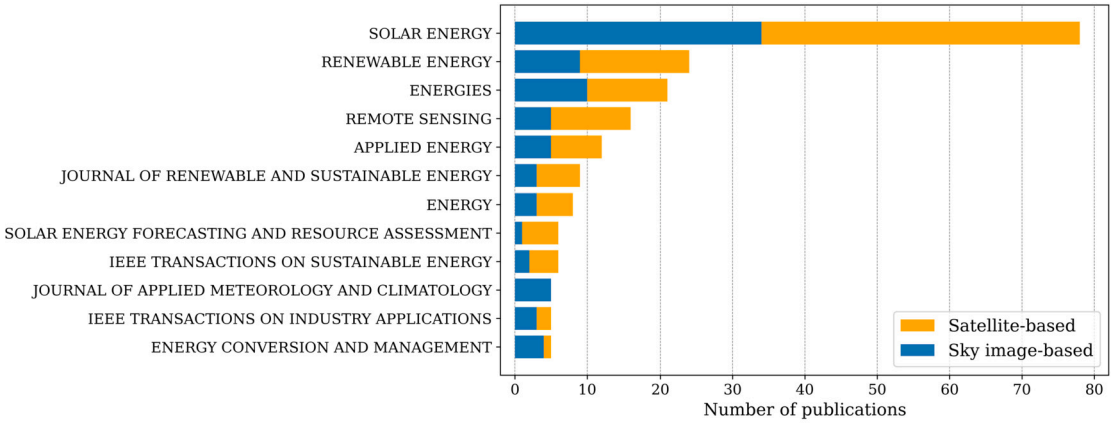

Fig. 6. Top 12 journals with the most computer vision-based solar forecasting publications.

Table 2
Solar forecasting review articles reference, publication year, and scope.

Article	Year	Scope
Inman et. al [8]	2013	Theory and application of utility-scale solar forecasting
Diagne et. al [41]	2013	GSI forecasting and proposition for small-scale insular grids
Law et. al [48]	2014	DNI forecasting
Antonanzas et. al [42]	2016	Latest advancements and future trends in solar power forecasting
Voyant et. al [4]	2017	Machine learning methods of GSI forecasting
Barbieri et. al [49]	2017	Very short-term photovoltaic power forecasting with cloud modeling
Sobri et. al [50]	2018	Photovoltaic power forecasting techniques
Kurzrock et. al [51]	2018	Geostationary satellite-based short-term cloud forecasting
Yang et. al [52]	2018	Technological infrastructure and key innovations in solar forecasting
Sweeney et. al [2]	2019	State-of-the-art and future solar and wind forecasting
Kumar et. al [53]	2020	Solar forecasting methods and sensor networks
Hong et. al [54]	2020	Energy (load, solar, wind, price) forecasting
Li et. al [55]	2020	Probabilistic solar forecasting applications in power systems
Guermoui et. al [56]	2020	Hybrid models for solar radiation forecasting
Ahmed et. al [57]	2020	Solar forecasting methods and optimization
Wang et. al [58]	2020	Taxonomy of AI for solar power forecasting
Juncklaus Martins et. al [59]	2021	Forecasting/nowcasting based on ground-based cloud imaging
Alkhayat et. al [43]	2021	deep learning-based solar and wind forecasting methods
Sharma et. al [46]	2021	Sky image-based short-term intra-hour solar prediction
Kumari et. al [44]	2021	deep learning GSI forecasting models
Moskolaï et. al [45]	2021	deep learning-based satellite image prediction
Sawant et. al [60]	2021	Cloud detection, identification, and forecasting
Chu et. al [9]	2021	Intra-hour GSI forecasting
Fan et. al [47]	2022	Ground-based sky image-based intra-hour solar forecasting
Erdener et. al [61]	2022	Aggregate regional behind-the-meter solar generation forecasting
Yang et. al [62]	2022	Solar forecasting from atmospheric science and power engineering perspectives
Lin et. al [12]	2023	Intra-hour solar forecasting with ground-based sky image methods
Krishnan et. al [63]	2023	How solar radiation forecasting impacts the utilization of solar energy

considers the diverse aspects of this field, from the datasets [34,64,65] to end-user applications [66] and cloud modeling techniques [67]. The review primarily focuses on computer vision methods using deep learning to analyze spatial data (images or videos) for solar power modeling [36,35,68–71].

The remainder of this article is organized as follows. Section 2 presents data acquisition and preprocessing techniques used to model solar power via cloud cover observations. Section 3 describes the fundamentals of computer vision-based solar forecasting, including computer vision tasks, evaluation methods, and end-user applications. A list of accessible resources, datasets, and codes is described in Sections 2.5 and 3.4. Section 4 focuses on the deep learning methods applied to solar power modeling with computer vision such as data fusion, transfer learning, multitask learning, data-centric techniques and interpretable AI. Future research challenges as well as the state of the adoption of vision-based forecasting technologies are discussed in the penultimate Section 5. Section 6 concludes the study.

2. Data collection and preprocessing

From the perspective of traditional computer vision methods, the information in a scene has both global and local features [72]. In solar forecasting, sky images contain local information about atmospheric conditions, whereas ground-level GSI measurements are global features represented by the sky images. The section about data is divided into atmospheric imagery and *in situ* measurements (Sections 2.1 and 2.2). In addition, effective image preprocessing methods for cloud cover observations are described in Section 2.3, and the derivation of the physical features to incorporate into physics-informed deep learning models is mentioned in Section 2.4.

2.1. Cloud cover observations

This section summarizes different data acquisition systems and their technical specifications, in addition to recent technological advances.

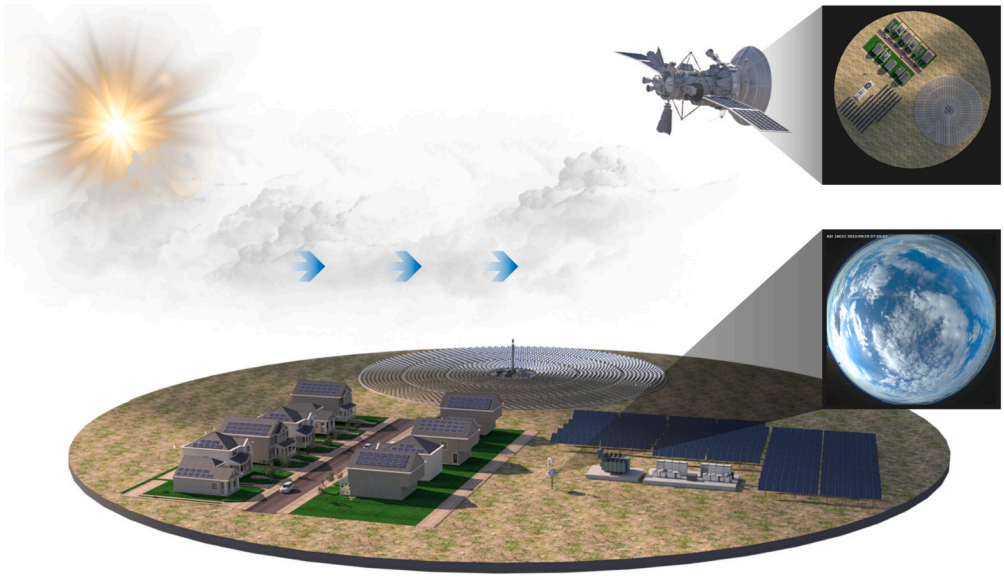

Fig. 7. Meteorological influences such as moving clouds can cause a significant variability in the production of energy from photovoltaic or concentrated solar power. Observing the cloud cover in the vicinity of solar sites via satellites or ground-level sky cameras helps to anticipate these fluctuations.

Information about publicly accessible datasets for direct download is presented in Section 2.5.

2.1.1. Satellite imagery

Geostationary satellites are the most common data acquisition system for solar forecasting, as they provide continuous imagery over large areas of Earth, albeit at lower spatial resolutions (around 1-3 km per pixel) than lower orbiting satellites such as Landsat. This enables them to quickly see changing cloud and atmospheric conditions over nearly any solar site, and be available as input for any forecast time. The Geostationary Operational Environmental Satellites (GOES-16) operated by the National Oceanic and Atmospheric Administration (NOAA) provides measurements covering 16 spectral bands every 5 to 10 minutes [73]. The satellite Fengyun-4A, managed by the China Meteorological Administration, provides measurements from 14 spectral bands [74]. The Communication Ocean and Meteorological Satellite equipped with Meteorological Imager (COMS-MI), operated by the Korean Meteorological Association, observes 8 spectral bands [75]. The Meteosat Second Generation (MSG), operated by EUMETSAT, is equipped with the Spinning Enhanced Visible and InfraRed Imager (SEVIRI) capable of sensing the Earth using 12 different spectral bands every 5 to 15 minutes [37,38,76,13]. The Himawari-8/9 satellite, operated by the Japan Meteorological Agency (JMA), provides 16 different spectral bands every 10 minutes [77]. The future generations of geostationary satellites like GOES-18 and Meteosat Third Generation (MTG) will provide improved spatiotemporal resolution and richer spectral information (e.g., from 12 channels for MSG to 16 channels for MTG, and from 5 to 15 minutes temporal resolution down to 2.5 to 10 minutes). Non-geostationary satellites, such as the Landsat series of imagers or MODIS satellite can provide higher resolution imagery, on the order of 0.5 to 30 meters per pixel, but with revisit times on the order of hours or days. Imagery from these satellites can be used for solar potential estimation [78–81] but are generally not suitable for solar nowcasting or short-term forecasting, because of their limited temporal resolution.

2.1.2. Ground-based sky imagers

The most commonly used sky images in solar forecasting applications are in the Red Green Blue (RGB) color model. The total sky imager (TSI) was first introduced in the atmospheric science community to quantify the fraction of the sky with clouds [82]. The TSI is a reflective sky imager that acquires sky images with a large FOV. A TSI records sky images by reflecting light beams using a convex mirror to converge on the focal point of a visible light camera. A decade later, the all-sky imager (ASI), i.e., skycam or whole-sky imager, was proposed as a low-cost alternative to the TSI [83]. The ASI uses an inexpensive camera with a fish-eye lens attached to enlarge the FOV. The TSI and ASI suffer from saturation of the pixels in the circumsolar area, but different alternatives to reduce the saturation of circumsolar pixels have been proposed since their introduction. Some of these alternatives use the Y16 brightness model (i.e., high dynamic range -HDR- and infrared images) instead of RGB.

2.1.3. Sun tracking

The sky conditions affect in situ GSI measurements mainly by passing clouds (i.e., stochastic effects) or other aerosols suspended in the atmosphere. These effects are commonly known as direct and diffuse components. In particular, assessing the effects of the direct component requires estimating when a cloud will intersect with the sun (i.e., inner circumsolar region), while the diffuse component effects require estimating the cloud density and coverage (i.e., outer circumsolar region). In any case, it is necessary to predict the future position of the sun in the sky images to identify which air parcel will cover the sun. The sun follows a trajectory in the sky varying daily, but it is deterministic and can be easily estimated.

A possible solution is mounting a sky imager on a solar tracker reducing the complexity of the problem to moving clouds [84,85]. Fast and accurate solar position algorithms exist [86–89]. However, there are precision errors in the estimation of the solar position that affect the accuracy of the clear sky index documented earlier [90]. These errors have been thoroughly assessed [91], and more recent research concluded that a consequence of the solar zenith angle estimation [92], which is particularly important for ground-based sky imagers mounted on a solar tracker. A proposed solution to this problem is to synchronize the solar tracker with satellite positioning [93] or use ground-based solar sensors [94]. Another alternative is to apply image processing methods and directly remove the sun from the images [95]. However, the uncertainty in the physical size of the pixels poses a limitation to this approach. An alternative to solar position algorithms is to detect the position of the sun in sky images to drive the solar tracker and center the images around the sun [96]. An approach following this trend proposed a model to predict the solar position throughout the day in sky images from past observations [97] (Fig. 8).

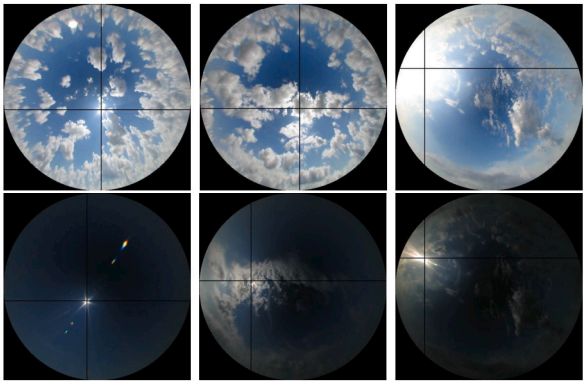

Fig. 8. Position of the sun in long- and short-exposure sky images predicted by an image-based sun tracker from past observations. Knowing the position of the sun when it is hidden by a cloud (middle column) or surrounded by a large saturated area (top right image) provides valuable information for short-term solar forecasting. Taken from [97].

2.1.4. Technological challenges

As shown in the top right image of Fig. 8, the brightness temperature of solar radiation saturates pixels in visible light sky imagers (i.e., RGB). This effect removes otherwise useful information for computer vision-based solar forecasting. For that reason, a sun-blocking mechanism is generally attached to a sky imager [98]. This mechanism is mounted on a 1-axis solar tracker and is similar to the shadow bands used to measure diffuse radiation with pyranometers [99]. Alternative mechanisms that remove less information from sky images exist but are not commercially available [100].

Visible light cameras record multiple frames per second (i.e., > 15 fps). It is possible to exploit this to improve the quality of the sky images and reduce the noise-to-signal ratio [85], and to adjust the exposure time (i.e., control the shutter) for recording frames with different exposure times [101]. This allows for a saturation reduction of circumsolar pixels via software. Other approaches following this trend propose nonparametric methods for fusing sun-centered sky images at multiple exposure times with reduced noise-to-signal ratios to generate HDR 16-bit grayscale sky images [85]. This method was developed for an ASI mounted on a 2-axis solar tracker (Fig. 9).

Optical filters are another alternative to reduce pixel saturation in the circumsolar area. Neutral density filters uniformly attenuate the solar radiation in the entire light spectrum [85], whereas near-infrared filters are capable of reducing the saturation of the pixels in the circumsolar area [98,102]. However, the most effective method to reduce the saturation of the circumsolar pixels is to use far-infrared sky images [103]. These types of cameras are made of low-cost uncooled microbolometers [104]. As visible light sky imagers, far-infrared imagers can have a large FOV when reflecting the entire sky over an aluminum sphere [105]. These approaches are similar to TSIs and are commercially available.[1] Additionally, it is possible to reproduce the capabilities of an ASI by fusing infrared images acquired from multiple sensors, producing static far-infrared sky images with a large FOV [106]. Similarly, when a small FOV far-infrared camera is mounted on a 2-axis solar tracker, it is possible to acquire sun-centered sky images with low saturation of the pixels in the circumsolar region [85].

2.2. In situ measurements

A computer vision-based solar forecasting model intrinsically aims to forecast GSI measured on the ground, or photovoltaic power output, by analyzing the movement of passing clouds using sky or satellite images. Consequently, a dataset for these applications must include consecutive sequences of sky or satellite images (i.e., covariates) paired with ground GSI measurements or photovoltaic power output (i.e., predictors).

2.2.1. Global solar irradiance

A pyranometer, located on a horizontal surface normal to the ground, measures GSI. The GSI, $\mathcal{R}_{GSI}$, can be decomposed in DNI, $\mathcal{R}_{Direct}$, and diffuse, $\mathcal{R}_{Diffuse}$, and reflected, $\mathcal{R}_{Reflected}$, irradiance, such as $\mathcal{R}_{GSI} = \mathcal{R}_{Direct} + \mathcal{R}_{Diffuse} + \mathcal{R}_{Reflected}$ [107]. The DNI is measured using a pyrheliometer, but its approximation is possible from GSI measurements [108]. DNI is necessary to estimate CSP output [109]. In contrast, GSI is a requirement to approximate the power output of photovoltaic power plants [110]. The GSI includes diffuse irradiance, which quantifies the scattering effect produced by particles or molecules floating in the atmosphere (i.e., clouds) [111]. When estimating the power output from a GSI forecast, it is necessary to know photovoltaic system design parameters; the number of photovoltaic arrays and active area (i.e., shadows and dust) [112,113]; the manufacturer's specific parameters, such as module and inverter efficiency; plus the local degradation pattern of the photovoltaic system, which requires an empirical model based on data for accurate estimation [114]. But there are simplified models [115] that are commonly used in operational planning applications [116].

2.2.2. Clear-sky index

The GSI signal has a deterministic and a stochastic (i.e., random) component. The deterministic component is considered to be the cyclostationary effects produced by Earth's rotation and revolution [95]. These movements cause the GSI to be a periodic function with local maxima at noon. The amplitude of the daily local maxima varies yearly, with global maxima in the summer solstice and a global minimum in the winter solstice. The effects produced by clouds and aerosols are the stochastic component. The random effects produced by aerosols and clouds depend on the distance that a light beam travels through the atmosphere [117]. These effects are greater during the sunrise and sunset hours. The clear-sky index (CSI) is a stochastic component, defined as $i_k = r_k / \hat{r}_k$, where r_k is the pyranometer signal, and $\hat{r}_k$ is the deterministic GSI computed from a physical model [118]. This practice is known as *detrending* in time series analysis (Fig. 10).

Previous work validated the performance of deep learning solar forecasting using CSI or GSI and found that the CSI reduces the performance [119]; however, more recent investigations used CSI as the predictor instead of GSI, which is becoming a common practice in the field to increase the performance of a solar forecast [117,120]. Additionally, the pyranometer signal might have biases with respect to the deterministic component that are only noticeable in high-resolution measurements [95]. These biases are produced by slight inclinations in the pyranometer's support or deviations with respect to the deterministic component. These biases are stationary and deterministic; thus, their removal increases the performance of a solar forecast [121,122].

2.3. Image preprocessing

This section describes existing image processing methods known for increasing the performance of solar forecasts. The key idea behind applying preprocessing to the sky images is to remove complexity from the input space to facilitate training a deep learning model, thus speeding up or increasing the performance.

2.3.1. Irradiance maps

There are other ground-based approaches available for indirectly visualizing cloud motion (i.e., projected shadows) using information recorded from the surface. These methods are particularly useful to derive photovoltaic power output from utility-scale photovoltaic power plants. For instance, it is possible to derive the shadows projected (i.e.,

[1] https://reuniwatt.com/en/247-all-sky-observation-sky-insight/.

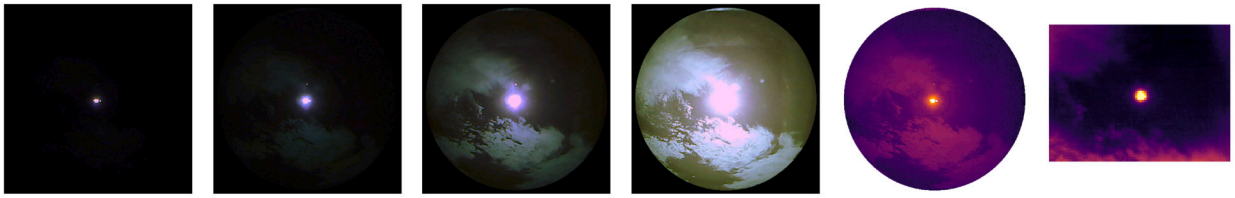

Fig. 9. From left to right, visible light images acquired at different exposure times (1, 4, 12, and 28 ms), HDR image resulting from fusing the visible light images, and infrared image of the circumsolar region. The resolution of the visible light and the HDR images is 450×450, and the resolution of the infrared image is 80×60.

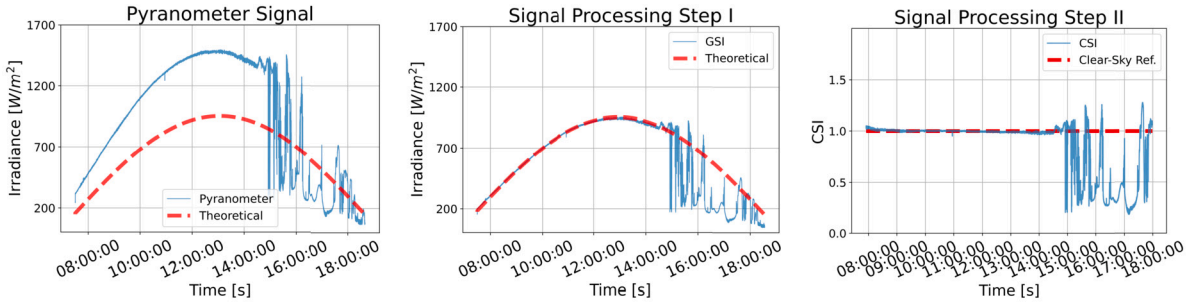

Fig. 10. Signal processing applied to the pyranometer measurements to obtain the CSI time series. From left to right, raw pyranometer measurements, after correcting amplitude and shifting bias, and CSI time series after detrending.

DNI map) by a cloud on the ground using multiple sky imagers [123]. The shadow camera is a visible light imager that records projected shadows instead of directly recording the clouds using sky images. The shadows are projected by passing clouds on the ground [124]. An alternative approach proposes visualizing passing clouds (in utility-scale power plants) by measuring the energy generated by photovoltaic modules and treating them as pixels. In this way, when a cloud crosses the photovoltaic modules, energy generation decreases, and an image of the shadow projected by a cloud is formed to track its motion [125]. Similarly, it is possible to scale this method in locations with multiple utility-scale photovoltaic plants [126]. To track the motion of the clouds across large space regions and use this information in solar forecasting, the energy generated at each photovoltaic plant can be defined as the pixels in an image [127].

2.3.2. Image reduction

The images acquired using visible light imagers (i.e., TSIs or ASIs) have a relatively high resolution for solar forecasting applications, generally ranging from 720×720 to 1280×1280. The resolution in the input space (Height $\times$ Width $\times$ Number of channels) increases the number of parameters in Convolutional Neural Networks (CNNs) (i.e., number of convolutional filters and dimensions) and adds complexity to the model without showing any improvement in the performance. To accelerate model training, the original sky image is downsized using common image processing libraries. Consistent results show that the optimal resolution is $\geq 128 \times 128$ [36] and $< 256 \times 256$ [120] (Fig. 11). To have a competitive performance in solar forecasting applications, the smallest resolution possible is ≥ 64 [119]. When downsizing sky or satellite images, a low-pass filter should be applied first to avoid aliasing effects [13], which have been shown to alter image content if not handled properly [128].

2.3.3. Image transformations

The sky images acquired using a fish-eye lens or a reflective surface have a distortion produced by the concentration of light beams on the imager's sensor plane [130] (Fig. 12). The images can be undistorted by detecting the corners of a checkerboard to numerically approximate the affine transformation [131]. Additionally, further work in solar forecasting developed a method to transform the pixels' coordinate system (i.e., Euclidean geometry) to a longitude and latitude coordinate system (i.e., spherical geometry) [132].

Fig. 11. Sky image at different pixel resolutions: 512×512, 128×128, 32×32. Source: SIRTA [129].

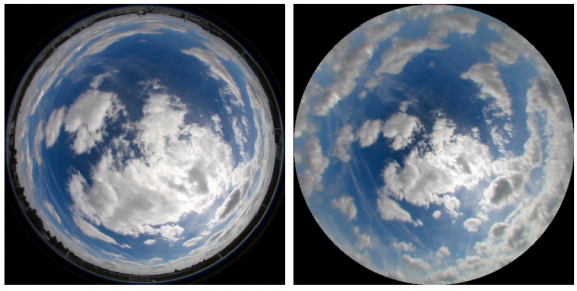

Fig. 12. Distorted image of the sky taken by an ASI and the corresponding undistorted image (azimuthal equidistant projection). Source: SIRTA [129].

Knowing the latitude and longitude of the air parcel corresponding to a pixel (i.e., voxel), the derivation of its area and volume is possible by applying a geospatial perspective reprojection [133]. A reprojection is particularly useful to approximate the cloud velocity vectors in sky images relative to the differences between consecutive sky images [134], which is a data processing (i.e., feature extraction) technique commonly applied in deep learning-based solar forecasting [103]; however, computing the absolute (i.e., actual) cloud velocity vectors is necessary to approximate the cloud height [135].

2.3.4. Ground-based image understanding

The circumsolar region has the information necessary to perform an accurate forecast when the forecast ranges from 30 seconds to 150 seconds [103]. When developing a multitask solar forecasting model ranging from 10 minutes to 60 minutes, it is necessary to use sky images with a large FOV [120]. Introducing knowledge based on image

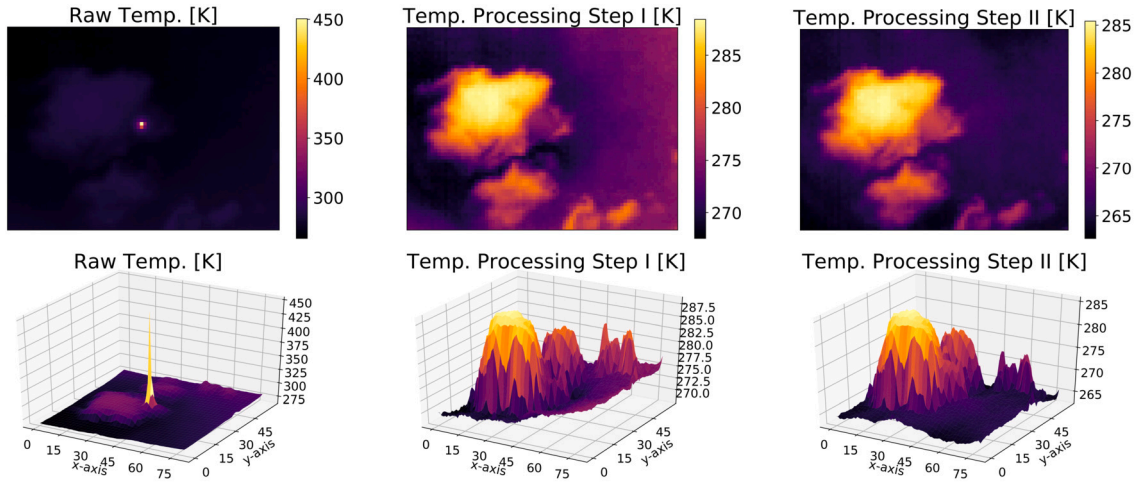

Fig. 13. Preprocessing applied to ground-based infrared images to remove radiation emitted by the sun (left), scattered radiation by particles in the atmosphere (middle), and radiation emitted by dust on the outside window of the sky imager (right). The bottom row shows the 3D graphs of the images in the top row.

understanding to the model allows for identifying the region of interest (ROI) in sky images.

Image understanding techniques to select potential ROI at different forecasting horizons are proposed in ground-based solar forecasting. Image transformation techniques discriminate between the circumsolar area (i.e., closeup of the sun) and the position of the sun in the sky (i.e., sun-centered) [136]. In particular, the ROI depends on the trajectory of the clouds and the sun (i.e., intersection). The *ladder* method was proposed to select an ROI in sky images by identifying which area in the ladder will cover the sun at a given forecasting horizon [137]. For that purpose, the *sun intercepting air parcel* method was introduced as an adaptive attention mechanism in which weights are the probability of a pixel in the image intersecting the sun at a particular forecasting horizon [121].

2.3.5. Satellite image understanding

In solar forecasting from satellite images, the position of the sun is key to defining the ROI because the part of the cloud cover affecting the generation of a photovoltaic system depends on the solar elevation. A proposed trigonometric method identifies the cloud cover ROI based on the angular position of the sun [70]. Additionally, an interpolation of this ROI is possible when the sampling frequency is too low. Another approach to detecting the ROI in satellite images assumes the Eulerian strategy in fluid mechanics as a simplification to the Lagrangian to identify the pixels (i.e., air parcels) that will intersect with the sun at a given forecasting horizon [121]. This method approximates the intersecting probability assuming a rectilinear trajectory [31]. An additional method for determining the ROI is to select the region around the photovoltaic system that is large enough to include all clouds that might move across the FOV [138,139,71]. This ensures that all existing clouds that might affect the radiation are included, other than those that form during the period of interest.

2.3.6. Detrending

Similar to detrending the GSI time series to obtain the CSI, it is possible to detrend the 2-dimenional time series of sky imagers to obtain the diffuse radiation emitted by clouds. Infrared sky images include the additive effect of direct solar radiation, diffuse radiation from the scattering effect produced by clouds and other water molecules, and the reflected radiation emitted by objects on the Earth's surface [95]. The direct radiation effect is stationary, and it can be removed. The diffuse radiation scattered by water molecules in the atmosphere produces cyclo-stationary effects that can be modeled using weather features (atmospheric pressure, relative humidity, and dew point). These weather features are available in standard weather stations [140]. The radiation emitted by debris on the camera lens (i.e., sediments) is static, and it can be removed as well. The result is a far-infrared image that registers the radiation emitted by the clouds [141] (Fig. 13).

2.4. Feature extraction for physics-informed deep learning

Adding physical features about the atmosphere dynamics (i.e., exogenous variables) is proven to increase the performance of a solar forecast. Deep learning models do not have access to knowledge gained empirically about the nonlinear atmospheric dynamics and how weather features affect the underlying process. This section describes computer vision methods used to derive features from cloud cover observations and weather station measurements.

2.4.1. Cloud albedo

The cloud index (i.e., cloud albedo), derived from satellite images, is a feature that can potentially increase the performance of a satellite-based solar forecast. The cloud index is a relative measure of the opacity of clouds derived from the short wave band [142]. A different feature is the ground albedo, which measures the radiation reflected by the Earth's surfaces. The cloud index can be derived from the ground albedo using the spectral bands provided by the Rapid Scan High Rate SEVIRI imaging instrumentation in a MSG [13]. Additionally, the input tensor can include other information to increase the performance: the pixel's elevation map, longitude, and latitude [38]. The SEVIRI instrument also provides an optical cloud product that gives cloud optical thickness, pressure, phase, and effective radius [143]. The GOES satellites have a similar set of cloud data products available [144].

2.4.2. Cloud height

The cloud height can be directly measured using a ceilometer [145], but this sensor is expensive. Nevertheless, the derivation of the cloud height is possible by detecting the shadows projected by passing clouds at different positions using a cloud speed sensor [146] or a pyranometer grid [147]. Another alternative is to use multiple sky images and apply stereographic methods [123]. This approach has been validated against a ceilometer for solar forecasting applications and has performed accurate estimations [148]. A less exploited approach to approximate the cloud height is using temperature measurements acquired with a far-infrared sky imager [133,149]. The temperature of a cloud can be estimated knowing the rate of temperature decrease of an object floating in the atmosphere (i.e., atmospheric lapses [150]), and the atmospheric lapse can be approximated by the moist adiabatic lapse rate and the dry adiabatic lapse rate when a standard weather station is available [151].

2.4.3. Cloud thickness

The extraction of physical cloud features from ground-based images is challenging since not all sky-imagers provide interpretable measurements. However, recent research in the field proposed a method to build 3D images of clouds, which allows us to approximate the cloud thickness [152], and deep learning methods can extract information in sky images or satellite imagery from cloud optical thickness for cloud segmentation applications [153]. This is important to quantify the aerosol (e.g., clouds) effects in the solar radiation transmissivity and diffuse proportion to estimate solar energy generation [154]. In addition, aerosol optical thickness provides information about the scattering produced in the atmosphere (i.e., atmospheric extinction [155]). It is possible to derive this feature when using satellite infrared images [156] in combination with physical models [157]. Additionally, an alternative metric for visible light imagers to increase the performance of a satellite-based solar forecast is the cloud quality index which quantifies cloud thickness. This index is derived from a grayscale channel (i.e., brightness) and estimates the thickness of the cloud with respect to a set of neighboring pixels [74].

Aerosol optical thickness extraction and quantification methods with direct application in solar forecasting exist [158]. Most research proposed to assimilate data from satellite imagery [159], and it is proven influential in day-ahead solar forecasting based on weather research and forecasting software [160] or hybrid models [161]. However, a study found the effects of aerosols in short-term solar forecasting to be significant as well [162]. The capabilities of deep learning have not been explored yet in great detail for assimilating aerosol thickness in solar forecasts but approaches based on computer vision with deep learning increased in the performances when retrieving it from satellite imagery [163–165]. The product produced by these methods can add information to intra-hour solar forecasting applications that use ground-based imagers.

2.4.4. Cloud coverage

The cloud cover index refers to the fraction of the sky covered by clouds, and it is correlated with other cloud features discussed previously (e.g., cloud index). This feature is known to ameliorate solar forecasts when combined with other meteorological features [166]. This information is provided by standard weather stations [167] or can be directly extracted from ASI [168] or satellite imaginary [169]. In fact, a recent study found that the derivation of the cloud cover from the distinct spectral bands of a satellite observation can be slightly different [170], pointing out that characterizing clouds may require fusing multispectra information. When the cloud height feature is known, deriving the cloud area from the cloud cover index is possible.

The extraction of the cloud coverage index requires the detection of pixels with clouds (see Section 3.3.4), and for that task, methods based on deep learning proposed to use spatiotemporal generative adversarial networks (GANs) and [171] or CNNs [172]. Solar forecasts based on deep learning can benefit from using cloud cover in the feature vector [173] and from using binary cloud cover images (i.e., cloud segmentation) in a CNN [174]. Other alternative approaches proposed to forecast the cloud cover to later derive solar generation based on GANs [175], and CNNs for nowcasting applications [176,130].

2.4.5. Cloud motion vectors

The cloud velocity vectors can be approximated using block matching to compute an error metric to find the most similar regions in two consecutive frames [25]. Block matching is computationally expensive, but the implementation of a smart search can potentially speed up the computation [177]. A similar approach to approximate the motion of objects (i.e., clouds) in two consecutive frames is particle image velocimetry (PIV) [178]. PIV computes the cross-correlation or normalized cross-correlation between the pixels in two images in the frequency domain [179]. The phase cross-correlation is an alternative to PIV used in images that is computationally less expensive [24].

The cloud velocity vectors in two consecutive images can also be approximated as the optical flow [180,181]. The Lucas-Kanade method [182] is a simple and efficient method to approximate the cloud velocity vectors [27], although the pyramidal Lucas-Kanade is most commonly applied [183]; however, solving optical flow equations via least-squares suffers the *aperture problem* [184]. The Horn-Schunck method [185] aims to solve the problem by applying a smoothness constraint. In addition, the variational implementation exists [186], and it is feasible for estimating the cloud velocity vectors [26]; however, the "total variation regularization" version of the Horn-Schunck method [187] was found to be the most efficient optical flow solution in cloud motion estimation applications [188]. Additionally, a formulation of weighted pyramidal Horn-Schunck for cloud motion vector estimation was recently proposed for satellite imagery applications [189].

Another alternative to approximate the cloud velocity vectors is the Farnebäck method [190]. This method can use prior knowledge, local weights, and be implemented in a pyramidal manner [191]. It has high performance when approximating the cloud velocity vectors in ground-based sky images [192], but it performs better with satellite images [193,194].

2.4.6. Cloud dynamics

The cloud velocity vectors allow for the derivation of second-order dynamics, such as vorticity and divergence [195]. The vorticity measures the angular velocity of a fluid (i.e., a cloud is rotating). The divergence measures the expansion rate (i.e., negative divergence means a cloud is dissipating and positive forming). Other methods available in computational fluid dynamics literature are still unexplored in solar forecasting applications (e.g., dynamic mode decomposition [196] and proper orthogonal decomposition [197]).

2.5. Open-source data

This section presents a range of publicly available datasets that have been or could be used in computer vision-based solar power modeling. To some extent, evaluating modeling approaches on such datasets offer the opportunity to compare their performance relative to already existing methods.

2.5.1. Ground-based sky images

Different research groups contributed to improving the accessibility of ground-based imagery datasets for solar forecasting and cloud segmentation [34]. In particular, some groups have contributed in extended efforts to collect data from multiple sensors and sites (see Fig. 14). Other groups have developed software to access publicly available datasets [34], such as *SolarData* [198] and *OpenSolar* [199].

- The Solar Radiation Research Laboratory at the National Renewable Energy Laboratory (NREL) developed a baseline measurement system [200]. This system provides multiple years of 10-minute sky images from a TSI (1,920×1,920) since July 2004 and from an ASI (288×352) since September 2017, plus 1-minute resolution GSI and meteorological measurements in Golden, Colorado, USA.
- The SIRTA Atmospheric Research Observatory released sky images collected by a TSI (480×640) and a short-exposure ASI (768×1024) during 7 and 8 years, respectively, with a resolution of 1 to 2 minutes, and 1-minute resolution GSI and meteorological measurements from Palaiseau, France [201].
- The *UCSD* dataset for solar forecasting models combines multiple data sources for Folsom, California, USA [202]. The dataset includes 3 years of high-resolution sky images (1536×1536), GSI measurements in 1-minute resolution, satellite imagery, NWPs, and secondary data (i.e., features extracted from images and GSI time series).

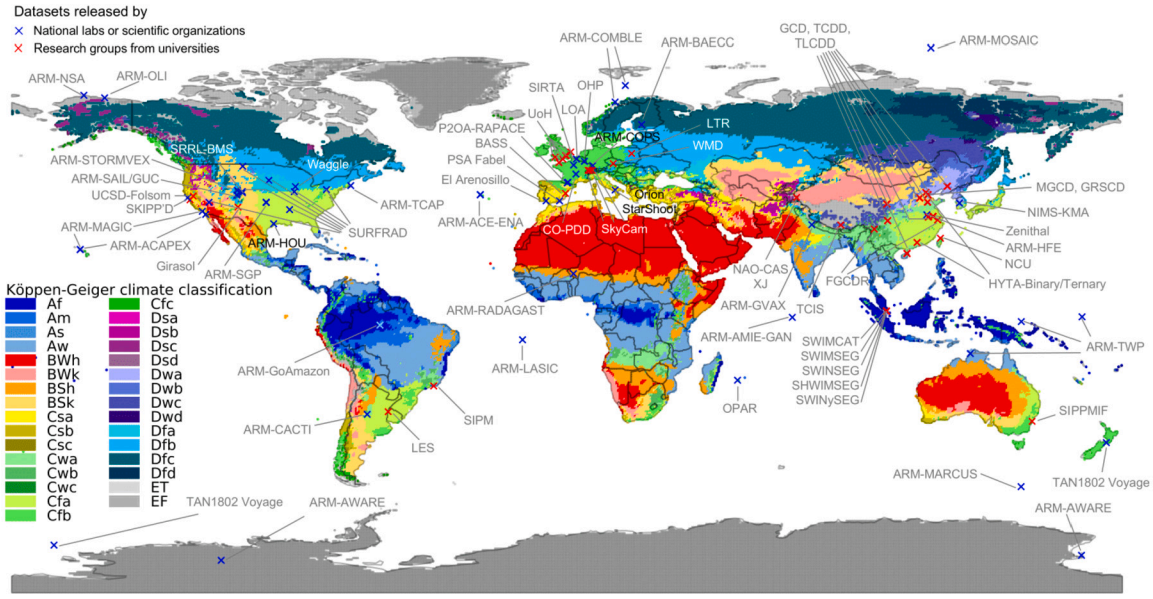

Fig. 14. Köppen–Geiger climate map with geographic locations of open-source sky image datasets annotated by blue (national labs or scientific organizations) and red (universities) crosses. This map highlights the diversity of open-source sky image datasets. Taken from [34].

- *SkyCam* has 1 year of HDR sky images (600×600) acquired using an ASI, paired with GSI measurements (logged every 10 seconds) from three locations in Switzerland (Neuchâtel, Bern, Alpnach) [203].
- *Girasol* provides sun-centered large FOV HDR multi-exposure visible (450×450) and small FOV radiometric infrared (80×60) sky images with 15-second resolution during 244 days. The dataset includes GSI and meteorological measurements (logged every 6 seconds) from Albuquerque, New Mexico, USA [85].
- *SKIPP'D* contains 3 years of ASI and photovoltaic power output data with a 1-minute resolution from Stanford, California, USA [204]. It provides both a processed benchmark dataset that contains pairs of down-sized sky images (64×64) and photovoltaic power output ready to use for computer vision-based solar forecasts as well as raw data containing sky videos, high-resolution sky images (2048×2048), and photovoltaic power output.

There are cloud segmentation datasets composed of ground-based sky images. For instance, *SURFRAD* provides hourly sky images (288×352) from 10 different locations in the USA during 2–10 years (two locations have 30-second sky images) [205]. In addition, there are multiple datasets collected over a year at a 1-minute resolution with cloud labels and corresponding sky images acquired by ASIs located in Singapore. *SWIMCAT* has sky images (125×125) acquired during daytime with 5 cloud classes [206], *SWIMSEG* is a sky image (600×600) dataset with 2 cloud classes acquired during nighttime [207], *SWINySEG* has a Nychthemeron sky images (300×300) dataset with 2 cloud classes [208], and *SHWIMSEG* is a 2-class HDR sky image (500×500) dataset acquired during nighttime [208].

2.5.2. Irradiance maps

GSI and DNI maps are publicly available for researchers and professionals. These maps provide GSI measurements at the ground level derived from satellite imagery. This information is useful for developing solar forecasting applications based on computer vision and remote-sensing. The publicly accessible databases are described here. The data are accessible through the websites or automatic API requests.

- *Helioclim* is maintained by MINES ParisTech, ARMINES, and TRANSVALOR S.A. [209]. It provides real-time data with 15-minute-ahead resolution measurement maps of GSI, DNI, diffuse, and reflected radiation at normal, tilted, and horizontal planes. The data are preprocessed images acquired from MSG-11. Helioclim contains historic data from 2004, and the maps have a spatial resolution that varies from 3 to 12 km.
- *ERA5* provides estimates of a large number of atmospheric, land, and oceanic climate variables, including direct and diffuse irradiance, to generate weather feature maps [210]. It is maintained by the European Centre for Medium-Range Weather Forecasts (ECMWF). It has a temporal resolution of 1 hour, with historic records from 1950. This dataset has a spatial resolution of 30 km and extends from 137 levels from the surface to a height of 80 km. The data have a delay and are generally available within 5 days of the real-time acquisition.
- A dataset equivalent to *ERA5* is the *MERRA*-2 reanalysis climate database managed by the National Aeronautics and Space Administration [211]. This dataset contains measurement maps for research applications from 1980 with a spatial resolution of 50 km.
- The *National solar radiation database (NSRDB)*, managed by NREL, is a GSI map database with a temporal resolution from 5 to 60 minutes [212]. The database contains historic measurements from 1998. The spatial resolution varies from 2 to 4 km. The data were acquired with Himawari, GOES, and MSG satellites.

2.5.3. Satellite imagery

Satellite imagery is also publicly available for end-users and researchers. These satellites provide measurements in multiple spectral channels, different spatial resolutions, and at various temporal resolutions as well. Geostationary satellites cover very large areas of the world constantly but at lower spatial resolution than lower-orbiting satellites such as Landsat. This constant imaging enables geostationary satellite imagery to be useful for short-term forecasting. Non-geostationary satellite imagery is useful for generating high-resolution irradiance maps or for detecting solar sites, but has limited usefulness for short-term forecasting of solar generation because of the long revisit times. In practice, most machine learning methods applied to satellite imagery are essentially interoperable with marginal adaptation to accommodate for different image formats (e.g., number of channels).

- *NOAA* provides satellite imagery covering the continents of North America and South America from 2016 with GOES-16, 17, and 18 satellites equipped 16 spectral channels. The resolutions vary from 0.5 to 2 km spatially, and from 5 to 15 minutes temporally [213].

- The *United States Geological Survey* offers access from multiple satellites, including the Landsat series of satellites. Landsat satellites image in up to 11 spectral bands with between 15-100 meter resolution and cover the entire world, with a revisit time of 8 days [214].
- The *European organization for the exploitation of meteorological satellites (EUMETSAT)*, which is the European operational satellite agency for monitoring weather, climate, and the environment from space, provides both real-time satellite and historic imagery from 1981 [215]. The images are acquired from MSG, Metop, and Sentinel-3 satellites. The satellite images are available over Europe [216] and over the Indian Ocean [217] from 2004 and 2017, respectively. The satellites have 12 spectral channels; one channel has 1-km resolution, and the other 11 have 3-km resolution. The temporal resolution varies from 5 to 15 minutes.
- The *JMA* provides satellite imagery from the Indian Ocean to the mid-Pacific. The images are acquired by Himawari satellite equipped with 16 spectral channels, and it is available from 2015. The temporal resolution ranges from 30 seconds to 10 minutes, and the spatial resolution varies from 0.5 to 2 km [218].

3. Solar power modeling with computer vision

Computer vision-based solar forecasting aims to predict the future solar power output at a location of interest using computer vision to analyze observations of the cloud cover, which accounts for most of the stochastic spatiotemporal solar variability (Fig. 7). Both imagery data (e.g., sky and satellite images) and sensor measurements (e.g., GSI, photovoltaic power output, wind speed, wind direction, temperature, pressure) need to be collected. Researchers can either set up devices to collect their own data (see Section 2) or acquire data from open-source datasets (see Section 2.5). Following this, quality control (Section 4.2.4) and feature engineering methods are applied. After preprocessing, the data are partitioned into training, validation, and testing sets (Section 3.5) for architecture development based on diverse metrics. The model performance is monitored after deployment, and adjustments on the model might be made. Further, online learning might be implemented to incorporate newly collected data and update the model [219].

3.1. Spatial characteristics

The spatial attribute of solar forecasting is crucial for many applications in terms of field of view and resolution. The complementary spatial characteristics of imaging techniques based on sky cameras and satellites facilitate the applicability of modeling techniques to an intermediate spatial extent via information fusion [13].

3.1.1. Sky images

Sky image-based models can offer high-spatial-resolution irradiance maps covering several square kilometers around the camera. In some conditions, local dense irradiance maps can be determined [220], but not all sites offer this possibility. For this reason, the majority of solar forecasting studies based on sky images currently focus on singular value prediction (e.g., GHI or GSI, DNI, photovoltaic power output) [35,119], image prediction [221,131], or cloud mask prediction [222,40].

3.1.2. Satellite imagery

The current geosynchronous weather satellites for cloud cover observations have, at best, an on-the-ground pixel size of 0.5 km – 2 km at the equator, which increases up to 4 km – 6 km per pixel at higher latitudes. Additionally, the pixels do not cover a uniform ground footprint, with pixels closer to the edge of the Earth's disk being more distorted than those near the center of the satellite's FOV. These characteristics mean that meteorological geostationary satellites do not have the spatial resolution to detect clouds smaller than a few kilometers in size, and how the clouds appear in the image changes depending on where in the image the clouds are located. Nearer the Earth's disk, clouds appear offset from the part of the Earth's surface they cover, whereas near the center of the satellite's FOV, they appear directly over the part of Earth's surface they cover. The region of the cloud cover blocking a solar site can be determined from the angular position of the sun as a preprocessing step [70]. In practice, satellite-based spatial forecasts are more flexible than ASI approaches because irradiance maps at a pixel level can be derived from radiative transfer models or with deep learning from ground-level measurements [75]. For this reason, the types of prediction from satellite observations include *in situ* measurements [40,223] but also cloud-index maps [13,224] and irradiance maps [38].

3.2. Temporal characteristics

Solar energy modeling can be characterized by various temporal variables: temporal resolution of *in situ* measurements or cloud cover observations, spectral resolution, past context, lead time, forecast horizon, and update rate (Fig. 15). Except for the spectral information, these attributes are primarily associated with time-dependent tasks or applications, including solar forecasting or video prediction, as opposed to static tasks, such as image segmentation.

3.2.1. Temporality in solar energy meteorology

Most temporal characteristics of a computer vision task can be split into two groups, past and future, which are optimized or constrained differently. On one hand, future temporal parameters are often set by the application. For instance, in a hybrid power plant optimization scheme, the horizon of the forecast is set by the warm-up time of the fossil fuel backup [225,226]. Further, an algorithm designed for energy trading must comply with market regulations [227] (Section 3.2.2).

In practice, the forecast horizon of sky images is also constrained by the FOV (up to 20/30 minutes, depending on the local cloud speed), whereas satellite observations can infer longer-term forecasts up to several hours. On the other hand, past temporal aspects are partially constrained by the source of data (e.g., fixed temporal resolution of satellite observations ranging from 5 min – 15 min for MSG to 2.5 min – 10 min for MTG), but they can also be tuned to a specific application to maximize the performance of the model [119]. Common hyperparameters defining the past context are the number of lag terms and the temporal resolution. Moreover, for a given computational capacity in operating conditions (e.g., edge computing), a trade-off between spatial and temporal resolutions of sky images can be reached.

Another key temporal aspect of any imaging technology is its spectral information. By capturing signal related to specific wavelengths, sky cameras and satellites can infer various characteristics of clouds, such as their temperature or composition. This facilitates cloud height estimation [133], sun localization [97], optical depth modeling [228] and cloud cover segmentation [229,230].

The diverse time attributes of sensing techniques (e.g., update frequency, spectral bands) represent a significant opportunity for richer detection capabilities (e.g., high temporal resolution, infrared sky cameras, multispectral imaging). However, this heterogeneity challenges the integration of multiple sources of information into a single modeling approach [13]. In that context, the flexibility of sky cameras in terms of temporal resolution can be exploited to match the update frequency of satellite imagery.

3.2.2. Operational solar forecasting

In an operational context, solar forecasting is defined by four time-related terms [231], the lead time, the horizon, the update rate, and the resolution, as shown in Fig. 15. The "boundary" between the short-term and very short-term solar forecasting is vague, due to the multidisciplinary nature of the problem and the involvement of multiple

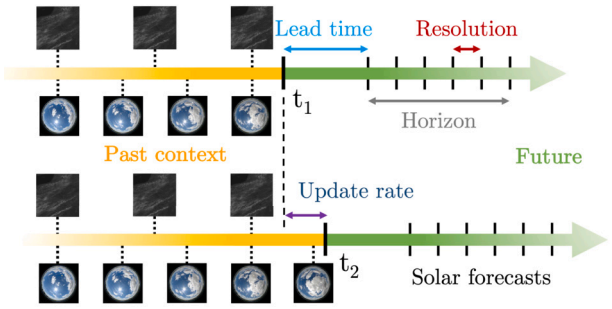

Fig. 15. Operational solar forecasting.

communities. First, different communities define the lead time differently. For example, the World Meteorological Organization refers to very short-term forecasting as forecasts 0-12 h ahead [232]. However, power system operators use day-ahead, intra-day, hour-ahead, or even intra-hour solar forecasts in their operations [233]. Second, even within the same community, the definition can also differ. For example, the energy forecasters differentiate short-term and very short-term solar forecasting by the availability of the numerical weather predictions (NWP) [234] that have various lead times from different models. In power systems, operators define the requirements for forecasts according to their own market, which are usually different from one to another. Third, there are also gaps between the literature and real world practice, since the processing and communication time is usually not considered in scientific publications but is important in power system daily operations.

3.3. Computer vision tasks in solar forecasting

Modern computer vision offers a wide range of solutions to various real-world challenges, from object detection and tracking, to modeling physical phenomena and generating synthetic data. Many studies in solar energy have demonstrated the applicability of vision algorithms to tasks, such as solar panel localization from remote imagery [235,236] or solar cell defect automatic detection [237,238]. Regarding solar forecasting, computer vision is key to modeling the complexity of the cloud cover spatiotemporal dynamics. From a general integrated learning task, such as predicting the future solar output from past sky observations, computer vision-based solar forecasting can also be split into several subtasks addressable by computer vision, such as cloud classification or solar estimation. We describe some of these tasks in the next subsections.

3.3.1. Solar estimation and radiative transfer modeling

Solar estimation is essentially building a mapping, f, from the image, $\mathcal{I}_t$ (captured at time t), to the concurrent sensor measurement, $\mathcal{M}_t$, either GSI or photovoltaic power output, i.e., $f : \mathcal{I}_t \mapsto \mathcal{M}_t$, which is similar to the computer vision task of estimating the age of people based on their facial images (Fig. 16). In situ measurements of irradiance and power output of a photovoltaic system are usually costly in devices and human labor for regular maintenance of the devices. Solar estimation models, in contrast, only require imagery data for training at the beginning, and they can then be applied with minimum cost; therefore, they can be used as an alternative to in situ measurements.

Depending on the spatial coverage, different imagery data are required for developing the solar estimation models. As shown in Fig. 2, ground-based sky images are suitable for a spatial extent below 1000 m, whereas satellite imagery is more useful for larger spatial coverages above 1000 m.

Numerous studies have examined the effectiveness of using end-to-end deep learning models, mostly CNN, for solar estimation [239]. In 2018, Sun et al. [36] developed for the first time a CNN model for solar estimation, called SUNSET, by using ground-based sky images, and

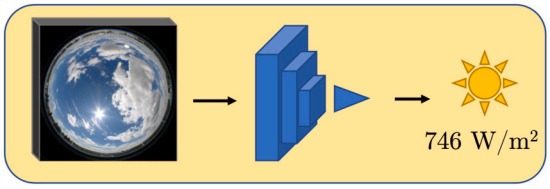

Fig. 16. Deep learning model for solar estimation (radiative transfer modeling) from cloud cover observation.

the model shows promising performance in correlating sky images to photovoltaic power output. The estimated value almost perfectly aligns with the ground truth in clear-sky days, whereas it struggles a bit with cloudy days. To deal with the challenge of solar estimation in cloudy days, Jiang et al. [240] built a CNN model for GSI estimation based on only the cloudy-day data, which achieved a relative RMSE of 8.7% on the test set. Nie et al. [241] developed a classification-prediction framework that first classifies input sky images into different sky conditions, before the classified images are sent to specific, fine-tuned CNNs for concurrent photovoltaic power output estimation.

For satellite imagery, one of the main non-deep learning approaches are the HelioSat methods [242–245], which map from geosynchronous satellite imagery to GSI using physics-based models. In recent years, new satellite-based retrieval methods using machine learning/deep learning have been used to directly infer solar irradiance from satellite images. Jiang et al. [246] investigated the spatial-scale effects on the accuracy of surface solar radiation retrieval using multivariate linear regression, artificial neural network and CNN models and found that scale effects could significantly influence the accuracy of satellite-based solar radiation estimation. In another study, Verbois et al. [247] examined the practical efficacy of using machine learning methods to directly infer the surface solar irradiance from satellite images compared to state-of-the-art physical retrieval methods. A multilayer perceptron model was trained using various spatial and temporal configurations of the development and evaluation datasets comprising radiance levels and colocated ground measurements. The authors concluded that the performance of the data-driven model is very dependent on the training dataset. The estimation of photovoltaic system output from satellite images can be performed via solar panel segmentation methods to infer the local solar capacity [248].

The seasonality of GSI, both over the course of the year and diurnally, can cause issues for solar forecasting models, so generally they should be taken out before giving the data to the model via the CSI [10]. One of the best methods for removing the seasonality is to use a clear-sky model [249–251]. This is especially important for satellite-based modeling approaches because sky image-based forecasting models can learn to correlate the CSI with the position of the sun in the sky.

3.3.2. Solar forecasting and nowcasting

In the past five years, computer vision-based solar forecasting has seen an increase in using end-to-end deep learning models to correlate the future irradiance level or photovoltaic power output with the sequence of past cloud cover observation (Fig. 17). A typical setup is to predict the T-minute-ahead future GSI or photovoltaic power output, referred to as measurement $\mathcal{M}$, based on an image sequence, $\mathcal{I}$, covering the past H minutes, and possibly together with concurrent historical measurements. Mathematically, it can be expressed as learning a mapping $f : (\mathcal{I}, \mathcal{M})_{t-H:\delta:t} \mapsto \mathcal{M}_{t+T}$, where δ is the interval between two lag terms.

CNNs are commonly used in these data-driven frameworks, either solely [119,120,252,253] or as a backbone, generally hybridized with recurrent neural network architectures, such as long short-term memory networks (LSTM) [101,39,40]. For example, Sun et al. [119] modified the CNN model architecture they developed for the solar estimation task [36] to solar forecasting by injecting sky images in the past 15

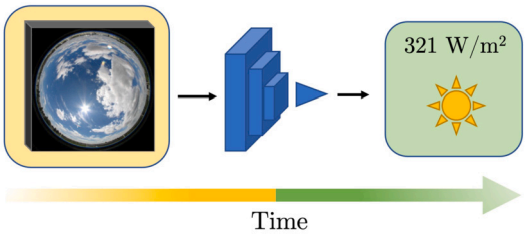

Fig. 17. Solar power forecasting with deep learning.

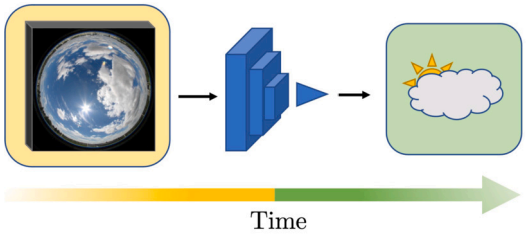

Fig. 18. Deep learning approach for event prediction.

minutes together with the concurrent photovoltaic power output history to predict photovoltaic power output 15 minutes ahead into the future. The study extensively explored the optimal model input and output configurations. The results suggest that using the same length of history as the forecasting horizon, i.e., $T = H$, is a good heuristic, and using hybrid input, i.e., images plus the photovoltaic power output history, could achieve better performance than using solely images or the photovoltaic power output history. Paletta et al. [39] established a benchmark for short-term GSI forecasting by comparing four commonly used deep learning architectures — CNN, LSTM, 3D-CNN and ConvLSTM — with different forecasting horizons from 2 to 30 minutes. The results show that these deep learning models can outperform by approximately 20% the reference persistence model for a 10-minute forecasting horizon; however, these models have similar limitations in anticipating fundamental events, causing large irradiance changes, such as clouds obscuring the sun. Furthermore, these four neural networks are shown to provide comparable predictions and forecast errors, with the best models marginally improving over the standard CNN architecture.

For solar nowcasting with satellite imagery, the task involves determining the amount of solar power being generated at the current time and a few hours into the future, corresponding to some amount of time steps into the future, for example, 48 time steps for a 4-hour forecast at 5-minute resolution. The task is generally framed as a regression task, trying to predict the exact amount of solar energy within the area or site of interest, and is an extension of the previous section on future times. Because satellite images are simply multichannel images, common deep learning models — such as ResNets, ConvLSTMs, and U-Nets — can and have been applied to this problem [254,73,255]. Yeom et al. [256] used a ConvLSTM model to predict short-term changes in solar radiation over South Korea, validated by ground pyranometers. In [257], satellite and NWP data were combined to forecast the future irradiance. Both ConvLSTM and 3D convolutional models were investigated for forecasting GSI up to 6 hours ahead in Italy in [258], with the ConvLSTM winning out over the smart persistence and the 3D convolutional model. The input to these models is usually a stack of satellite images covering the area surrounding the region of interest (e.g., a solar power plant), potentially much larger than the are of interest to better capture clouds that might move over the area of interest within the forecast horizon [138,139]. To work with models not designed for time series, such as U-Nets and ResNets, one common approach is to combine the time and channel dimensions of the inputs [255].

Predicting irradiance is different than predicting photovoltaic power output. Irradiance predictions are generally dense predictions for every pixel in the input images, predicting the irradiance at those points, whereas photovoltaic power output forecasting tends to be more sparse, predicting the actual power output for specific sites in the FOV. Photovoltaic forecasting is also quite directly linked to the specificities of the photovoltaic panels (e.g., size, orientation, soiling) and site-specific data (e.g., shadowing effects), rather than irradiance predictions, which can be adapted to different types of panels and site-specific data after the fact.

3.3.3. Event prediction

Passing clouds obscure (or show) the sun and significantly attenuate (or increase) the irradiance reaching the ground in the short term, consequently leading to a sudden drop (rise) of the power output of photovoltaic solar panels. These significant power output changes of local photovoltaic systems within a short time period are often referred to as ramp events, which are crucial information for grid operation and management. The cloud dynamics can be captured by ground-based sky imagers or satellites; however, existing deep learning models used in solar forecasting are usually lacking in their ability to anticipate these events, evidenced by recurrent temporal lags in predictions [39].

Several studies have tried to address these issues by either directly predicting the ramp events or predicting the future states of the sky using sky images as a way of assisting solar forecasting (Fig. 18). Pothineni et al. [259] used CNNs to predict the 5-minute-ahead sky condition to be either clear or occluded. The work experimented with different neural network architectures and concluded that an 18-layer ResNet performed the best, with 91%–93% accuracy, though no follow-up experiments further showed the usage of this information for solar forecasting. Abuella and Chowdhury [260] developed a post-processing adjusting approach to improve the ramp event forecasting capability of hour-ahead ensemble solar forecasting models. The ramp event forecasting can be formulated as a classification problem, where four types of ramp events are defined based on the direction and rate of the ramp: ramp-up high rate, ramp-up low rate, ramp-down high rate, and ramp-down low rate. The results demonstrate the efficacy of this adjusting approach. Leelaruji and Teerakawanich [261] combined image processing techniques with a CNN based on ResNet for alerting of trigger events before the sun cover happens, 1 to 2 minutes in advance. The results show a prediction error of 27.50%. On the other hand, Paletta et al. [40] developed a deep learning model called ECLIPSE, which consists of spatial and temporal encoders to extract features from the past sky image sequence to predict the future segmentation map (i.e., as a means of indicating whether the sun is obscured by the clouds) and the future irradiance at the same time. Besides minimizing the irradiance prediction error, a regularization term associated with the segmentation map prediction is included in the loss function of the deep learning model.

Commonly used evaluation metrics — such as MAE, mean square error (MSE), and RMSE — are not able to capture the fluctuations of irradiance or power output time series, and they are not suitable metrics for assessing the model performance on detecting ramp events. To bridge this gap, Vallance et al. [262] proposed a new ramp metric, called the ramp score, which compares the ramps extracted from the forecast with those extracted from the measurements (details can be found in Section 3.5 and in [39]).

3.3.4. Image segmentation

Cloud cover observations are widely used to perform accurate segmentation maps. Such accurate detection of clouds assists remote-sensing analysts and meteorologists in performing automatic computations of cloud cover values. Traditionally, the cloud cover values are reported via *oktas*; however, with the introduction of sky cameras, it is now possible to perform automatic and accurate segmentation of clouds, and thereby report the cloud cover value. Researchers in the field have used various statistical image processing techniques over

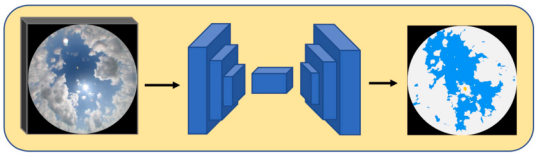

Fig. 19. Encoder-decoder neural network architecture for cloud cover segmentation.

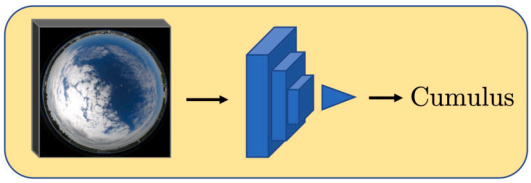

Fig. 20. Deep learning architecture for cloud classification.

the last decade in the segmentation of sky/cloud images, including superpixels [263], threshold methods [263], graph cuts [264,265], as well as probabilistic approaches [266]. Apart from classic statistical methods, supervised [149] and unsupervised [267] fully probabilistic approaches and kernel learning methods were used for cloud segmentation in ground-based infrared images [268]. In addition, unsupervised fully probabilistic methods enable cloud semantic segmentation [141].

Recently, deep learning techniques have also been used to improve the segmentation accuracy of the various approaches (Fig. 19). Researchers in [208] proposed a lightweight deep learning architecture, called CloudSegNet, for efficient segmentation of sky/cloud images. It is the first to accomplish state-of-the-art results on open datasets by combining daylight and nighttime (also known as nychthemeron) image segmentation in a single framework. Hasenbalg et al. [67] compared six benchmarking cloud segmentation algorithms on images captured by a standard security camera: a color-channel threshold-based algorithm; a Clear Sky Library based approach, a region-increasing algorithm, the Hybrid Thresholding Algorithm (HYTA), and an improved HYTA+ development. Additionally, a CNN is modified for this issue via transfer learning. Further, Xie et al. [269] proposed SegCloud, a new deep CNN model for precise cloud segmentation based on ground-based observation. The SegCloud architecture has a symmetric encoder-decoder structure in terms of architecture. While the decoder network restores the high-level cloud feature maps produced by the encoder network to the same resolution as the input images, the encoder network combines low-level cloud features to create high-level, low-resolution cloud feature maps. The SegCloud approach can automatically partition whole-sky images captured by an ASI and has a powerful cloud-discriminating capacity. Transformer-based cloud segmentation approaches are also recently explored in [270].

In satellite imagery, cloud segmentation is used to compute the cloud cover and to identify pixels that are covered by clouds [271]. Pugazhenthi and Kumar [272] proposed an improved fuzzy c-means and an improved k-means clustering algorithms that segment far-infrared images of the INSAT-3D satellite into regions with low-, middle-, and high-level clouds as well as areas without clouds. Further, Francis et al. [273] examined the issue of cloud detection in visible and multispectral satellite data from two high-resolution sensors, Carbonite-2 and Landsat 8. In addition to binary segmentation, Wieland et al. [274] provided a multiclass, data-driven method for semantic segmentation of clouds and cloud shadows in single-date images based on a modified U-Net CNN. On a large-scale library of Landsat images, they trained the network to classify objects into five categories: shadow, cloud, water, land, and snow/ice. These algorithms are often modified to run on onboard edge devices. Bahl et al. [275] proposed low-power neural networks for satellite image semantic segmentation [275]. These networks are designed to function on edge devices with limited resources, such as phones, drones, or satellites. Other types of computer vision-based detection tasks consist of identifying rooftop solar panels via remote-sensing imagery and estimating some of their main characteristics (e.g., capacity, tilt angle, azimuth) for modeling purposes [276–279].

In short, Table 3 provides a summary of the various available deep networks for the purpose of cloud image segmentation.

3.3.5. Cloud classification

In more recent times, deep learning classifiers have been trained to produce superior outcomes without any need for feature identification prior to training (Fig. 20). A CNN was implemented to extract features that are then processed and sent to a support vector machine classifier for classification [281]. The network's average accuracy was evaluated across the six classes and claimed an accuracy of 89.5% on its dataset. Later, to categorize cloud images, Zhang et al. [282] developed AlexNet [283] and published the CloudNet architecture. The author-released the cirrus cumulus stratus nimbus dataset and the SWIMCAT dataset were both used to test the model. Recently, Wang et al. [284] introduced CloudA, in which they trained a unique deep CNN using a support vector machine classifier.

In summary, the task of cloud classification has been attempted by researchers using both machine-learning and deep-learning methods. Some of these methods offer good accuracy in a handful of annotated cloud classification datasets; however, we feel that there is still a lot of scope for improvement in this area, primarily in the accuracy of the cloud classification task and the availability of open-access cloud classification annotated datasets.

3.3.6. Cloud motion prediction

In video prediction, the objective is to predict the next set of frames into the future given the last N frames as history (Fig. 21). In relation to solar forecasting, the main application of video prediction is to predict where clouds will move in the future and therefore how clouds visible at the inference time will affect the output from solar energy systems.

Defining what a good video prediction is remains difficult. With metrics such as RMSE, and MAE to a lesser extent, deep learning models tend to blur details, causing clouds to become more of a white fog as the forecast time lengthens [13,38,221,285,286] (Fig. 22). Although this blurriness is rarely representative of the actual future scenario, it can be beneficial to some operational applications because it describes the uncertainty associated with predictions. A resulting drawback is the low variance of the forecasts, which mitigates steep solar ramps [39]. To force more realistic outputs, deep learning models such as GANs have been shown to create much more realistic forecasts of precipitation [287] or cloud displacement [288] compared to non-generative models trained with RMSE or related metrics. Alternatively, structure-preserving loss functions have been applied to produce more realistic predictions by also measuring nonstructural distortions, such as luminance and contrast changes [224].

In relation to satellite-image video-based prediction, each frame is taken between 5 and 15 minutes apart and covers extended areas. This large FOV means that satellite-based methods can see clouds that are hundreds of kilometers away from the site of interest, potentially allowing for more accurate long-term forecasts of cloud movement than sky images, with their more limited FOV. Current works build neural networks trained on satellite observations to predict the future cloud cover. These sequence-to-sequence architectures take raw and preprocessed images (e.g., irradiance or cloud-index maps) as well as auxiliary data encoded in additional channels (e.g., irradiance values, time spatial coordinates) as input [13,38].

Video prediction with sky images exploits similar approaches: predicting future sky observations from a context of several past frames (Fig. 23). In practice, sky cameras offer much higher spatial and temporal resolutions of the local cloud cover, revealing clouds that cannot

Table 3
Summary of various deep learning networks for cloud image segmentation.

Network	Image Type	Advantages	Disadvantages
DeeplabV3+ [280]	Ground-based	High accuracy	Computationally expensive
CloudSegNet [208]	Ground-based	Lightweight architecture, efficient segmentation	Limited performance on complex scenes
SegCloud [269]	Ground-based	Precise cloud segmentation	Symmetric encoder-decoder structure limits scalability
Transformer-based models [270]	Ground-based	Captures long-range dependencies	Higher training complexity
Pugazhenthi and Kumar [272]	Satellite	Multi-label segmentation	Dependent on thresholds
Francis et al. [273]	Satellite	Works on multispectral data	Low performance on snow or icy terrain
Wieland et al. [274]	Satellite	Five-class classification	Variance in performances across sensors and locations
Bahl et al. [275]	Satellite	Designed to function on limited resources	Does not work in multi-class image segmentation

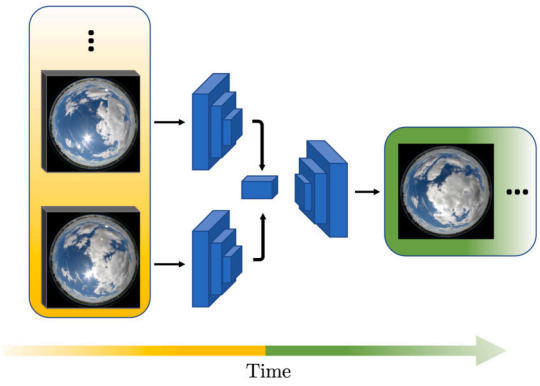

Fig. 21. Deep learning network for cloud motion prediction.

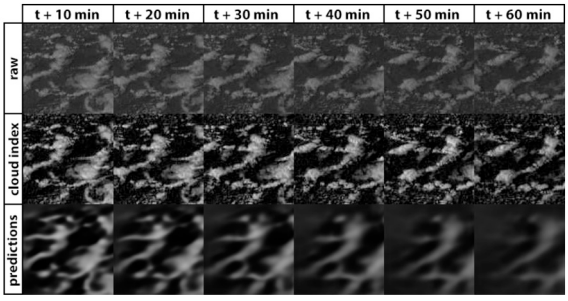

Fig. 22. Prediction of future satellite observations by a deep learning model. The longer the horizon, the fuzzier the predictions from the model. Taken from [13].

be observed from satellites; however, the FOV of a unique camera remains limited to several square kilometers centered on the device. This limits the forecast horizon of methods based on a single sky camera to the amount of time taken by clouds to hide the sun from the moment they were visible in the image. Typically, clouds cross the FOV within 20 to 30 minutes, depending on the wind speed. For this reason, deep learning models usually observe a 10-minute context window to predict future frames from 5 to 20 minutes in the future.

A range of deep learning architectures have been applied to video prediction from sky images. Siddiqui and Bharadwaj [222] learns semantic masks of both past and future frames using ResNet to generate a representation tensor for each context frame. Future masks and corresponding irradiance levels are obtained from spatial attention mechanisms combined with ConvLSTM layers. To address the fuzziness of sky image predictions, a method based on a GAN was proposed by [288]. A generator is trained to predict the next frame from a context of four sky images while the discriminator tries to distinguish real sequences of five consecutive real frames from sequences resulting from the generating process (i.e., four real frames plus the corresponding prediction of the

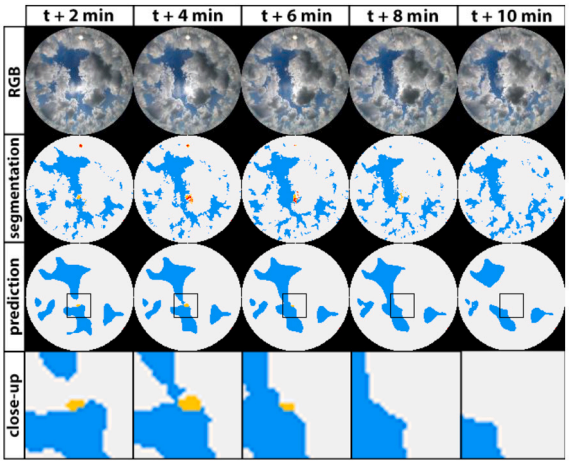

Fig. 23. Cloud motion prediction with sky images. A close-up of the circumsolar area shows how the model predicts that the sun is going to be hidden by a cloud within the next 10 minutes. Taken from [40].

generator). Observing that physical phenomena such as cloud displacement can be described by advection-diffusion equations, another model, called PhyDNet, aims to constrain predictions with partial differential equations in the latent space [221]. PredNet [289], which uses the error associated with previous generated images to improve the subsequent frame prediction, was also used to predict irradiance from the learned representations of future sky images [285]. Another method iteratively predicts cloud masks frame by frame with a CNN [290]. A deep learning model, named ECLIPSE, generates a spatiotemporal representation of the past sequence of sky or satellite images using 2D and 3D convolutional layers [40]. A recurrent convolutional module iteratively predicts future states that can then be decoded into various signals: irradiance level, irradiance distribution, or cloud mask. Because fish-eye lenses induce a strong distortion, some approaches first unwrap sky images as a preprocessing step prior to feeding a deep learning model [40,131]. This improves the shape consistency of clouds as they move across the FOV.

3.4. Open-source code and models

Increasingly, solar forecasting models are being made open source, either only the code or the code and the trained model weights. These releases allow for anyone to easily build upon the existing work, better compare approaches, reproduce the original results, or improve the open code. Platforms for machine learning model hosting, such as Hugging Face, are also sometimes used to publish trained models and reduce the barriers for others to build upon and use the models.

For satellite-based solar forecasting, some examples of open code and model weights include PVNet [291], which takes historical satellite data, NWPs, and live photovoltaic system readings to predict regional

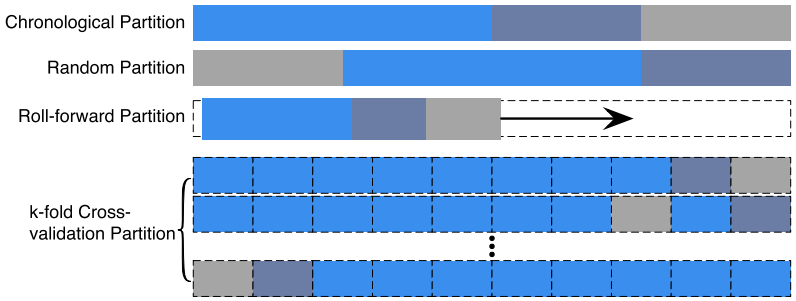

Fig. 24. Data partitioning strategies. Blue, purple, and gray indicate training, validation, and testing datasets, respectively.

photovoltaic power output for the United Kingdom, or transformer-based models, such as Power Perceiver [68], which takes similar data and predicts both site-level solar output and regional forecasts and builds on the work of the more general Perceiver and PerceiverIO architectures [292,293]. Showing the benefits of open code, other, related open-source models for rain forecasting have been adapted for solar forecasting [138,139,287]. These models were trained on open datasets [64,216] and released on Hugging Face [65] for use by other researchers and practitioners.

A combination of sky image, satellite, NWP, and photovoltaic power output dataset and baseline model code was made open in [294], providing a set of simple benchmark models for comparing approaches. Some simple open models include [295], which uses an LSTM to forecast photovoltaic power output. SUNSET [296] is an open-source CNN model that uses both imagery and photovoltaic power output history to predict short-term solar generation.

The International Energy Agency PVPS collaboration is working to evaluate current and emerging resources for solar forecasting, including both models and data. The group is planning on releasing their findings and both data and model products by the end of 2023 [297].

3.5. Quantitative and qualitative evaluation

With decades of development, a consensus has been reached on how to validate a proposed solar forecasting model [298,299]. When applied to computer vision-based solar forecasting, the same standards and practices should be followed. Generally, a data-driven model should be selected, constructed, and optimized using in-sample period data, during which hyperparameters and parameters are tuned with the training and validation datasets. Then, the model will be tested on the testing (or forecasting) dataset in the out-of-sample period. Evaluation metrics are required in both processes to guide the training or verify the performance. The proposed method is proven to be superior if it has better performance compared to the benchmarks based on the same metrics and testing dataset; however, there are several common issues in data partition, metric selection, and competitive model selection in the computer vision-based solar forecasting evaluation and validation. Therefore, we will discuss the three critical components in evaluating a new model: the data partitioning, benchmark setting, and evaluation metric selection.

The intention of data partitioning in solar forecasting is to simulate the real-world situation where only historical data are available for training and updating the model; therefore, data partitioning normally separates the data into training, validation, and testing subsets. Solar time series is chronological and has evident diurnal and seasonal trends, which makes the data partitioning more important in the model evaluation.

The most natural partitioning method for time-series prediction is chronological partitioning, where the training dataset consists of the most ancient samples, the testing dataset has the most recent samples, and the validation dataset contains the remaining samples. This data partitioning method requires multiple years of data to ensure that the evaluation is unbiased. For example, six years of sky image data were used in [117], where the testing dataset included two years of data with more than 52,000 samples. In a CNN-based satellite image solar forecasting work, three years of data were used for training, and the last year of data was used for testing [300]. The second widely used data partitioning method is random partitioning, which leaves one or multiple period(s) for testing and the rest for training and validation. This partitioning method does not require the temporal orders of the three subsets, which means the testing period can be sampled anywhere in the time series. The most famous example is the global energy forecasting competitions [301]. In [302], two years of GOES-13 satellite images data were used to develop irradiance forecasts up to 5 hours ahead, where the 2017 data were reserved for algorithm training and the 2016 data were used for evaluation. This method can ensure fair comparisons, but it cannot reflect the real-world forecasting practices and might miss the long-term trend patterns and heteroscedasticity in the forecast time series.

These two methods are usually nonoverlapping partitioning methods. Two overlapping partitioning methods are widely used in computer vision-based solar forecasting, shown in Fig. 24. The first is roll-forward partitioning, which uses a fixed-length moving window to partition the dataset with updated information. The forecasting model is retrained in each step with the newly constructed subsets. This method is usually used in traditional statistical methods that take less time to train. For example, the Bayesian model averaging model was combined with a moving window to generate probabilistic forecasts by post-processing the deterministic solar forecast scenarios [303]. The second overlapping partitioning method is the k-fold cross-validation. It splits the data into k groups, holds one group of data for testing, and uses the rest of the data for training/validation. The procedure is repeated k times to cover the entire dataset in the testing, and the results are evaluated and summarized. k-fold cross-validation is a resampling method usually applied to limited data. For example, a 10-fold cross-validation method was used in a study on cloud motion speed estimation to augment a dataset with only 500 images [304]. Although k-fold cross-validation can mitigate a lack of data to some extent, this method is only powerful when applied to datasets with decent sizes. All four methods can be applied to validate the computer vision-based solar forecasting models. But there are several bottom-line rules: (i) models should be tested with out-of-sample data, (ii) the same data partitioning method should be applied to the proposed forecasting model and the competitive models for fair comparisons, (iii) at least one year of data should be included in the testing dataset to maintain seasonal patterns and various weather conditions, and (iv) the data partitioning method should be described in detail and should be reproducible.

Another important aspect when evaluating a new model is benchmarks, which are a collection of competitive models for comparison. Benchmark models should be a mix of classic baseline models, state-of-the-art models, and similar models in the immediate family. For example, in sky image-based very short-term solar forecasting, the persistence methods are usually used as the baseline method. Traditional time-series methods, such as the autoregressive integrated moving aver-

age method (ARIMA), and standard shallow machine learning methods — such as neural network, SVR, random forest, and GBM — are always used as benchmark methods. Taking transformer models as an example, their immediate competitive models include CNN without an attention mechanism and CNN with different attention mechanisms. With the advances in open-source research, a number of easily implemented models are available to compare with computer vision-based solar forecasting models [39,305]. Detailed descriptions of these models can be found in Section 3.4. In addition to the benchmark selection, model construction and optimization are also critical for fair comparisons. It was criticized in [54] that model parameters were manipulated to allow the competing models to be dominated by the proposed models; hence, both the proposed model and the benchmark models should be designed and optimized using the same strategy and method. It is also important to show the optimization process and results for reproductibility.

The two important types of goodness defining a good forecast are quality and value [298,306]. The former measures the correspondence between forecasts and observations, and the latter measures the benefits of accurate forecasts to end users. Most computer vision-based solar forecasting research uses one or more quantitative evaluation metric(s) to assess the quality of forecasts. There are a redundant number of review articles discussing the quality evaluation metrics in solar forecasting [57,298,307]; however, only a limited number of articles focus on both algorithm development and benefit assessment in computer vision-based solar forecasting. For example, sky image-based solar forecasts were developed to mitigate the photovoltaic power fluctuations through a battery smoothing control method [308] and a battery-less proactive ramp down strategy [309], respectively. Similarly, sky image-based solar forecasts were used for photovoltaic power ramp-rate control with a higher control rate [310]. A possible reason for a lack of forecasting articles favoring the value of forecasts is that the forecast value highly depends on the end users, which need additional power system modeling and simulations. It is also challenging to set up a unified standard to assess the benefit and value of forecasts; hence, in this review, we only briefly introduce the quality metrics and give a few examples of evaluating the value of forecasts.

Solar forecasts can be evaluated both qualitatively and quantitatively. Depending on the objective in the forecasting methodology workflow and the output format, the quantitative evaluation metrics can be divided into regression metrics and classification metrics, or deterministic metrics and probabilistic metrics. Table 4 lists a collection of metrics in each group. The most widely used metrics are forecasting errors, which quantify the discrepancies between observations and forecasts, including MAE, RMSE, MSE, mean bias error (MBE), and their variants [307]. Error metrics are also used to compare the developed model with the baseline to show the improvement, which is defined as the forecasting skill. RMSE is usually used in the solar forecasting literature [298]. The coefficient of determination [76] and the correlation coefficient [77] are also used to assess the accuracy of the forecasts. In probabilistic solar forecasting, reliability and sharpness are the two major qualitative characteristics to assess [61]. Reliability refers to the correspondence between the forecast probability and the true probability. Sharpness measures the uncertainty density or the predictive distribution narrowness. The former can be assessed by the prediction interval coverage probability, the average coverage error, and the latter one can be quantified by the prediction interval averaged width [299,311]. The continuous ranked probability score (CRPS) is a metric to jointly measure the reliability and sharpness; it can be complemented by several other scores, including the Winkler score [312], quantile score, interval score, and ignorance score [299].

The regression predictions can also be qualitatively validated. The most widely used is by plotting the time series of the actual values, forecasts, and errors, which directly shows the discrepancies between the actual and forecast values. Another common approach is plotting the distributions. For example, the histogram, quantile-quantile plot, and the cumulative distribution plot of the deterministic forecast errors are used to assess the goodness of the solar forecasts or to investigate the correlation between solar and wind power output forecast errors [313–315]. Another way of using distribution to time-independently verify the forecasts is the joint distribution of observations and forecasts, which can illustrate the bias corresponding to the actual target values. Probabilistic forecasting performance can also be visually evaluated. For example, a rank histogram is used to assess the dispersion of ensemble forecasts by looking at the flatness. A probability integral transform histogram is used to evaluate the calibration property of cumulative predictive distributions of the probabilistic forecasts. The prediction interval coverage probability (PICP) is a metric of the reliability of a forecast, while the prediction interval normalized averaged width (PINAW) measures the sharpness. Reliability and sharpness diagrams demonstrate the reliability and sharpness indices for different confidence levels. These metrics are commonly used, but they are not the most appropriate for solar irradiance forecasting. The definitions and discussions of these probabilistic evaluation plots can be found in [316].

Solar forecasting also involves some classification problem, such as event prediction, cloud segmentation, and cloud classification. Satellite images or meteorological data are used to analyze the presence of clouds or their types. Evaluation of the classification results is different but could also be performed quantitatively and qualitatively. The most commonly used quantitative evaluation metrics are confusion matrix-based metrics, including accuracy, precision, recall, specificity, and error rate. These metrics can be used for binary classification problems in solar forecasting, such as ramp detection and event existence prediction, and also for multiclass classification problems, such as cloud type classification. Three more comprehensive metrics that can also be derived from the confusion matrix are the F-score, the J-statistic, and the Matthews correlation coefficient. The first measures the harmonic mean of precision and sensitivity, the second uses sensitivity and specificity, and the last is the correlation between the observed and predicted class considering the class imbalance impact. The receiver operating characteristic (ROC) curve is qualitative that measures the misclassification rate of one class and the accuracy of the other. The corresponding quantitative metric is the area under the ROC curve that measures the quality of binary classifiers.

Some metrics are especially useful to evaluate possible class imbalances in the cloud segmentation problem, such as the intersection over union, the Dice coefficient, and the Jaccard index. In the literature, there have been a few cloud classification methods [317,318]. The experimental results show that adding the cloud classification step to solar forecasting improves the forecasting performance [122,149,121]. The overall performance of the forecasting model with the cloud classification step can be evaluated based on the metrics in Table 4.

Solar variables have diurnal and seasonal patterns and are highly impacted by weather conditions; therefore, it is always encouraged to separate the evaluation by hour, by month, and by weather condition to take a closer look at the forecasts. As an unsupervised process, clustering is used to distinguish and identify the type of each time period in the training data. Due to the customization of data labels, evaluation of the clustering results is challenging. The three deterministic metrics that are commonly used as quantitative metrics to assess the clustering performance are connectivity, silhouette, and the Dunn's index.

3.6. Applications and end users of vision-based forecasting

Forecasts of solar and wind power have been traditionally used by power plant operators for economic and system reliability benefits. In surveys on the adoption of forecasts of variable energy generation in the Western Interconnection conducted in 2012 and 2014, many surveyed balancing areas reported that they regarded forecasts as a necessity for electrical system reliability and effectiveness [319,320]. These surveys demonstrated economic benefits in which a 1% reduction of forecast MAE could be worth up to millions of dollars per year in some op-

Table 4
Different metrics used to evaluate computer vision-based cloud segmentation, sky (i.e., atmospheric) condition classification, and solar forecasts with deterministic and probabilistic deep learning models.

Evaluation	Deterministic	Probabilistic
Quantitative	MAE, RMSE, MSE, MBE, NMAE, NRMSE, MAPE, RMSPE, R^2, forecasting skill	Skewness, kurtosis, PICP, PINAW, negative log-predictive density, CRPS, pinball loss Winkler, quantile, interval and ignorance scores
Qualitative	Confusion matrix, ROC curve, J-statistic, F-score, Matthews correlation coefficient, Jaccard index, Dice coefficient	Bayesian and Akaike information criterion, entropy, reliability, sharpness, integrated complete likelihood

erating entities [320]. Previous studies also show the economic and flexibility benefits of improved forecast accuracy in electric power systems [321,322]. Forecasts can also be used for other purposes, such as scheduling and operations of electricity markets, procurement of operating reserves, determination of optimal market bids for power plants, and improvement of situational awareness [323–326].

Electricity market participants include producers, such as power plants that provide electricity to the grid, and consumers, i.e., end-use customers who consume electricity. Unlike market operators, the operations of market participants are profit-oriented, and their goals are typically maximizing their revenues from electricity markets by bidding into energy and/or ancillary markets. Solar forecasts can be used in the determination of optimal operating schedules of market participants. These models usually represent solar power uncertainty and market price volatility with probability distributions, scenarios, or uncertainty sets, and they optimize their bidding strategies using stochastic optimization, robust optimization, and chance-constrained optimization [327–333]. Satellite data, such as measurements of GSI, can be used as input to produce short-term solar power forecasts and to inform the optimal bids into electricity markets for both photovoltaic and CSP plants. Previous studies have shown both financial and reliability improvements in different markets by using forecasts from satellite data [334,335]. In addition to energy markets, solar forecasts can add additional value to solar power plants in ancillary service markets. For example, [336] demonstrated that photovoltaic can provide frequency regulation when satellite-derived solar power forecasts were used. On the demand side, electricity consumers can adjust their load to mitigate load imbalance or to improve economic performance in response to time-varying electricity rates. Demand response actions can be realized by simply selecting the on/off settings [337] or by dynamically varying levels of end-use electric load, such as HVAC (heating, ventilating, and air conditioning), based on satellite-derived solar power forecasts [338,339].

Operating reserves are key ancillary services that serve to stabilize power system frequency, which is an indicator of the balance of real power [340]. Although the names, types, and functions of these operating reserves might vary with markets, most markets procure a variety of operating reserves with response times ranging from approximately 5 minutes (e.g., regulating reserves) to 30 minutes (e.g., nonspinning reserves) [341]. Forecasting plays an increasingly important role in the determination of the requirements of operating reserves because of increasing renewable penetrations in modern power systems and because too high or too low requirements can sacrifice cost-effectiveness or system reliability, respectively. Methods of determining requirements of operating reserves can be categorized into endogenous and exogenous methods [342]. Endogenous methods usually rely on market dispatch models to co-optimize the operations of energy and operating reserves, and they represent renewable and load uncertainties explicitly using a variety of techniques. These models give the amount of required reserves to achieve predefined reliability levels, which usually comply with market standards [343–345]. Despite their popularity in the literature, these methods are rarely adopted by real-world market operators because they are computationally prohibitive. Exogenous methods, in contrast, are less computationally expensive and are more widely used in the real world. These methods determine the requirements of operating reserves based on uncertainty levels of net load (i.e., total electric demand minus non-dispatchable power, such as wind and solar). Typically, distributions of net load are constructed from historical data [346]; however, because of increasing renewable penetration, historical data might fail to reflect the latest system states or weather conditions; therefore, the latest studies propose addressing this issue by using forecasts [347,348]. Because net load is a linear combination of gross load, wind power, and solar power, distributions of net load forecasting errors are determined by distributions of all constituent components. Although these components can be assumed to be independent [116], studies suggest that they often lead to conservative results [346,349,350]; therefore, some studies use copula to account for correlations across variables [351–354]. In addition, forecasts of solar power, including sky images and satellite data, can be further processed to estimate distributions of net load forecasting errors using a variety of techniques, such as time-series models [355], k-nearest neighbors [347], regressions [348,356], and neural networks [116,357]. Previous studies suggest better economic and reliability performance from using weather-informed requirements of operating reserves [347,355,358–361].

Because of their dependence on meteorological conditions, both solar and wind power are subject to power ramps, which can significantly impact grid security; therefore, utilities usually rely on active power curtailment or energy storage to reduce ramp rates and smooth solar power output [362–366]. Ramp forecasts enable operators to take informed actions prior to the occurrence of solar ramps and thus improve grid reliability and economic performance [367]. For example, Wen et al. [364], Saleh et al. [365] made solar power forecasts using sky images, and they developed ramp control strategies that comply with grid regulations based on their ramp forecasts. The improved ramp control strategies can ameliorate system cost-effectiveness, and they can sometimes even reduce the battery degradation of a hybrid photovoltaic and battery system by reducing the energy throughput over a battery's lifetime [367]. Although most studies use deterministic forecasts, probabilistic forecasts can also be used to inform ramp control strategies [363].

4. Deep learning techniques for vision-based solar energy meteorology

This section presents diverse deep learning methods used in vision-based solar energy modeling. These techniques focus on various aspects of the general modeling pipeline including architecture tuning, data processing, model training, interpretability and uncertainty quantification.

4.1. Architecture tuning

Implementing deep learning models often involves numerous architecture design choices (e.g., number of layers, size of convolutional filters, and number of neurons) or different learning setups (e.g., learning rate and batch size). Tuning these hyperparameters to improve the performance of deep learning models is a nontrivial job. Normally, for

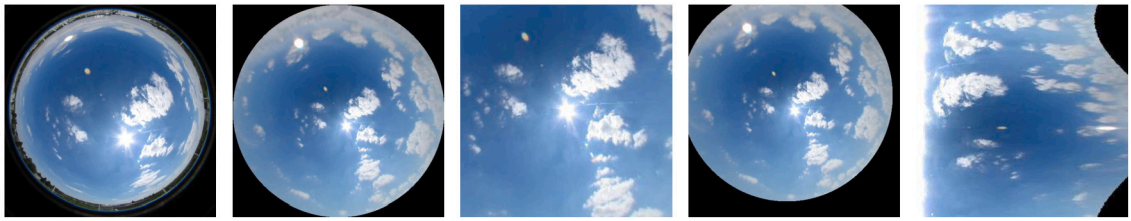

Fig. 25. Different scene representations of a cloud cover observation [136] (source: SIRTA [129]). From left to right: 1. raw (distorted) image of the sky taken with a fish-eye camera, 2. undistorted sky image, 3. close-up on the circumsolar area, 4. sky image centered on the sun's position, and 5. polar coordinates.

each hyperparameter, a range of possible values are defined. An exhaustive search (i.e., grid search) including every combination of these parameters is often impractical given the constraints on computational resources and time. Further, hyperparameters could be dataset dependent [368], i.e., the optimal hyperparameter settings obtained for a given dataset might not be optimal for another one; thus, grid search is not efficient for hyperparameter searching. In view of these issues, sampling methods (i.e., random search) are usually employed. Instead of a discrete set of values, a statistical distribution is defined for each hyperparameter from which the values can be randomly sampled. In most cases, hyperparameters are not equally important [368]. Random search has more exploratory power and can focus on finding the optimal values for the important hyperparameters, whereas grid search might waste time in exploring unimportant parameters [368]. In addition to random search, Bayesian optimization has recently emerged as a powerful tool for hyperparameter tuning. Unlike random search, which needs a lot of parallel but isolated experiments to find the optimal hyperparameter settings, Bayesian optimization is a machine learning algorithm that can be used to automatically search for the optimal hyperparameter settings based on multiple iterations [369]. The Gaussian process is often used to estimate the prior probability of model performance across the hyperparameter space [370]. The results from previous iterations can be used to determine the sampling method for the next iteration based on an acquisition function until it converges to an optimum [369].

For solar forecasting using deep learning models, few studies have shown systematic experiments on architecture tuning with different searching strategies. For categorical hyperparameters, a uniform probability distribution was used, whereas for continuous hyperparameters, the Latin hypercube sampling strategy was applied [371]. In [122] the authors used Bayesian optimization instead of grid search for cross-validating the hyperparameters.

4.2. Data-centric methods

In addition to model-centric approaches aiming to improve the model architecture or the training strategy, some works try to facilitate modeling by improving the data. These data-centric techniques cover a range of aspects, such as feature engineering and data augmentation.

4.2.1. Feature engineering and scene representation

Feature engineering aims to use domain knowledge to extract new features from raw data. For instance, a common preprocessing step in vision-based solar forecasting is to unwrap sky images taken by fish-eye lenses, which cause a strong distortion of the scene (see panels 1 and 2 in Fig. 25). This can be done by projecting clouds on a rectangular grid assuming, for example, median cloud height [178,372]. The resulting scene representation aims to retrieve the actual shape and relative size of the clouds distorted by the lens, hence resembling satellite observations. In deep learning studies, this method was applied to provide object trajectory consistency (sun and clouds) [97] or to facilitate the prediction of distant cloud displacements [131]. In contrast, the original distortion imposed by the lens was also shown to improve solar predictions by providing more detail on the center of the image where the sun and surrounding clouds are visible in high solar flux conditions (high solar zenith angle) [40]. Providing more details on the point of interest (the sun in sky images or a solar plant/meteorological station in satellite observations) can also simply be performed by magnifying the ROI. This was shown to improve shorter-term forecasts by enabling the model to focus on nearby clouds or by facilitating the estimation of the current irradiance level from a more detailed circumsolar area in sky images (third panel in Fig. 25) [136]. Similarly, centering the whole image on the point of interest (fourth panel in Fig. 25) provides information on its location even if it is hidden by a cloud. In sky images, for instance, the position of the sun is a crucial indicator of the level of clear-sky irradiance.

Computer vision-based solar irradiance forecasting is approximately invariant by rotation around the point of interest because future irradiance shifts are independent from the direction from which clouds hide the sun (in sky images) or a solar plant (in satellite observations). To leverage this property, the data can be augmented with rotations (see subsequent section on data augmentation) or with the use of polar coordinates [373], which turn the rotation invariance of the problem into a shift invariance (fifth panel in Fig. 25). The resulting shift invariance of the scene can be better exploited by convolutional architectures with pooling operations, which are translational invariant (Fig. 25): a given sun-cloud (or solar plant-cloud in satellite images) spatial configuration can be learned from a single image without having to augment the data [136]. In addition, the polar representation magnifies the ROI, leading to improved short-term irradiance predictions. This approach can be further augmented by centering the polar representation on the incoming flow of clouds, which can be determined by an optical flow algorithm [374].

4.2.2. Data augmentation

Data augmentation aims to artificially increase a dataset by generating modified versions of existing samples. Instead of collecting additional data, which can be expensive or impracticable, data augmentation tries to better exploit available data to improve a model's generalizability. In practice, synthetic data can be obtained from generative models, such as GANs, or by modifying existing samples with visual transformations, such as noise addition, cropping, rotations, or flipping.

Various data augmentation approaches have been applied to vision-based solar forecasting (see Fig. 26). For instance, noise injection was performed by adding Gaussian noise to pixel values [375]. A different color space transformation technique consists of randomly changing the intensity level of the three RGB channels independently (colorcasting) [375,376]. Alternatively, the pixel values of the image can be increased or decreased by a constant value across all three channels simultaneously (brightness adjustment) [375]. Applied to solar modeling from sky images, these approaches have been shown to benefit the nowcasting task of correlating an image with the corresponding solar value, whereas the impact on the forecasting task is not significant [375].

Another set of data augmentation techniques involves mixing images. The synthetic minority over-sampling technique [377] for regression [378] creates data by fusing an observation with a randomly selected neighbor from the same set (see Fig. 26). The corresponding

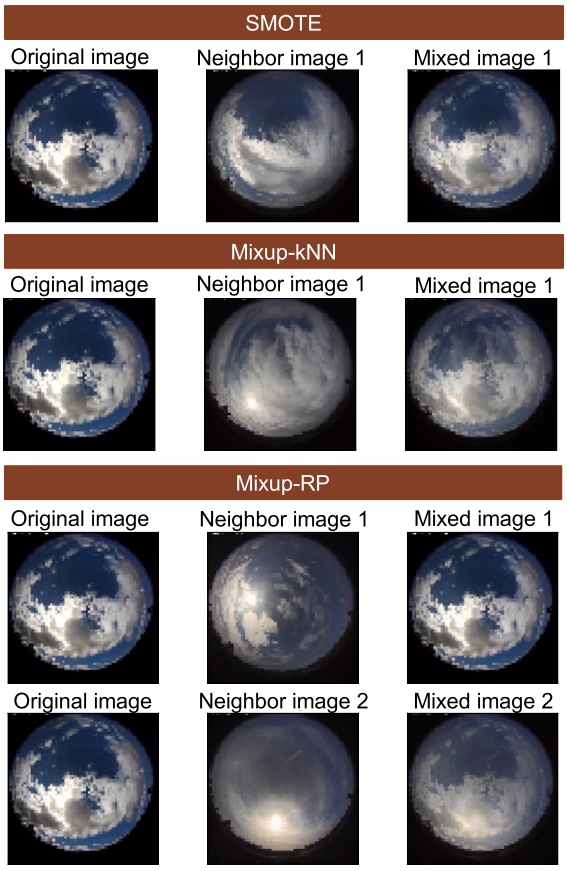

Fig. 26. Demonstration of different data augmentation techniques applied to sky images. Source: [375].

target variable is defined by the distance between the generated sample and each of the two seed samples [375]. Alternately, the *mixup* method [379] constructs virtual samples by taking a convex combination of example pairs and their labels [375]. Original images can be mixed with a random sample or with one of its k-nearest neighbors. Similar to the color space transformation methods presented in the previous paragraph, mixing images was shown to facilitate nowcasting predictions the most [375].

Image transformation — such as rotations, cropping, or vertical/horizontal flip — have also been used in recent works [136,380–384]. For instance, random cropping is a common strategy in satellite-based machine learning approaches that deal with very large Earth observations covering countries or continents [38]. In addition, rotations applied to sun-centered sky images or satellite images centered on a solar site leverage the rotational invariance of vision-based solar irradiance forecasting [136]. Note that this method might be less effective with photovoltaic power output forecasting because the spatial distribution, tilt, and orientation of the panels impede this rotational invariance. Further, a polar representation can be augmented with vertical translations that correspond to rotations of the original image. Finally, temporal flip consists of randomly flipping image sequences to predict the past instead of the future, hence producing more diverse temporal dynamics [136].

Although augmenting the data by applying various transformations provides some additional sample variability during training, its potential remains constrained by the diversity of cloud patterns in the dataset. A physics-based simulator of sky camera observations has been developed, but it has not been exploited in a data-driven approach [385]. Alternatively, Nie et al. [375] present cloud image samples generated by a Deep Convolutional GAN (DCGAN) (Fig. 27); however, the co-generation of the images and corresponding continuous prediction targets, i.e., photovoltaic power output or GSI, remains a key challenge of GAN-based data augmentation for solar forecasting.

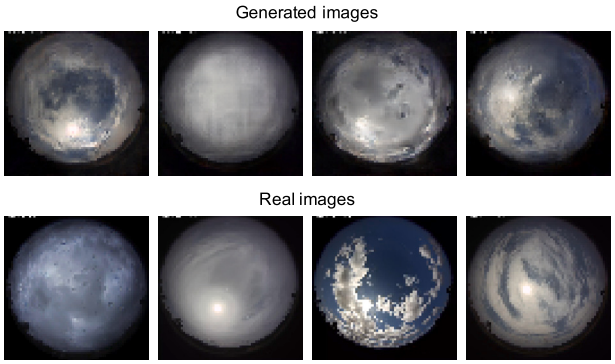

Fig. 27. Samples of cloudy images generated from DCGAN (the first row) using random Gaussian noise and real cloudy images used for training DCGAN (the second row). Note that the generated images are from random seed and do not correspond to the real images. Adapted from [375].

In this regard, cloud classification and segmentation are more suitable for the application of GAN-based data augmentation because the labels can be either inherited from the original data (e.g., in cloud category classification, the synthetic cloud images share the same labels as the data used for training the GAN), generated by humans or estimated by algorithms (e.g., in cloud segmentation, the synthetic images can be segmented with human knowledge or algorithms). For example, Jain et al. [386] demonstrate the effectiveness of using GANs to augment datasets for the cloud segmentation task with the corresponding binary segmentation maps estimated by an unsupervised clustering algorithm.

4.2.3. Sampling strategies

Like many real world datasets, satellite observations and sky image datasets are unbalanced in different ways. For instance, the distribution of cloud types strongly depends on the weather conditions at a given geographic location. This results in some cloud patterns being under- or overrepresented in the original dataset. If mini-batches are uniformly sampled from a training set representative of the dataset, the distribution learned by the model will be site-specific, which might impact its performance in different climate conditions. To address this limitation, Nie et al. [375] presents different sampling approaches to overrepresent the minority class (cloudy sky images), and hence best match the target distribution (test set). The experiments conducted in the article show that the proposed sampling strategy mainly benefited the nowcasting task. Similarly, Pothineni et al. [382] augmented the minority class with various data augmentation techniques.

4.2.4. Quality control

In addition to the size of a dataset, its quality can have a large impact on the performance of the model and its generalization properties. For instance, wrongly labeled samples or irradiance mismeasurements can be detrimental to the model training by inducing an erroneous supervision signal and to the model exploitation if it operates in unknown conditions. For these reasons, quality control is an essential aspect of machine learning projects. In vision-based solar power monitoring, the causes of anomalies include equipment failure (e.g., temperature response, shade ring misalignment, spectral selectivity) and operational disturbances (e.g., dust, snow, dew, water droplets, or bird droppings on the camera) [387]. Several methods, detailed here have been developed to accordingly detect these abnormalities.

Sky cameras are exposed to various external hazards impairing the collection of cloud cover observations: animals, soiling, snow, or rain. Inspecting outliers in a dataset is a common strategy to filter these anomalies. For example, by measuring the distance between samples in a feature space, one can define outliers as samples that significantly

Fig. 28. Examples of sky images marked as outliers by a CVAE [388].

differ from the average representation; however, comparing sky images in the large original RGB feature space is limited because of the curse of dimensionality. To overcome this difficulty, a filtering strategy based on a convolutional variational autoencoder (CVAE) model was proposed by [388]. An autoencoder was trained to reconstruct sky images from a low dimension feature space representation. Outliers derived from this low-dimensional representation are then manually checked to differentiate actual anomalies (e.g., birds or human beings) from visually uncommon sky images (e.g., rare or complex cloud patterns); however, this filtering method might not catch common anomalies, such as rain or dust in sandy regions (Fig. 28).

Quality control of ground-based measurements, such as GSI or photovoltaic power output, entails different signal analysis approaches. A common strategy involves the comparison of measurements with a reference to flag anomalies. For instance, extraterrestrial and simulated GSI levels under clear-sky or overcast conditions help detect abnormal solar flux values [389–393]. Successive measurements or measurements from neighboring stations can also be subject to statistical or spatial coherence tests [394]. In addition, the comparison of the relative duration of sunshine hours with daily global solar radiation provides indications on systemic and nonsystemic errors [395]. Another strategy consists of comparing satellite estimates with *in situ* measurements [396]. More recently, visual tools were developed to support the various quality control approaches [387,397].

4.3. Data fusion

Data fusion is an important area of research in machine learning that aims to integrate data from different sources to produce more consistent and accurate information. It is based on the expectation that multiple data sources are more informative than a single data source. For computer vision-based solar forecasting, several scenarios of data fusion have been explored.

4.3.1. Images and auxiliary data

Computer vision-based solar forecasting often involves heterogeneous input. Besides cloud cover observations, diverse sensor measurements (e.g., GSI, photovoltaic power output, wind speed, wind direction, sun angles) provide crucial local information on the atmospheric and operating conditions of a solar site. In particular, the thermal environment (i.e., air temperature, wind speed, humidity, and air pressure) plays a key role in the overall efficiency of solar panels [398]. In addition to the different scales of data, another challenge is how to make the deep learning system pay due attention to each type of data. The problem arises because imagery data are often high dimensional, i.e., an array with hundreds of thousands of entries, whereas sensor measurements might only be a vector of tens of entries. It is likely that the deep learning model pays more attention to the high-dimensional imagery information than the low-dimensional sensor measurements. This is an active field of research in applications such as self-driving [399] and robotics [400], but very limited studies have investigated this problem in solar forecasting. In 2019, Venugopal et al. [401] first systematically investigated 28 methods of fusion (MOF), which belongs to 4 families: mix-in; activation map combination; activation map stacking; and two-step, for integrating the hybrid input of a sky image sequence and photovoltaic power output history to forecast 15-minute-ahead photovoltaic power output by using CNN as the backbone. The results show that a two-step autoregressive CNN MOF has the best performance, closely followed by a mix-in MOF that performs feature expansion and reduction to give appropriate importance to the two types of inputs. Similarly, Ajith and Martínez-Ramón [103] developed a multimodal fusion network based on CNN and LSTM for studying GSI forecasts by using infrared images and past GSI data with forecasting horizons ranging from 15 to 150 s. The extracted spatial and temporal features are fused using a fully connected neural network. The proposed model shows up to 46% improvement compared with benchmark machine learning and deep learning models using solely irradiance data. Another approach investigated by [402,40] consists of augmenting images by stacking additional channels containing concomitant auxiliary information, such as the sun distance or the irradiance level. More recently, Terrén-Serrano and Martínez-Ramón [122] explored fusing information from infrared sky images with various other sensors — including a pyranometer, a solar tracker, and a weather station — using a multitask deep learning architecture based on RNNs. The accuracy of an 8-minute-ahead forecast is improved by nearly 20% in terms of forecasting skill.

4.3.2. Camera network

Networks of ground sky cameras are starting to be deployed to offer high-spatiotemporal observations of the cloud cover [403]. A preliminary study was conducted to evaluate the benefit of integrating observations from three cameras collocated at the Abengoa Solar Platform of Solúcar near Seville [402]. Results show that combining the three sources of information with a shared encoder leads to a performance gain.

4.3.3. Satellite and sky images

Often used separately, satellite observations and sky images offer two complementary points of view on the cloud cover. For this reason, some approaches try to combine both sources of images into a single modeling framework [404] or try to evaluate in which weather conditions one prevails over the other [405,406]. In deep learning, both sources of data can be independently processed by parallel spatial encoders prior to being recombined into a single state representation for solar forecasting [13]. Although the method shows valuable improvement over single-vision approaches (sky images only or satellite observations only), some challenges remain, such as the integration in the modeling of observations with different temporal resolutions.

4.4. Transfer learning — domain adaptation

Transfer learning is a commonly used strategy in machine learning to help improve performance or more quickly solve new problems on target domains by transferring the knowledge learned from different (but related) source domains [407]. For vision-based solar forecasting, a solar site could benefit from knowledge carried by models trained on images collected in other locations to improve the accuracy of its site-specific algorithm. Indeed, some common features learned from other sites, such as the sun position or the cloud distribution, can be shared across different locations. This could be especially beneficial for new solar facilities that have limited data collection at the beginning. A recent study by [408] suggests that transferring learning from a large and diverse source dataset to a local target dataset can save up to 80% of the training data while achieving comparable performance for 15-minute-ahead solar forecasting. With more and more sky image datasets being open source in recent years, pretraining a general solar

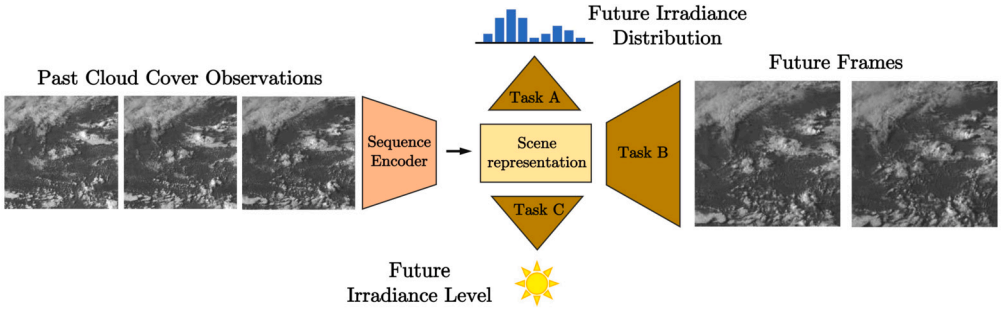

Fig. 29. Neural network architecture for MTL.

forecasting model based on a large-scale centralized dataset with massive and diverse sky image samples is facilitated. Similar to pretraining strategies based on ImageNet, transferring the knowledge from such a model to local sites can potentially save data and jump-start local model development; however, the various types of heterogeneity observed in data collected from different locations remain challenging for transfer learning approaches: different prediction variables (i.e., photovoltaic power output versus GSI), different measurement distributions given local weather conditions, and different camera types (i.e., TSI versus ASI) and orientations. Processing and reconciliation of these datasets is thus a critical step for building a large-scale dataset for knowledge transfer.

4.5. Multitask learning

A Multitask learning (MTL) model aims to address multiple related tasks at once (Fig. 29). Intra-task information can be used to increase the performance of a model and ameliorate prediction consistency such as inter-task consistency (e.g., cloud masking and cloud index mapping, deterministic and probabilistic solar forecasting) and inter-horizon consistency (e.g., short- and long-term horizons). This is generally done using a single model to learn multiple tasks instead of using multiple models to learn each task individually [409]. In deep learning, the multiple tasks do not need to be directly combined using a single model (i.e., architecture). A model can share representations (i.e., hidden space) between its different structures to improve the overall performance with respect to task-specific models.

When MTL is applied to forecast time series, the output space is that of a classic statistical functional model, but in deep learning models, exogenous variables are added to the input space. In addition, performance is improved by including information about past cloud cover from ground-based sky imagers (i.e., tensor signals) in the input space [40,221] or satellite images [13]. From the perspective of the input and output spaces, MTL can be divided into two categories: multi-input multi-output (MIMO) or single-input multi-output (SIMO) [410]. Depending on the inter-task correlation level, the tasks can be considered independent (i.e., uncorrelated), with directional correlation (e.g., time domain), or fully correlated. A MIMO model is a multitask model made of multiple models. Each model can potentially have a different input feature vector (or tensor). If tasks are independent, a multitask model can be assembled from several output-specific models. In that case, the feature vector can also be different (i.e., independent multitask model). These types of MTL models are common in solar forecasting applications [36,103,253].

A SIMO model corresponds to single models (i.e., architecture) that generate multiple outputs from a feature vector or tensor. When the output variables have a time structure, using the sequential correlation between outputs is beneficial. A chain of models is commonly used in deep learning models for language processing. These are known as recursive architectures [411]. In solar forecasting applications, they are proven to improve performance with respect to MIMO models [122]. Chains of deep learning models can form SIMOs, sharing representations from sequential forecasts and exploiting the directional structure in GSI with an *attention mechanism* [223]. In addition, deep learning-based SIMOs can have encoded representations between decoding structures in a sequential (i.e., directional) manner to forecast CSI and future spatial sky conditions (i.e., cloud cover maps) from consecutive past satellite [13] or ground-based images [40].

A common method to develop SIMO models in deep learning is to define the last dense layer as having multiple outputs. This approach was proposed in solar forecasting applications, using cloud features extracted from multiple images [122] or using batches of multiple sky images [70] to forecast a batch of sky images. In solar forecasting applications, it is possible to implement a SIMO deep learning model to forecast tasks in different output spaces, such as a future sky image and a GSI measurement [412]. This forecasting problem can be solved by using the same architecture with attention mechanisms [222] or by dividing it into multiples ones [221]. The resulting output space is the same, but the forecasting application is different [413]. A SIMO model trained using a single probabilistic loss independently weighting the terms that form each model [414] can be considered as an additional class of MTL models.

4.6. Interpretable deep learning

Often described as *black boxes*, deep learning models suffer from a lack of transparency that hinders their applicability to many sensitive domains, such as transport, healthcare, or justice. Interpretable AI (or explainable AI (XAI)), aims to make such models more intelligible to humans [415]. This research domain helps to justify, control, discover, or improve the behavior of a data-driven method [416]. In practice, model-agnostic interpretability approaches fall into four categories: visualization (visualization of the mapping learned by the model), knowledge extraction (extraction of the knowledge acquired during training and encoded as an internal representation), influence methods (evaluation of the influence of an input change on the model prediction), and example-based explanation (selection of specific instances of the dataset to interpret the prediction of the model) [416]. In addition, note that in some cases, improving the explainability of a deep learning model impacts its performance [415].

In solar energy, the International Energy Agency Task 16 alerts on the lack of interpretability of neural network: “Yet the lack of transparency that usually accompanies artificial intelligence models (i.e., retracing the path that the model took to reach its conclusion) has drawbacks: the difficulty of translating the information generated into basic principles (or physics) and interpreting the information to determine what is happening in the natural world and apply the knowledge gained at a particular project site to other regions. Consequently, an appropriate strategy could benefit from the optimized combination of both physical and artificial intelligence-based models.” [417]. Moreover, increasing the transparency of deep learning solar modeling would have various benefits. By developing trust in AI systems, XAI would increase their acceptance by policy makers or grid operators. In addition, operational actions would be better supported by model insights. Developers

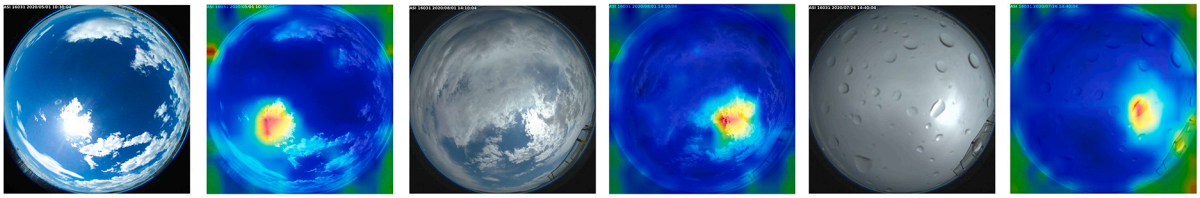

Fig. 30. Visualization of sky images and their corresponding attention maps by a transformer-based nowcasting network on the TSI880 dataset (top) and ASI16 dataset (bottom) from the National Renewable Energy Laboratory (NREL). Taken from [418].

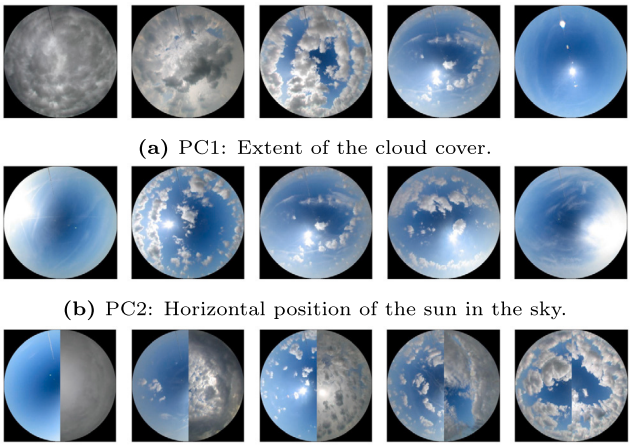

(a) PC1: Extent of the cloud cover.

(b) PC2: Horizontal position of the sun in the sky.

(c) PC3: Spatial variability of the cloud cover: from fully cloudy or fully sunny to partly cloudy. Each image illustrates two neighboring samples from the distribution.

(d) PC4: Vertical position of the sun in the sky. Each image illustrates two neighboring samples from the distribution.

Fig. 31. Four principal components (PCs) of the spatiotemporal representation of past sky images encoded by a video and irradiance prediction deep learning model. Taken from [40].

would gain understanding on the capabilities but also limitations of the AI system, which might trigger further improvements.

Several works in solar energy have presented experiments that aim to improve our understanding of neural network for computer vision. For example, observing feature maps corresponding to particular instances of the dataset provides insights into the types of features extracted by convolutional layers [252,364,380]. In practice, some filters seem to focus on specific elements in the image, such as clouds, the sun, the sky, or the solar tracker [120,380,419]. In addition, the specific visual pattern recognized by a filter can be generated by tuning the input image to maximize the average response of that filter [252]. Another approach aims to generate *hyper columns* (the vector of activations of all CNN units above an input pixel) [420] to derive a heat map that indicates the focus of CNNs in sky images [413]. For transformer-based models, attention maps clearly show the focus on the circumsolar area (see Fig. 30). A principal component analysis of the learned spatiotemporal representation of the past sequence of sky images highlighted the most significant features used by a deep learning model: the extent of the cloud cover, the horizontal and vertical position of the sun, the spatial variability of the cloud cover (from fully cloudy or fully clear-sky to partly cloudy) [40] (Fig. 31). This method achieved similar results when applied to the polar representation of sky images [136].

In addition to these purely explainable AI approaches, some training objectives provide additional interpretability and transparency for deep learning modeling. For instance, providing the uncertainty associated with a forecast informs on the confidence of the model in its prediction [38,40]. Similarly, predicting sky or satellite observations as well as insolation levels provides visual feedback on the future cloud cover expected by the model. From that perspective, the blurrier the predicted cloud cover, the higher the associated uncertainty.

4.7. Probabilistic forecasting

In a recent review of the field of AI applied to solar power forecasting, the investigation of probabilistic methods was seen as a critical research direction [421]. Advancing the quantification of prediction uncertainties would benefit power systems [422] while increasing the interpretability of deep learning modeling (see Section 4.6). In mathematical terms, a probabilistic model aims to predict the probability distribution, $P(Y|X)$, of a predicted value, Y (e.g., future photovoltaic power output or GSI value, cloud type) conditioned by some observations X, (e.g., past sky or satellite images, historical measurements).

In solar forecasting, the variability observed at a short-term timescale mainly comes from the formation, dissipation, and displacement of clouds; thus, vision-based solar forecasting could play a major role in improving the quantification of this type of uncertainty (Fig. 32). A common strategy in deep learning consists of predicting a histogram instead of a single value (Fig. 29). This probabilistic framework can be applied to local or regional solar forecasting [38,13,40].

Likewise, probabilistic modeling is commonly used in other computer vision tasks involving classification, including segmentation [423–425] or cloud type classification [426,427]. The output of the model is passed through a Softmax activation function (or eventually a Sigmoid activation function for binary classification) to retrieve the probability of each category. Alternatively, the quantile loss function associated with a quantile q, which is

$$\mathrm{QL}(\hat{y}, y) = \max\left[q(\hat{y} - y), (q-1)(\hat{y} - y)\right], \tag{1}$$

where $\hat{y}$ the model prediction and y the ground truth, has been applied to probabilistic radiative transfer modeling [428] and solar power forecasting [429].

5. Discussion

This review study highlights the considerable advances observed in recent years in the field of vision based-solar energy modeling. Despite this rapid progress, many technical limitations and implementation challenges have still to be overcome to fully benefit from the development of deep learning. The following subsections describe some of the research areas that require further investigation, and discuss potential solutions to facilitate the operational adoption of these rapidly advancing techniques.

5.1. Road map for future research

The demand for cloud cover-informed solar predictions has motivated an increased interest toward computer vision-based solar forecasting approaches. In this context, the increasing availability of open-source sky and satellite image datasets has paved the way to the application of data-driven methods to address this challenging task. In particu-

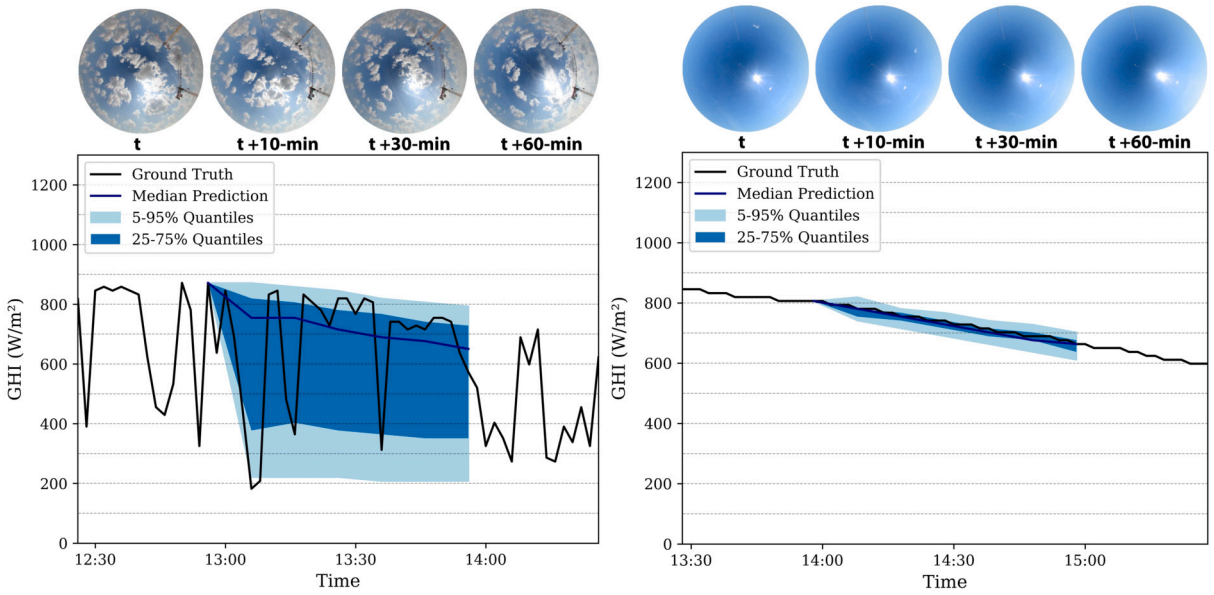

Fig. 32. Probabilistic predictions based on past sky and satellite images in diverse weather conditions. The uncertainty predicted by the model adapts to the situation: high uncertainty in partly cloudy conditions, and low uncertainty in clear-sky days. Taken from [13].

lar, neural network is capable of (i) modeling large-scale spatiotemporal solar data, (ii) handling multimodal data, and (iii) providing accurate predictions with significantly less computing time. In addition, this rapidly evolving field benefits from the maturity of some computer vision research areas (e.g., image classification or image segmentation) while remaining open to new advances (e.g., physics-informed neural network or video prediction). Despite promising results, some theoretical and practical challenges listed here remain or could be further investigated to facilitate the applications of solar forecasting in power system management and operations.

5.1.1. Forecast verification

Forecast verification is crucial to evaluating and comparing the performance of solar forecasting models. There exists a wide range of methods and metrics (see Section 3.5) to expend beyond the limited evaluation scheme of assessing a model's performance based on a metric corresponding to the training loss (e.g., RMSE and L_2 loss). In particular, few works have tried to propose or apply more advanced loss functions adapted to particular objectives (e.g., decreasing temporal distortion, prediction of sharp solar power changes). Further, contributions on the topic of value-oriented solar forecasting verification and training would strongly benefit many downstream applications.

5.1.2. Benchmark datasets

Existing solar forecasting models are mostly developed and evaluated based on different datasets, making it hard to consistently compare the performance of these models. Although there are studies benchmarking certain types of solar forecasting models based on a single dataset [39], there are currently very limited studies cross-comparing different types of solar forecasting models, i.e., deep learning-based models (e.g., CNN, LSTM, ConvLSTM, etc.), machine learning-based models (e.g., extreme grading boosting, random forest, SVR), time-series models (e.g., autoregressive, ARIMA), and physics deterministic models (e.g., cloud motion vector, advection) on standardized datasets. Another challenge is to reproduce the models published in existing studies. Erroneous implementation of the existing models can lead to false comparisons. With more and more open-source datasets and models available in recent years (see descriptions in Sections 2.5 and 3.4), we highly encourage the researchers to report their model performance by comparing with open-source models (e.g., SUNSET [119], PhyDNet [221]) and standardized datasets (e.g., *UCSD* [202], *SKIPP'D* [204], *SIRTA* [201], *Girasol* [430]), and we further call on the efforts to build a large-scale sky image datast by assembling suitable open-source datasets for solar forecasting to benchmark different types of models and to accelerate solar forecasting methods development.

5.1.3. Probabilistic forecasts

Probabilistic modeling can provide valuable feedback on the uncertainties associated with solar power forecasting, including the stochastic nature of the cloud cover dynamics, the lack of information on distant clouds, such as their location and spatial configuration. To date, few studies have investigated the potential of the probabilistic framework to ameliorate the prediction of deep learning models for solar forecasting [13,431]. An application of a probabilistic forecast is stochastic electric grid planning, which requires generating random realizations of future renewable energy generation outcomes [432]. This is especially important to consider the risk introduced by certain generators in the realization of a potential extreme weather scenario. This application requires a fully probabilistic instead of a probabilistic approach. A fully probabilistic approach allows for drawing random samples from a predictive probability density [122].

5.1.4. Explainable artificial intelligence

A major downside of current deep learning methods is the lack of interpretability of their predictions [417]. Although probabilistic deep learning approaches can provide some insights on the predictions of a network, a stronger focus on more diverse explainable AI techniques will foster the acceptation for deep learning-based solar power forecasts. Moreover, a deeper understanding of solar modeling with neural networks is likely going to clarify some limitations and trigger new technical development.

5.1.5. Site adaptation

The limited generalization skills of current deep learning models are a strong limitation to their widespread implementation. Recent work on sky images has shown that domain adaptation strategies could significantly facilitate the transfer of knowledge from large datasets to new solar sites [408]. The main challenge to address in that context is how to provide valuable solar forecast, with no or limited local data. This difficult problem could be tackled by building more robust and general foundation models based on the large number of diverse open-source

datasets that are capable of being adapted to a wide range of downstream tasks [34].

5.1.6. Edge computing and privacy-preserving algorithms

Coupling solar forecasting with edge computing and distributed sensing to facilitate the fusion of global and local information is another critical research direction. Further, designing data-sharing mechanisms and privacy-preserving deep learning algorithms that protect privacy while improving power and energy system efficiency is a valuable emerging topic in solar forecasting.

5.1.7. Synthetic data generation

Generating synthetic data to guide a deep learning model training is an appealing strategy to address edge cases, improve generalization properties, pretrain deep learning models, and adapt a training to specific environments or weather conditions. A solution to that problem would be to develop realistic simulations of the cloud cover dynamics and its physical properties, as in [385]. Alternatively, GANs or VAEs are powerful tools to produce new observations from an approximated data distribution [375]. These models could help generating realistic sequences of cloud cover observations as well as corresponding solar values.

5.1.8. Physics informed deep learning

Introducing prior knowledge (e.g., physics laws) into deep learning models can potentially increase their performance while improving their interpretability by (re)discovering realistic physical equations from observations. For instance, PhyDNet [221] constrains a neural network to learn partial differential equations that best describe the cloud cover dynamics to predict future cloud displacements. Streamlines are the paths that floating clouds trace in the atmosphere. Machine learning methods based on computer vision are capable of visualizing streamlines in satellite images [433] and ground-based sky images [134] but in a suboptimal manner. In this context, a physics informed deep learning method has the potential to optimally visualize fluid mechanics field lines.

5.1.9. Morphology-informed solar power modeling

Integrating the solar panel spatial configuration and local shadowing effects caused by vegetation, buildings or terrain variation, has the potential to ameliorate the accuracy of solar forecasts. This information could be inferred from irradiance measurements [387], object detection from sky images [434] or high resolution remote sensing observations [435,279], LiDAR data [436], and other *in situ* 3D mapping measurements [437]. Although local shadowing and morphological effects could be learnt by the model providing enough cloud cover observations and corresponding solar data, approaches based on transfer learning and multilocation dataset fusion might benefit from the development of morphology-informed methods.

5.2. Industry adoption and implementation

In addition to improving the technique, advancing its operational implementation is vital to reduce the uncertainties associated with weather variability and to contribute toward an effective integration of clean energy into energy systems. Some companies in the industry and private sector have adopted satellite imagery and ground-based sky imagers solar forecasting. For example, Steadysun and Reuniwatt provide intra-day and day-ahead solar forecasts combining machine learning with sky images and geostationary satellite imagery. Similarly, Solcast (recently acquired by DNV in January 2023) uses sky images, weather satellite imagery, machine learning, and computer vision for day-ahead solar forecasting models. Open Climate Fix, a UK-based startup, relies on satellite imagery, NWP, vertical cloud profiles, geographic information, and machine learning to predict several hours-head photovoltaic power output for UK's National Grid. SolarAnywhere fuses data from multiple sources, including satellite imagery, using deep learning in their forecasting models.

However, industry adoption of solar forecasting techniques and tools remains slow compared to the pace of development and innovation introduced by research teams. This can be explained by several factors:

1. Lack of resources to assimilate the innovations and deploy them in the operational tools.
2. Lack of computing capacity to implement the methods, monitor the forecasts, and evaluate the added-value.
3. Difficulty to integrate new and potentially complex tools in existing operational processing chains, including to build the links with the necessary input data (e.g., satellite image fluxes in real time).
4. Inadequacy and lack of adaptability of operational tools to integrate forecasting models. For instance, some forecasting tools are still based on old models, including at least, in part, the use of spreadsheets and macros, which are not ready to interface with Python-based models (or other advanced programming languages).
5. Lack of skills in the workforce to handle and assimilate AI/deep learning methodologies.

The main limitation to the wide adoption of innovative computer vision-based solar forecasting using deep learning can be summarized as a lack of coordination between providers and end users at the utility level (i.e., grid operators). This is a significant barrier that can, however, be overcome by putting effort into understanding the needs and processes of the user (i.e., grid operators) on the one side and developing the products with the users on the other side. Further, grid operators might need to upgrade their skills via dedicated training to gain the required knowledge to understand and use recent computer vision-based forecasting models.

In summary, there is a strong need for developers to interact with grid operators at the concept stage of the development of new products. From that context, some insight might come from a weather and climate service ecosystem, which, if developed, could provide an efficient provider/user interaction processes based on stakeholder engagement and co-production principles (co-design, co-development, co-evaluation, etc.) [438].

6. Conclusion

Solar energy meteorology using computer vision is essential to address the variability of solar generation caused by changing cloud cover, and thus facilitate its integration into the electric grid. In this context, machine learning offers a valuable modeling framework capable of analyzing and combining large amounts of complex data originating from Earth observations (i.e., remote-sensing), ground-based sky imagers, and *in situ* measurement devices. An extensive review of the resulting computer vision tasks and associated deep learning approaches for solar forecasting is presented in this article. Additionally, accessible resources, validation methods, and promising research topics — such as probabilistic modeling, video prediction, transfer learning, and explainable artificial intelligence — are thoroughly described. Despite several ongoing challenges, including improving the generalization skill of the models and facilitating the adoption of the techniques by the industry, this detailed analysis shows that machine learning has the capacity to improve the modeling of solar energy generation.

CRediT authorship contribution statement

Quentin Paletta: Conceptualization, Funding acquisition, Investigation, Project administration, Supervision, Visualization, Writing – original draft, Writing – review & editing. **Guillermo Terrén-Serrano:** Funding acquisition, Investigation, Project administration, Visualization, Writing – original draft, Writing – review & editing. **Yuhao**

Nie: Funding acquisition, Investigation, Visualization, Writing – original draft, Writing – review & editing. **Binghui Li:** Funding acquisition, Investigation, Writing – original draft. **Jacob Bieker:** Funding acquisition, Investigation, Writing – original draft, Writing – review & editing. **Wenqi Zhang:** Funding acquisition, Investigation, Writing – review & editing. **Laurent Dubus:** Funding acquisition, Investigation, Writing – original draft. **Soumyabrata Dev:** Funding acquisition, Investigation, Writing – original draft. **Cong Feng:** Conceptualization, Funding acquisition, Investigation, Project administration, Supervision, Visualization, Writing – original draft, Writing – review & editing.

Declaration of competing interest

The authors declare that they have no known competing financial interests or personal relationships that could have appeared to influence the work reported in this paper.

Data availability

Data will be made available on request.

Acknowledgements

This work was authored in part by the National Renewable Energy Laboratory, operated by Alliance for Sustainable Energy, LLC, for the U.S. Department of Energy (DOE) under Contract No. DE-AC36-08GO28308. Funding provided by the Lab-Directed R&D Director's Postdoctoral Fellowships program. The views expressed in the article do not necessarily represent the views of the DOE or the U.S. Government. The U.S. Government retains and the publisher, by accepting the article for publication, acknowledges that the U.S. Government retains a nonexclusive, paid-up, irrevocable, worldwide license to publish or reproduce the published form of this work, or allow others to do so, for U.S. Government purposes. B.L acknowledges support from Idaho National Laboratory (INL). G.T.S. acknowledges support from the Research Seed Grant Program 2022-2023 from the Institute for Energy Efficiency of the University of California, Santa Barbara (UCSB), the ARPA-E PERFORM program under grant DE-AR0001289, and the Environmental Studies program of the UCSB. J.B. acknowledges support from Open Climate Fix. L.D. acknowledges support from Réseau de Transport d'Électricité and the World Energy & Meteorology Council. Q.P. acknowledges support from the ϕ-Lab at the European Space Research Institute (ESRIN) and the Climate Office at the European Centre for Space Applications and Telecommunications (ECSAT) of the European Space Agency (ESA), ENGIE Lab CRIGEN, EPSRC (EP/R513180/1), and the University of Cambridge. S.D. acknowledges support from Science Foundation Ireland under Grant Agreement No. 13/RC/2106_P2 at the ADAPT SFI Research Centre at University College Dublin. Y.N. acknowledges support from Dubai Electricity and Water Authority (DEWA) through their membership in the Stanford Energy Corporate Affiliates (SECA) program.

References

[1] World Meteorological Organization (WMO). 2022 State of Climate Services: energy (WMO-no. 1301). Geneva: WMO. ISBN 978-92-63-11301-6, 2022.
[2] Sweeney Conor, Bessa Ricardo J, Browell Jethro, Pinson Pierre. The future of forecasting for renewable energy. Wiley Interdiscip Rev Energy Environ 2020;9(2):e365. https://doi.org/10.1002/wene.365.
[3] Mathiesen Patrick, Kleissl Jan. Evaluation of numerical weather prediction for intra-day solar forecasting in the continental United States. Sol Energy 2011;85(5):967–77. https://doi.org/10.1016/j.solener.2011.02.013.
[4] Voyant Cyril, Notton Gilles, Kalogirou Soteris, Nivet Marie-Laure, Paoli Christophe, Motte Fabrice, et al. Machine learning methods for solar radiation forecasting: a review. Renew Energy 2017;105:569–82. https://doi.org/10.1016/j.renene.2016.12.095.
[5] Mayer Martin János. Benefits of physical and machine learning hybridization for photovoltaic power forecasting. Renew Sustain Energy Rev 2022;168:112772. https://doi.org/10.1016/j.rser.2022.112772.
[6] Chen Qi, Li Xinyuan, Zhang Zhengjia, Zhou Chao, Guo Zhiling, Liu Zhengguang, et al. Remote sensing of photovoltaic scenarios: techniques, applications and future directions. Appl Energy March 2023;333:120579. https://doi.org/10.1016/j.apenergy.2022.120579.
[7] Saunders Roger. The use of satellite data in numerical weather prediction. Weather 2021;76(3):95–7. https://doi.org/10.1002/wea.391.
[8] Inman Rich H, Pedro Hugo TC, Coimbra Carlos FM. Solar forecasting methods for renewable energy integration. Prog Energy Combust Sci 2013;39(6):535–76. https://doi.org/10.1016/j.pecs.2013.06.002.
[9] Chu Yinghao, Li Mengying, Coimbra Carlos FM, Feng Daquan, Wang Huaizhi. Intra-hour irradiance forecasting techniques for solar power integration: a review. iScience 2021;24(10):103136. https://doi.org/10.1016/j.isci.2021.103136.
[10] Yang Dazhi, Wang Wenting, Gueymard Christian A, Hong Tao, Kleissl Jan, Huang Jing, et al. A review of solar forecasting, its dependence on atmospheric sciences and implications for grid integration: towards carbon neutrality. Renew Sustain Energy Rev June 2022;161:112348. https://doi.org/10.1016/j.rser.2022.112348.
[11] Kurzrock Frederik, Cros Sylvain, Ming Fabrice Chane, Otkin Jason A, Hutt Axel, Linguet Laurent, et al. A review of the use of geostationary satellite observations in regional-scale models for short-term cloud forecasting. Meteorol Z November 2018:277–98. https://doi.org/10.1127/metz/2018/0904.
[12] Lin Fan, Zhang Yao, Wang Jianxue. Recent advances in intra-hour solar forecasting: a review of ground-based sky image methods. Int J Forecast January 2023;39(1):244–65. https://doi.org/10.1016/j.ijforecast.2021.11.002.
[13] Paletta Quentin, Arbod Guillaume, Lasenby Joan. Omnivision forecasting: combining satellite and sky images for improved deterministic and probabilistic intra-hour solar energy predictions. Appl Energy April 2023;336:120818. https://doi.org/10.1016/j.apenergy.2023.120818.
[14] Antonanzas J, Osorio N, Escobar R, Urraca R, Martinez-de-Pison FJ, Antonanzas-Torres F. Review of photovoltaic power forecasting. Sol Energy October 2016;136:78–111. https://doi.org/10.1016/j.solener.2016.06.069.
[15] Blum Niklas Benedikt, Nouri Bijan, Wilbert Stefan, Schmidt Thomas, Lünsdorf Ontje, Stührenberg Jonas, et al. Cloud height measurement by a network of all-sky imagers. Atmos Meas Tech July 2021;14(7):5199–224. https://doi.org/10.5194/amt-14-5199-2021.
[16] Nouri Bijan, Blum Niklas, Wilbert Stefan, Zarzalejo Luis F. A hybrid solar irradiance nowcasting approach: combining all sky imager systems and persistence irradiance models for increased accuracy. Solar RRL 2021;6(5):2100442. https://doi.org/10.1002/solr.202100442.
[17] Sawant Manisha, Shende Mayur Kishor, Feijóo-Lorenzo Andrés E, Bokde Neeraj Dhanraj. The state-of-the-art progress in cloud detection, identification, and tracking approaches: a systematic review. Energies January 2021;14(23):8119. https://doi.org/10.3390/en14238119.
[18] Li Qingyong, Lu Weitao, Yang Jun. A hybrid thresholding algorithm for cloud detection on ground-based color images. J Atmos Ocean Technol October 2011;28(10):1286–96. https://doi.org/10.1175/JTECH-D-11-00009.1. ISSN 1520-0426.
[19] Escrig H, Batlles FJ, Alonso J, Baena FM, Bosch JL, Salbidegoitia IB, et al. Cloud detection, classification and motion estimation using geostationary satellite imagery for cloud cover forecast. Energy June 2013;55:853–9. https://doi.org/10.1016/j.energy.2013.01.054.
[20] Mueller Richard, Trentmann Jörg, Träger-Chatterjee Christine, Posselt Rebekka, Stöckli Reto. The role of the effective cloud albedo for climate monitoring and analysis. Remote Sens November 2011;3(11):2305–20. https://doi.org/10.3390/rs3112305.
[21] Nouri B, Wilbert S, Segura L, Kuhn P, Hanrieder N, Kazantzidis A, et al. Determination of cloud transmittance for all sky imager based solar nowcasting. Sol Energy March 2019;181:251–63. https://doi.org/10.1016/j.solener.2019.02.004.
[22] Oberländer D, Prahl C, Wilbert S, Müller S, Stanicki B, Hanrieder N. Cloud shadow maps from whole sky imagers and voxel carving. In: International conference energy and meteorology; 2015. p. 10.
[23] Blanc Philippe, Massip Pierre, Kazantzidis Andreas, Tzoumanikas Panagiotis, Kuhn Pascal, Wilbert Stefan, et al. Short-term forecasting of high resolution local DNI maps with multiple fish-eye cameras in stereoscopic mode. AIP Conf Proc June 2017;1850(1):140004. https://doi.org/10.1063/1.4984512.
[24] Huang Hao, Yoo Shinjae, Yu Dantong, Huang Dong, Qin Hong. Cloud motion detection for short term solar power prediction. In: Proceedings - international conference on machine learning; 2011. p. 4.
[25] Cros S, Sébastien N, Liandrat O, Schmutz N. Cloud pattern prediction from geostationary meteorological satellite images for solar energy forecasting. In: Comerón Adolfo, Kassianov Evgueni I, Schäfer Klaus, Picard Richard H, Stein Karin, Gonglewski John D, editors. SPIE remote sensing; October 2014. p. 924202.
[26] Chow Chi Wai, Belongie Serge, Kleissl Jan. Cloud motion and stability estimation for intra-hour solar forecasting. Sol Energy May 2015;115:645–55. https://doi.org/10.1016/j.solener.2015.03.030.
[27] Wood-Bradley P, Zapata J, Pye J. Cloud tracking with optical flow for short-term solar forecasting. 2012.
[28] Urbich Isabel, Bendix Jörg, Müller Richard. The seamless solar radiation (SESORA) forecast for solar surface irradiance—method and validation. Remote Sens January 2019;11(21):2576. https://doi.org/10.3390/rs11212576.

[29] Peng Zhenzhou, Yu Dantong, Huang Dong, Heiser John, Yoo Shinjae, Kalb Paul. 3D cloud detection and tracking system for solar forecast using multiple sky imagers. Sol Energy August 2015;118:496–519. https://doi.org/10.1016/j.solener.2015.05.037. ISSN 0038092X.

[30] Cros S, Sébastien N, Liandrat O, Schmutz N. Cloud pattern prediction from geostationary meteorological satellite images for solar energy forecasting. In: Remote sensing of clouds and the atmosphere XIX; and optics in atmospheric propagation and adaptive systems XVII, vol. 9242. SPIE; October 2014. p. 924202.

[31] Carrière Thomas, Amaro e Silva Rodrigo, Zhuang Fuqiang, Saint-Drenan Yves-Marie, Blanc Philippe. A new approach for satellite-based probabilistic solar forecasting with cloud motion vectors. Energies January 2021;14(16):4951. https://doi.org/10.3390/en14164951.

[32] Peng Zhenzhou, Yu Dantong, Huang Dong, Heiser John, Yoo Shinjae, Kalb Paul. 3D cloud detection and tracking system for solar forecast using multiple sky imagers. Sol Energy August 2015;118:496–519. https://doi.org/10.1016/j.solener.2015.05.037.

[33] Cros Sylvain, Badosa Jordi, Szantaï André, Haeffelin Martial. Reliability predictors for solar irradiance satellite-based forecast. Energies January 2020;13(21):5566. https://doi.org/10.3390/en13215566.

[34] Nie Yuhao, Li Xiatong, Paletta Quentin, Aragon Max, Scott Andea, Adam. Brandt.Open-source ground-based sky image datasets for very short-term solar forecasting, cloud analysis and modeling: a comprehensive survey. https://doi.org/10.48550/arXiv.2211.14709, November 2022.

[35] Zhang Jinsong, Verschae Rodrigo, Nobuhara Shohei, Lalonde Jean-François. Deep photovoltaic nowcasting. Sol Energy December 2018;176:267–76. https://doi.org/10.1016/j.solener.2018.10.024.

[36] Sun Yuchi, Szűcs Gergely, Brandt Adam R. Solar PV output prediction from video streams using convolutional neural networks. Energy Environ Sci July 2018;11(7):1811–8. https://doi.org/10.1039/C7EE03420B.

[37] Pérez Emilio, Pérez Javier, Segarra-Tamarit Jorge, Beltran Hector. A deep learning model for intra-day forecasting of solar irradiance using satellite-based estimations in the vicinity of a PV power plant. Sol Energy April 2021;218:652–60. https://doi.org/10.1016/j.solener.2021.02.033.

[38] Nielsen Andreas H, Iosifidis Alexandros, IrradianceNet Henrik Karstoft. Spatiotemporal deep learning model for satellite-derived solar irradiance short-term forecasting. Sol Energy November 2021;228:659–69. https://doi.org/10.1016/j.solener.2021.09.073.

[39] Paletta Quentin, Arbod Guillaume, Lasenby Joan. Benchmarking of deep learning irradiance forecasting models from sky images – an in-depth analysis. Sol Energy August 2021;224:855–67. https://doi.org/10.1016/j.solener.2021.05.056.

[40] Paletta Quentin, Hu Anthony, Arbod Guillaume, Lasenby Joan. ECLIPSE : Envisioning cloud induced perturbations in solar energy. Appl Energy November 2022;326:119924. https://doi.org/10.1016/j.apenergy.2022.119924.

[41] Diagne Maimouna, David Mathieu, Lauret Philippe, Boland John, Schmutz Nicolas. Review of solar irradiance forecasting methods and a proposition for small-scale insular grids. Renew Sustain Energy Rev 2013;27:65–76. https://doi.org/10.1016/j.rser.2013.06.042.

[42] Antonanzas Javier, Osorio Natalia, Escobar Rodrigo, Urraca Ruben, Martinez-de Pison Francisco J, Antonanzas-Torres Fernando. Review of photovoltaic power forecasting. Sol Energy 2016;136:78–111. https://doi.org/10.1016/j.solener.2016.06.069.

[43] Alkhayat Ghadah, Mehmood Rashid. A review and taxonomy of wind and solar energy forecasting methods based on deep learning. Energy AI 2021;4:100060. https://doi.org/10.1016/j.egyai.2021.100060.

[44] Kumari Pratima, Toshniwal Durga. Deep learning models for solar irradiance forecasting: a comprehensive review. J Clean Prod 2021;318:128566. https://doi.org/10.1016/j.jclepro.2021.128566.

[45] Moskolaï Waytehad Rose, Abdou Wahabou, Dipanda Albert, et al. Application of deep learning architectures for satellite image time series prediction: a review. Remote Sens 2021;13(23):4822. https://doi.org/10.3390/rs13234822.

[46] Sharma Ekanki, Elmenreich Wilfried. A review on physical and data-driven based nowcasting methods using sky images. In: Future of information and communication conference. Springer; 2021. p. 352–70.

[47] Lin Fan, Zhang Yao, Wang Jianxue. Recent advances in intra-hour solar forecasting: a review of ground-based sky image methods. Int J Forecast 2022. https://doi.org/10.1016/j.ijforecast.2021.11.002.

[48] Law Edward W, Prasad Abhnil A, Kay Merlinde, Taylor Robert A. Direct normal irradiance forecasting and its application to concentrated solar thermal output forecasting–a review. Sol Energy 2014;108:287–307. https://doi.org/10.1016/j.solener.2014.07.008.

[49] Barbieri Florian, Rajakaruna Sumedha, Ghosh Arindam. Very short-term photovoltaic power forecasting with cloud modeling: a review. Renew Sustain Energy Rev 2017;75:242–63. https://doi.org/10.1016/j.rser.2016.10.068.

[50] Sobri Sobrina, Koohi-Kamali Sam, Rahim Nasrudin Abd. Solar photovoltaic generation forecasting methods: a review. Energy Convers Manag 2018;156:459–97. https://doi.org/10.1016/j.enconman.2017.11.019.

[51] Kurzrock Frederik, Cros Sylvain, Chane-Ming Fabrice, Otkin Jason, Hutt Axel, Linguet Laurent, et al. A review of the use of geostationary satellite observations in regional-scale models for short-term cloud forecasting. Meteorol Z 2018;27(4):277–98. https://doi.org/10.1127/metz/2018/0904.

[52] Yang Dazhi, Kleissl Jan, Gueymard Christian A, Pedro Hugo TC, Coimbra Carlos FM. History and trends in solar irradiance and pv power forecasting: a preliminary assessment and review using text mining. Sol Energy 2018;168:60–101. https://doi.org/10.1016/j.solener.2017.11.023.

[53] Kumar Dhivya Sampath, Mert Yagli Gokhan, Kashyap Monika, Srinivasan Dipti. Solar irradiance resource and forecasting: a comprehensive review. IET Renew Power Gener 2020;14(10):1641–56. https://doi.org/10.1049/iet-rpg.2019.1227.

[54] Hong Tao, Pinson Pierre, Wang Yi, Weron Rafał, Yang Dazhi, Zareipour Hamidreza. Energy forecasting: a review and outlook. IEEE Open Access J Power Energy 2020;7:376–88. https://doi.org/10.1109/OAJPE.2020.3029979.

[55] Li Binghui, Zhang Jie. A review on the integration of probabilistic solar forecasting in power systems. Sol Energy 2020;210:68–86. https://doi.org/10.1016/j.solener.2020.07.066.

[56] Guermoui Mawloud, Melgani Farid, Gairaa Kacem, Lamine Mekhalfi Mohamed. A comprehensive review of hybrid models for solar radiation forecasting. J Clean Prod 2020;258:120357. https://doi.org/10.1016/j.jclepro.2020.120357.

[57] Ahmed Razin, Sreeram V, Mishra Y, Arif MD. A review and evaluation of the state-of-the-art in pv solar power forecasting: techniques and optimization. Renew Sustain Energy Rev 2020;124:109792. https://doi.org/10.1016/j.rser.2020.109792.

[58] Wang Huaizhi, Liu Yangyang, Zhou Bin, Li Canbing, Cao Guangzhong, Voropai Nikolai, et al. Taxonomy research of artificial intelligence for deterministic solar power forecasting. Energy Convers Manag 2020;214:112909. https://doi.org/10.1016/j.enconman.2020.112909.

[59] Martins Bruno Juncklaus, Cerentini Allan, Mantelli Neto Sylvio Luiz, Loureiro Chaves Thiago Zimmermann, Moreira Branco Nicolas, von Wangenheim Aldo, et al. Systematic review of nowcasting approaches for solar energy production based upon ground-based cloud imaging. Solar Energy Adv July 2022:100019. https://doi.org/10.1016/j.seja.2022.100019.

[60] Sawant Manisha, Kishor Shende Mayur, Feijóo-Lorenzo Andrés E, Dhanraj Bokde Neeraj. The state-of-the-art progress in cloud detection, identification, and tracking approaches: a systematic review. Energies 2021;14(23):8119. https://doi.org/10.3390/en14238119.

[61] Erdener Burcin Cakir, Feng Cong, Doubleday Kate, Florita Anthony, Hodge Bri-Mathias. A review of behind-the-meter solar forecasting. Renew Sustain Energy Rev 2022;160:112224. https://doi.org/10.1016/j.rser.2022.112224.

[62] Yang Dazhi, Wang Wenting, Gueymard Christian A, Hong Tao, Kleissl Jan, Huang Jing, et al. A review of solar forecasting, its dependence on atmospheric sciences and implications for grid integration: towards carbon neutrality. Renew Sustain Energy Rev 2022;161:112348. https://doi.org/10.1016/j.rser.2022.112348.

[63] Krishnan Naveen, Kumar K Ravi, Inda Chandrapal Singh. How solar radiation forecasting impacts the utilization of solar energy: a critical review. J Clean Prod February 2023;388:135860. https://doi.org/10.1016/j.jclepro.2023.135860.

[64] Dudfield Peter, Bieker Jacob, Kelly Jack. Predict PV yield. https://huggingface.co/datasets/openclimatefix/uk_pv, 2022.

[65] Bieker Jacob, Kelly Jack, Dudfield Peter. Open climate fix hugging face repository. https://huggingface.co/openclimatefix, 2022.

[66] Adil Ahmed, Khalid Muhammad. A review on the selected applications of forecasting models in renewable power systems. Renew Sustain Energy Rev 2019;100:9–21. https://doi.org/10.1016/j.rser.2018.09.046.

[67] Hasenbalg M, Kuhn P, Wilbert S, Nouri B, Kazantzidis A. Benchmarking of six cloud segmentation algorithms for ground-based all-sky imagers. Sol Energy May 2020;201:596–614. https://doi.org/10.1016/j.solener.2020.02.042.

[68] Kelly Jack, Dudfield Peter, Bieker. Power perceiver Jacob. https://github.com/openclimatefix/power_perceiver, 2022.

[69] Bieker Jacob, Kelly Jack, Satflow Peter Dudfield. https://github.com/openclimatefix/satflow, 2022.

[70] Si Zhiyuan, Yang Ming, Yu Yixiao, Ding Tingting. Photovoltaic power forecast based on satellite images considering effects of solar position. Appl Energy November 2021;302:117514. https://doi.org/10.1016/j.apenergy.2021.117514.

[71] Andrychowicz Marcin, Espeholt Lasse, Li Di, Merchant Samier, Merose Alexander, Zyda Fred, et al. Deep learning for day forecasts from sparse observations. https://doi.org/10.48550/arXiv.2306.06079, 2023.

[72] O'Mahony Niall, Campbell Sean, Carvalho Anderson, Harapanahalli Suman, Velasco Hernandez Gustavo, Krpalkova Lenka, et al. Deep learning vs. traditional computer vision. In: Arai Kohei, Kapoor Supriya, editors. Advances in computer vision. Cham: Springer International Publishing; 2020. p. 128–44.

[73] Singh Bansal Akansha, Bansal Trapit, Irwin David. A moment in the sun: solar nowcasting from multispectral satellite data using self-supervised learning. In: Proceedings of the thirteenth ACM international conference on future energy systems; 2022. p. 251–62.

[74] Wang Fei, Lu Xiaoxing, Mei Shengwei, Su Ying, Zhen Zhao, Zou Zubing, et al. A satellite image data based ultra-short-term solar pv power forecasting method considering cloud information from neighboring plant. Energy 2022;238:121946. https://doi.org/10.1016/j.energy.2021.121946.

[75] Yeom Jong-Min, Deo Ravinesh C, Adamowski Jan F, Park Seonyoung, Lee Chang-Suk. Spatial mapping of short-term solar radiation prediction incorporating geostationary satellite images coupled with deep convolutional LSTM networks for South Korea. Environ Res Lett August 2020;15(9):094025. https://doi.org/10.1088/1748-9326/ab9467.

[76] Nikitidou E, Zagouras A, Salamalikis V, Kazantzidis A. Short-term cloudiness forecasting for solar energy purposes in Greece, based on satellite-derived information.

Meteorol Atmos Phys 2019;131(2):175–82. https://doi.org/10.1007/s00703-017-0559-0.
[77] Blanc Philippe, Remund Jan, Vallance Loic. Short-term solar power forecasting based on satellite images. In: Renewable energy forecasting. Elsevier; 2017. p. 179–98.
[78] Murat Ates Ali, Yilmaz Osman Salih, Gulgen Fatih. Using remote sensing to calculate floating photovoltaic technical potential of a dam's surface. Sustain Energy Technol Assess 2020;41:100799.
[79] Bellaoui Mebrouk, Bouchouicha Kada, Oulimar Ibrahim. Estimation of daily global solar radiation based on MODIS satellite measurements: the case study of Adrar region (Algeria). Measurement 2021;183:109802. https://doi.org/10.1016/j.measurement.2021.109802.
[80] Dubayah R. Estimating net solar radiation using Landsat thematic mapper and digital elevation data. Water Resour Res 1992;28(9):2469–84. https://doi.org/10.1029/92WR00772.
[81] Wang Jianjun, White Kevin, Robinson Gary John. Estimating surface net solar radiation by use of Landsat-5 TM and digital elevation models. Int J Remote Sens 2000;21(1):31–43. https://doi.org/10.1080/014311600210975.
[82] Long CN, Slater DW, Tooman Tim P. Total sky imager model 880 status and testing results. Richland, Wash, USA: Pacific Northwest National Laboratory; 2001.
[83] Fu Chia-Lin, Cheng Hsu-Yung. Predicting solar irradiance with all-sky image features via regression. Sol Energy 2013;97:537–50. https://doi.org/10.1016/j.solener.2013.09.016.
[84] Chu Yinghao, Li Mengying, Coimbra Carlos FM. Sun-tracking imaging system for intra-hour DNI forecasts. Renew Energy 2016;96:792–9. https://doi.org/10.1016/j.renene.2016.05.041. ISSN 18790682.
[85] Terrén-Serrano Guillermo, Bashir Adnan, Estrada Trilce, Martínez-Ramón Manel. Girasol, a sky imaging and global solar irradiance dataset. Data Brief April 2021;35:106914. https://doi.org/10.1016/j.dib.2021.106914.
[86] Blanc Philippe, Wald Lucien. The SG2 algorithm for a fast and accurate computation of the position of the Sun for multi-decadal time period. Sol Energy 2012;86(10):3072–83. https://doi.org/10.1016/j.solener.2012.07.018. ISSN 0038092X.
[87] Grena Roberto. Five new algorithms for the computation of Sun position from 2010 to 2110. Sol Energy 2012;86(5):1323–37. https://doi.org/10.1016/j.solener.2012.01.024.
[88] Rizvi Arslan A, Addoweesh Khaled, El-Leathy Abdelrehman, Al-Ansary Hany. Sun position algorithm for sun tracking applications. In: IECON 2014-40th annual conference of the IEEE industrial electronics society. IEEE; 2014. p. 5595–8.
[89] Blanco Manuel J, Milidonis Kypros, Bonanos Aristides M. Updating the PSA sun position algorithm. Sol Energy 2020;212:339–41. https://doi.org/10.1016/j.solener.2020.10.084.
[90] Hay John E. Calculation of solar irradiances for inclined surfaces: validation of selected hourly and daily models. Atmos-Ocean 1986;24(1):16–41. https://doi.org/10.1080/07055900.1986.9649238.
[91] Reda Ibrahim, Andreas Afshin. Solar position algorithm for solar radiation applications. Sol Energy 2004;76(5):577–89. https://doi.org/10.1016/j.solener.2003.12.003. ISSN 0038092X.
[92] Stein Joshua S, Hansen Clifford W, Reno Matthew J. Global horizontal irradiance clear sky models: implementation and analysis. Technical report. Albuquerque, NM, and Livermore, CA: Sandia National Laboratories (SNL); 2012.
[93] Liu Ying, Jiang Du, Yun Juntong, Sun Ying, Li Cuiqiao, Jiang Guozhang, et al. Self-tuning control of manipulator positioning based on fuzzy PID and PSO algorithm. Front Bioeng Biotechnol 2022;9:817723. https://doi.org/10.3389/fbioe.2021.817723.
[94] Salgado-Conrado Lizbeth. A review on sun position sensors used in solar applications. Renew Sustain Energy Rev 2018;82:2128–46. https://doi.org/10.1016/j.rser.2017.08.040.
[95] Terrén-Serrano Guillermo, Martínez-Ramón Manel. Data acquisition and image processing for solar irradiance forecasting. https://doi.org/10.48550/arXiv.2011.12401, 2020.
[96] Wei Ching Chuan, Song Yu Chang, Chang Chia Chi, Lin Chuan Bi. Design of a solar tracking system using the brightest region in the sky image sensor. Sensors (Switz) 2016;16(12):1–11. https://doi.org/10.3390/s16121995. ISSN 14248220.
[97] Paletta Quentin, Lasenby Joan. A temporally consistent image-based sun tracking algorithm for solar energy forecasting applications. In: NeurIPS 2020 workshop on tackling climate change with machine learning; 2020. p. 10. https://www.climatechange.ai/papers/neurips2020/8.
[98] Dev Soumyabrata, Savoy Florian, Hui Lee Yee, Wahrsis Stefan Winkler. A low-cost high-resolution whole sky imager with near-infrared capabilities. In: Proceedings of SPIE - the international society for optical engineering, vol. 9071. 05 2014. p. 90711L.
[99] Kuo Wen-Chi, Chen Chiun-Hsun, Chen Sih-Yu, Wang Chi-Chuan. Deep learning neural networks for short-term PV power forecasting via sky image method. Energies 2022;15(13).
[100] Oktavia Kamadinata Jane, Ken Tan Lit, Suwa Tohru. Sky image-based solar irradiance prediction methodologies using artificial neural networks. Renew Energy 2019;134:837–45. https://doi.org/10.1016/j.renene.2018.11.056.
[101] Zhang Jinsong, Verschae Rodrigo, Nobuhara Shohei, Lalonde Jean François. Deep photovoltaic nowcasting. Sol Energy September 2018;176:267–76. https://doi.org/10.1016/j.solener.2018.10.024.
[102] Mammoli A, Ellis A, Menicucci A, Willard S, Caudell T, Simmins J. Low-cost solar micro-forecasts for PV smoothing. In: 2013 1st IEEE conference on technologies for sustainability (SusTech); 2013. p. 238–43.
[103] Ajith Meenu, Martínez-Ramón Manel. Deep learning based solar radiation micro forecast by fusion of infrared cloud images and radiation data. Appl Energy July 2021;294:117014. https://doi.org/10.1016/j.apenergy.2021.117014.
[104] Roxhed Niclas, Niklaus Frank, Fischer Andreas C, Forsberg Fredrik, Höglund Linda, Ericsson Per, et al. Low-cost uncooled microbolometers for thermal imaging. Optical sensing and detection, vol. 7726. International Society for Optics and Photonics; 2010. p. 772611.
[105] Redman Brian J, Shaw Joseph A, Nugent Paul W, Trevor Clark R, Piazzolla Sabino. Reflective all-sky thermal infrared cloud imager. Opt Express Apr 2018;26(9):11276–83. https://doi.org/10.1364/OE.26.011276.
[106] Mammoli Andrea, Terrén-Serrano Guillermo, Menicucci Anthony, Caudell Thomas P, Martínez-Ramón Manel. An experimental method to merge far-field images from multiple longwave infrared sensors for short-term solar forecasting. Sol Energy 2019;187:254–60. https://doi.org/10.1016/j.solener.2019.05.052.
[107] Masters GM, online library Wiley. Renewable and efficient electric power systems. Wiley - IEEE Series. Wiley. ISBN 9780471280606, 2004.
[108] Ineichen Pierre, Perez RR, Seal RD, Maxwell EL, Zalenka AJAT. Dynamic global-to-direct irradiance conversion models. ASHRAE Trans 1992;98(1):354–69.
[109] Crespi Francesco, Toscani Andrea, Zani Paolo, Sánchez David, Manzolini Giampaolo. Effect of passing clouds on the dynamic performance of a CSP tower receiver with molten salt heat storage. Appl Energy 2018;229:224–35.
[110] Ramadhan Raden AA, Heatubun Yosca RJ, Tan Sek F, Lee Hyun-Jin. Comparison of physical and machine learning models for estimating solar irradiance and photovoltaic power. Renew Energy 2021;178:1006–19. https://doi.org/10.1016/j.renene.2021.06.079.
[111] Imene Yahyaoui. Advances in renewable energies and power technologies: volume 1: solar and wind energies. Elsevier; 2018.
[112] Lappalainen Kari, Valkealahti Seppo. Output power variation of different PV array configurations during irradiance transitions caused by moving clouds. Appl Energy 2017;190:902–10. https://doi.org/10.1016/j.apenergy.2017.01.013.
[113] Lappalainen Kari, Wang Guang C, Kleissl Jan. Estimation of the largest expected photovoltaic power ramp rates. Appl Energy 2020;278:115636. https://doi.org/10.1016/j.apenergy.2020.115636.
[114] Kaaya Ismail, Ascencio-Vásquez Julián, Weiss Karl-Anders, Topič Marko. Assessment of uncertainties and variations in PV modules degradation rates and lifetime predictions using physical models. Sol Energy 2021;218:354–67. https://doi.org/10.1016/j.solener.2021.01.071.
[115] Rodríguez Fermín, Martín Fernando, Fontán Luis, Galarza Ainhoa. Ensemble of machine learning and spatiotemporal parameters to forecast very short-term solar irradiation to compute photovoltaic generators' output power. Energy 2021;229:120647. https://doi.org/10.1016/j.energy.2021.120647.
[116] Yan Xingyu, Abbes Dhaker, Francois Bruno. Uncertainty analysis for day ahead power reserve quantification in an urban microgrid including PV generators. Renew Energy 2017;106:288–97. https://doi.org/10.1016/j.renene.2017.01.022.
[117] Feng Cong, SolarNet Jie Zhang. A sky image-based deep convolutional neural network for intra-hour solar forecasting. Sol Energy July 2020;204:71–8. https://doi.org/10.1016/j.solener.2020.03.083.
[118] Engerer NA, Mills. Kpv FP. A clear-sky index for photovoltaics. Sol Energy 2014;105:679–93. https://doi.org/10.1016/j.solener.2014.04.019.
[119] Sun Yuchi, Venugopal Vignesh, Brandt Adam R. Short-term solar power forecast with deep learning: exploring optimal input and output configuration. Sol Energy August 2019;188:730–41. https://doi.org/10.1016/j.solener.2019.06.041.
[120] Feng Cong, Zhang Jie, Zhang Wenqi, Hodge Bri-Mathias. Convolutional neural networks for intra-hour solar forecasting based on sky image sequences. Appl Energy March 2022;310:118438. https://doi.org/10.1016/j.apenergy.2021.118438.
[121] Terrén-Serrano G, Martínez-Ramón M. Kernel learning for intra-hour solar forecasting with infrared sky images and cloud dynamic feature extraction. Renew Sustain Energy Rev 2023;175:113125. https://doi.org/10.1016/j.rser.2022.113125.
[122] Terrén-Serrano Guillermo, Martínez-Ramón Manel. Deep learning for intra-hour solar forecasting with fusion of features extracted from infrared sky images. Inf Fusion 2023.
[123] Nouri Bijan, Kuhn P, Wilbert Stefan, Hanrieder Natalie, Prahl C, Zarzalejo L, et al. Cloud height and tracking accuracy of three all sky imager systems for individual clouds. Sol Energy 2019;177:213–28. https://doi.org/10.1016/j.solener.2018.10.079.
[124] Kuhn P, Wilbert S, Prahl C, Schüler D, Haase T, Hirsch T, et al. Shadow camera system for the generation of solar irradiance maps. Sol Energy 2017;157:157–70. https://doi.org/10.1016/j.solener.2017.05.074.
[125] Inage Shin-ichi. Development of an advection model for solar forecasting based on ground data first report: development and verification of a fundamental model. Sol Energy 2017;153:414–34. https://doi.org/10.1016/j.solener.2018.12.068.
[126] Inage Shin-ichi. Development of an advection model for solar forecasting based on ground data. Part ii: verification of the forecasting model over a wide geographical area. Sol Energy 2019;180:257–76. https://doi.org/10.1016/j.solener.2018.12.068.
[127] Zang Haixiang, Liu Li Sun Ling, Cheng Lilin, Wei Zhinong, Sun Guoqiang. Short-term global horizontal irradiance forecasting based on a hybrid CNN-LSTM model

with spatiotemporal correlations. Renew Energy 2020;160:26–41. https://doi.org/10.1016/j.renene.2020.05.150.
[128] Parmar Gaurav, Zhang Richard, Zhu Jun-Yan. On buggy resizing libraries and surprising subtleties in FID calculation. arXiv:2104.11222 [cs], April 2021.
[129] Haeffelin M, Barthès L, Bock O, Boitel C, Bony S, Bouniol D, et al. SIRTA, a ground-based atmospheric observatory for cloud and aerosol research. Ann Geophys February 2005;23(2):253–75. https://doi.org/10.5194/angeo-23-253-2005.
[130] Rajagukguk Rial A, Kamil Raihan, Lee Hyun-Jin. A deep learning model to forecast solar irradiance using a sky camera. Appl Sci 2021;11(11):5049.
[131] Leron Julian, Sankaranarayanan Aswin C. Precise forecasting of sky images using spatial warping. In: Proceedings of the IEEE/CVF international conference on computer vision; 2021. p. 1136–44.
[132] Richardson Walter, Krishnaswami Hariharan, Vega Rolando, Cervantes Michael. A low cost, edge computing, all-sky imager for cloud tracking and intra-hour irradiance forecasting. Sustainability 2017;9(4):482. https://doi.org/10.3390/su9040482.
[133] Terrén-Serrano Guillermo, Martínez-Ramón Manel. Geospatial perspective reprojections for ground-based sky imaging systems. IEEE Trans Geosci Remote Sens 2022;60:1–7. https://doi.org/10.1109/TGRS.2022.3154710.
[134] Terrén-Serrano Guillermo, Martínez-Ramón Manel. Multi-layer wind velocity field visualization in infrared images of clouds for solar irradiance forecasting. Appl Energy 2021;288:116656. https://doi.org/10.1016/j.apenergy.2021.116656.
[135] Nguyen Dung Andu, Kleissl Jan. Stereographic methods for cloud base height determination using two sky imagers. Sol Energy 2014;107:495–509. https://doi.org/10.1016/j.solener.2014.05.005.
[136] Paletta Quentin, Hu Anthony, Arbod Guillaume, Blanc Philippe, Lasenby Joan. SPIN: Simplifying polar invariance for neural networks application to vision-based irradiance forecasting. In: Proceedings of the IEEE/CVF conference on computer vision and pattern recognition workshops; 2022. p. 5182–91.
[137] Caldas M, Alonso-Suárez R. Very short-term solar irradiance forecast using all-sky imaging and real-time irradiance measurements. Renew Energy 2019;143:1643–58.
[138] Kaae Sønderby Casper, Espeholt Lasse, Heek Jonathan, Dehghani Mostafa, Oliver Avital, Salimans Tim, et al. A neural weather model for precipitation forecasting. CoRR. arXiv:2003.12140 [abs], 2020.
[139] Espeholt Lasse, Agrawal Shreya, Sønderby Casper, Kumar Manoj, Heek Jonathan, Bromberg Carla, et al. Skillful twelve hour precipitation forecasts using large context neural networks. https://arxiv.org/abs/2111.07470, 2021.
[140] Dombrowski Olga, Hendricks Franssen Harrie-Jan, Brogi Cosimo, Bogena Heye Reemt. Performance of the ATMOS 41 all-in-one weather station for weather monitoring. Sensors 2021;21(3). https://doi.org/10.3390/s21030741.
[141] Terrén-Serrano Guillermo, Martínez-Ramón Manel. Detection of clouds in multiple wind velocity fields using ground-based infrared sky images. arXiv preprint. arXiv:2105.03535, 2021.
[142] Ineichen Pierre, Perez Richard. Derivation of cloud index from geostationary satellites and application to the production of solar irradiance and daylight illuminance data. Theor Appl Climatol 1999;64(1):119–30. https://doi.org/10.1007/s007040050116.
[143] EUMETSAT. Optimal cloud analysis - MSG - 0 degree. https://navigator.eumetsat.int/product/EO:EUM:DAT:MSG:OCA?query=Cloud&filter=satellite_MSG&results=30&s=advanced, 2022.
[144] NOAA. GOES-R data products: cloud optical depth. https://www.goes-r.gov/products/baseline-cloud-opt-depth.html, 2022.
[145] Morris Victor R. Ceilometer instrument handbook. Technical report. DOE Office of Science Atmospheric Radiation Measurement (ARM); 2016.
[146] Wang Guang, Kurtz Ben, Kleissl Jan. Cloud base height from sky imager and cloud speed sensor. Sol Energy 2016;131:208–21. https://doi.org/10.1016/j.solener.2016.02.027.
[147] Chao Wang Guang, Urquhart Bryan, Kleissl Jan. Cloud base height estimates from sky imagery and a network of pyranometers. Sol Energy 2019;184:594–609. https://doi.org/10.1016/j.solener.2019.03.101.
[148] Kuhn P, Wirtz M, Killius N, Wilbert S, Bosch JL, Hanrieder N, et al. Benchmarking three low-cost, low-maintenance cloud height measurement systems and ECMWF cloud heights against a ceilometer. Sol Energy 2018;168:140–52. Advances in Solar Resource Assessment and Forecasting.
[149] Terrén-Serrano Guillermo, Martínez-Ramón Manel. Comparative analysis of methods for cloud segmentation in ground-based infrared images. Renew Energy 2021;175:1025–40. https://doi.org/10.1016/j.renene.2021.04.141.
[150] Stone Peter H, Carlson John H. Atmospheric lapse rate regimes and their parameterization. J Atmos Sci 1979;36(3):415–23. https://doi.org/10.1175/1520-0469(1979)036<0415:ALRRAT>2.0.CO;2.
[151] Hess SL. Introduction to theoretical meteorology. Holt: Holt-Dryden Book; 1959.
[152] Chen Yuxuan, Chen Jing, Huang Wumeng. 3D cumulus cloud scene modelling and shadow analysis method based on ground-based sky images. Int J Appl Earth Obs Geoinf 2022;109. https://doi.org/10.1016/j.jag.2022.102765:102765.
[153] Nataraja Vikas, Schmidt Sebastian, Chen Hong, Yamaguchi Takanobu, Kazil Jan, Feingold Graham, et al. Segmentation-based multi-pixel cloud optical thickness retrieval using a convolutional neural network. Atmos Meas Tech 2022;15(17):5181–205. https://doi.org/10.5194/amt-15-5181-2022.
[154] Alhmoud Lina. Why does the PV solar power plant operate ineffectively? Energies 2023;16(10):4074. https://doi.org/10.3390/en16104074.
[155] Carra Elena, Marzo Aitor, Ballestrín Jesús, Polo Jesús, Barbero Javier, Alonso-Montesinos Joaquín, et al. Atmospheric extinction levels of solar radiation using aerosol optical thickness satellite data. Validation methodology with measurement system. Renew Energy 2020;149:1120–32. https://doi.org/10.1016/j.renene.2019.10.106.
[156] Jethva Hiren, Torres Omar, Yoshida Yasuko. Accuracy assessment of modis land aerosol optical thickness algorithms using aeronet measurements over North America. Atmos Meas Tech 2019;12(8):4291–307. https://doi.org/10.5194/amt-12-4291-2019.
[157] Kokhanovsky AA, Smirnov A, Korkin SV, Wind G, Slutsker I. The retrieval of cloud properties based on spectral solar light diffuse transmittance measurements under optically thick cloud cover conditions. J Quant Spectrosc Radiat Transf 2020;251:107008. https://doi.org/10.1016/j.jqsrt.2020.107008.
[158] Ben-tayeb Abdelmoula, Diouri Mohammed, Meziane Rajae, Steli Hanae. Solar radiation attenuation by aerosol: application to solar farms. Air Qual Atmos Health 2020;13(2):259–69. https://doi.org/10.1007/s11869-020-00790-1.
[159] Bunn Patrick TW, Holmgren William F, Leuthold Michael, Castro Christopher L. Using GEOS-5 forecast products to represent aerosol optical depth in operational day-ahead solar irradiance forecasts for the southwest United States. J Renew Sustain Energy 2020;12(5).
[160] Cheng Xinghong, Ye Dong, Shen Yanbo, Li Deping, Feng Jinming. Studies on the improvement of modelled solar radiation and the attenuation effect of aerosol using the WRF-Solar model with satellite-based aod data over North China. Renew Energy 2022;196:358–65. https://doi.org/10.1016/j.renene.2022.06.141.
[161] Kumar Astitva, Rizwan M, Nangia Uma. A hybrid intelligent approach for solar photovoltaic power forecasting: impact of aerosol data. Arab J Sci Eng 2020;45:1715–32. https://doi.org/10.1007/s13369-019-04183-0.
[162] Yang Liwei, Gao Xiaoqing, Hua Jiajia, Wu Pingping, Li Zhenchao, Jia Dongyu. Very short-term surface solar irradiance forecasting based on FengYun-4 geostationary satellite. Sensors 2020;20(9):2606. https://doi.org/10.3390/s20092606.
[163] She Lu, Zhang Hankui K, Li Zhengqiang, de Leeuw Gerrit, Huang Bo. Himawari-8 aerosol optical depth (AOD) retrieval using a deep neural network trained using aeronet observations. Remote Sens 2020;12(24):4125. https://doi.org/10.3390/rs12244125.
[164] Yeom Jong-Min, Jeong Seungtaek, Ha Jong-Sung, Lee Kwon-Ho, Lee Chang-Suk, Park Seonyoung. Estimation of the hourly aerosol optical depth from GOCI geostationary satellite data: deep neural network, machine learning, and physical models. IEEE Trans Geosci Remote Sens 2021;60:1–12. https://doi.org/10.1109/TGRS.2021.3107542.
[165] Zbizika Renee, Pakszys Paulina, Zielinski Tymon. Deep neural networks for aerosol optical depth retrieval. Atmosphere 2022;13(1):101. https://doi.org/10.3390/rs14061411.
[166] Yakoubi H, El Mghouchi Y, Abdou N, Hajou A, Khellouki A. Correlating clearness index with cloud cover and other meteorological parameters for forecasting the global solar radiation over Morocco. Optik 2021;242:167145. https://doi.org/10.1016/j.ijleo.2021.167145.
[167] Yang Dazhi, Jirutitijaroen Panida, Walsh Wilfred M. Hourly solar irradiance time series forecasting using cloud cover index. Sol Energy 2012;86(12):3531–43. https://doi.org/10.1016/j.solener.2012.07.029.
[168] Azhar Mohammad Afiq Dzuan Mohd, Hamid Nurul Shazana Abdul, Kamil Wan Mohd Aimran Wan Mohd, Mohamad Nor Sakinah. Daytime cloud detection method using the all-sky imager over permatapintar observatory. Universe 2021;7(2):41. https://doi.org/10.3390/universe7020041.
[169] Li Chao, Ma Jinji, Yang Peng, Li Zhengqiang. Detection of cloud cover using dynamic thresholds and radiative transfer models from the polarization satellite image. J Quant Spectrosc Radiat Transf 2019;222:196–214. https://doi.org/10.1016/j.jqsrt.2018.10.026.
[170] Son Yongju, Yoon Yeunggurl, Cho Jintae, Choi Sungyun. Cloud cover forecast based on correlation analysis on satellite images for short-term photovoltaic power forecasting. Sustainability 2022;14(8):4427. https://doi.org/10.3390/su14084427.
[171] Sarukkai Vishnu, Jain Anirudh, Uzkent Burak, Ermon Stefano. Cloud removal from satellite images using spatiotemporal generator networks. In: Proceedings of the IEEE/CVF winter conference on applications of computer vision; 2020. p. 1796–805.
[172] Jeppesen Jacob Høxbroe, Jacobsen Rune Hylsberg, Inceoglu Fadil, Toftegaard Thomas Skjødeberg. A cloud detection algorithm for satellite imagery based on deep learning. Remote Sens Environ 2019;229:247–59. https://doi.org/10.1016/j.rse.2019.03.039.
[173] Si Zhiyuan, Yu Yixiao, Yang Ming, Li Peng. Hybrid solar forecasting method using satellite visible images and modified convolutional neural networks. IEEE Trans Ind Appl 2020;57(1):5–16. https://doi.org/10.1109/TIA.2020.3028558.
[174] Park Seongha, Kim Yongho, Ferrier Nicola J, Collis Scott M, Sankaran Rajesh, Beckman Pete H. Prediction of solar irradiance and photovoltaic solar energy product based on cloud coverage estimation using machine learning methods. Atmosphere 2021;12(3):395. https://doi.org/10.3390/atmos12030395.
[175] Andrianakos George, Tsourounis Dimitrios, Oikonomou Spiros, Kastaniotis Dimitris, Economou George, Kazantzidis Andreas. Sky image forecasting with generative adversarial networks for cloud coverage prediction. In: 2019 10th international conference on information, intelligence, systems and applications (IISA). IEEE; 2019. p. 1–7.

[176] Berthomier Léa, Pradel Bruno, Perez Lior. Cloud cover nowcasting with deep learning. In: 2020 tenth international conference on image processing theory, tools and applications (IPTA). IEEE; 2020. p. 1–6.

[177] Barjatya Aroh. Block matching algorithms for motion estimation. IEEE Trans Evol Comput 2004;8(3):225–39. https://doi.org/10.1109/ICELIE.2013.6701287.

[178] Marquez Ricardo, Coimbra Carlos FM. Intra-hour DNI forecasting based on cloud tracking image analysis. Sol Energy May 2013;91:327–36.

[179] Adrian Ronald J, Westerweel Jerry. Particle image velocimetry. Cambridge University Press; 2011.

[180] Shakya Snehlata, Kumar Sanjeev. Characterising and predicting the movement of clouds using fractional-order optical flow. IET Image Process 2019;13(8):1375–81. https://doi.org/10.1049/iet-ipr.2018.6100.

[181] Zhang Songiie, Dong Zhekang, Yang Xinyi, Chai Songiian, Xu Zhao, Qi Donglian. Intrahour cloud tracking based on optical flow. In: 2019 Chinese Control Conference (CCC). IEEE; 2019. p. 3023–8.

[182] Lucas Bruce D, Kanade Takeo, et al. An iterative image registration technique with an application to stereo vision, vol. 81. Vancouver; 1981.

[183] Bouguet Jean-Yves, et al. Pyramidal implementation of the affine Lucas Kanade feature tracker description of the algorithm. Intel corporation, Microprocessor Research Labs 2001;5(1–10):4.

[184] Beauchemin Steven S, Barron John L. The computation of optical flow. ACM Comput Surv 1995;27(3):433–66. https://doi.org/10.1145/212094.212141.

[185] Horn Berthold KP, Schunck Brian G. Determining optical flow. Artif Intell 1981;17(1–3):185–203. https://doi.org/10.1016/0004-3702(81)90024-2.

[186] Chantas Giannis, Gkamas Theodosios, Nikou Christophoros. Variational-bayes optical flow. J Math Imaging Vis 2014;50(3):199–213. https://doi.org/10.1007/s10851-014-0494-3.

[187] Zach Christopher, Pock Thomas, Bischof Horst. A duality based approach for real-time TV-L 1 optical flow. In: Joint pattern recognition symposium. Springer; 2007. p. 214–23.

[188] Aicardi D, Musé P, Alonso-Suárez R. A comparison of satellite cloud motion vectors techniques to forecast intra-day hourly solar global horizontal irradiation. Sol Energy 2022;233:46–60. https://doi.org/10.1016/j.solener.2021.12.066.

[189] Cheng Lilin, Zang Haixiang, Trivedi Anupam, Srinivasan Dipti, Ding Tao, Wei Zhinong, et al. Prediction of non-stationary multi-head cloud motion vectors for intra-hourly satellite-derived solar power forecasting. IEEE Trans Power Syst 2023:1–10. https://doi.org/10.1109/TPWRS.2023.3284559.

[190] Farnebäck Gunnar. Two-frame motion estimation based on polynomial expansion. In: Scandinavian conference on image analysis. Springer; 2003. p. 363–70.

[191] Baker Simon, Matthews Iain. Lucas-Kanade 20 years on: a unifying framework. Int J Comput Vis 2004;56(3):221–55. https://doi.org/10.1023/B:VISI.0000011205.11775.fd.

[192] Tiwari Soumya, Sabzehgar Reza, Rasouli Mohammad. Short term solar irradiance forecast based on image processing and cloud motion detection. In: 2019 IEEE Texas power and energy conference (TPEC); 2019. p. 1–6.

[193] Cheng Lilin, Zang Haixiang, Wei Zhinong, Ding Tao, Sun Guoqiang. Solar power prediction based on satellite measurements–a graphical learning method for tracking cloud motion. IEEE Trans Power Syst 2021;37(3):2335–45. https://doi.org/10.1109/TPWRS.2021.3119338.

[194] Cheng Lilin, Zang Haixiang, Wei Zhinong, Ding Tao, Xu Ruiqi, Sun Guoqiang. Short-term solar power prediction learning directly from satellite images with regions of interest. IEEE Trans Sustain Energy 2022;13(1):629–39. https://doi.org/10.1109/TSTE.2021.3123476.

[195] Terrén-Serrano Guillermo. Intra-hour solar forecasting using cloud dynamics features extracted from ground-based infrared sky images. PhD dissertation. Univesity of New Mexico, School of Engineering; 2022 0.5555/AAI29067225.

[196] Schmid Peter J. Dynamic mode decomposition of numerical and experimental data. J Fluid Mech 2010;656:5–28. https://doi.org/10.1017/S0022112010001217.

[197] Berkooz Gal, Holmes Philip, Lumley John L. The proper orthogonal decomposition in the analysis of turbulent flows. Annu Rev Fluid Mech 1993;25(1):539–75. https://doi.org/10.1146/annurev.fl.25.010193.002543.

[198] Solardata Dazhi Yang. An R package for easy access of publicly available solar datasets. Sol Energy 2018;171:A3–12. https://doi.org/10.1016/j.solener.2018.06.107.

[199] Feng Cong, Yang Dazhi, Hodge Bri Mathias, OpenSolar Jie Zhang. Promoting the openness and accessibility of diverse public solar datasets. Sol Energy aug 2019;188:1369–79. https://doi.org/10.1016/j.solener.2019.07.016.

[200] Stoffel T, Andreas A. NNREL Solar Radiation Research Laboratory (SRRL): Baseline Measurement System (BMS); Golden, Colorado (data). Technical report. Golden, CO, United States: National Renewable Energy Lab. (NREL); 1981.

[201] Haeffelin M, Barthès L, Bock O, Boitel C, Bony S, Bouniol D, et al. SIRTA, a ground-based atmospheric observatory for cloud and aerosol research. Ann Geophys 2005;23(2):253–75. https://doi.org/10.5194/angeo-23-253-2005. https://angeo.copernicus.org/articles/23/253/2005/.

[202] Pedro Hugo TC, Larson David P, Coimbra Carlos FM. A comprehensive dataset for the accelerated development and benchmarking of solar forecasting methods. J Renew Sustain Energy May 2019;11(3):036102. https://doi.org/10.1063/1.5094494.

[203] Ntavelis Evangelos, Remund Jan, SkyCam Philipp Schmid. A dataset of sky images and their irradiance values. arXiv:2105.02922 [cs], May 2021.

[204] Nie Yuhao, Li Xiatong, Scott Andea, Sun Yuchi, Venugopal Vignesh, Brandt Adam. SKIPP'D: a SKy images and photovoltaic power generation dataset for short-term solar forecasting. arXiv preprint. arXiv:2207.00913, 2022.

[205] Augustine John A, DeLuisi John J, Long Charles N. SURFRAD–a national surface radiation budget network for atmospheric research. Bull Am Meteorol Soc 2000;81(10):2341–58. https://doi.org/10.1175/1520-0477(2000)081<2341:SANSRB>2.3.CO;2.

[206] Dev Soumyabrata, Hui Lee Yee, Winkler Stefan. Categorization of cloud image patches using an improved texton-based approach. In: 2015 IEEE international conference on image processing (ICIP). IEEE; 2015. p. 422–6.

[207] Dev Soumyabrata, Hui Lee Yee, Winkler Stefan. Color-based segmentation of sky/cloud images from ground-based cameras. IEEE J Sel Top Appl Earth Obs Remote Sens 2016;10(1):231–42. https://doi.org/10.1109/JSTARS.2016.2558474.

[208] Dev Soumyabrata, Nautiyal Atul, Hui Lee Yee, Cloudsegnet Stefan Winkler. A deep network for nychthemeron cloud image segmentation. IEEE Geosci Remote Sens Lett 2019;16(12):1814–8. https://doi.org/10.1109/LGRS.2019.2912140.

[209] Espinar Bella, Blanc Philippe, Wald Lucien, Gschwind Benoît, Menard Lionel, Wey Etienne, et al. HelioClim-3: a near-real time and long-term surface solar irradiance database. In: Workshop on "Remote sensing measurements for renewable energy"; 05 2012. p. 4.

[210] Copernicus Climate Change Service (C3S). ERA5: fifth generation of ECMWF atmospheric reanalyses of the global climate. Copernicus Clim Change Serv Clim Data Store 2017;15(2):2020.

[211] Gelaro Ronald, McCarty Will, Suárez Max J, Todling Ricardo, Molod Andrea, Takacs Lawrence, et al. The modern-era retrospective analysis for research and applications, version 2 (MERRA-2). J Climate 2017;30(14):5419–54. https://doi.org/10.1175/JCLI-D-16-0758.1.

[212] Sengupta Manajit, Xie Yu, Lopez Anthony, Habte Aron, Maclaurin Galen, Shelby James. The national solar radiation data base (NSRDB). Renew Sustain Energy Rev 2018;89:51–60. https://doi.org/10.1016/j.rser.2018.03.003.

[213] GOES. NOAA geostationary operational environmental satellites (GOES). 16, 17 & 18. https://registry.opendata.aws/noaa-goes/, 2022.

[214] US Geological Survey. Landsat. https://www.usgs.gov/landsat-missions, 2023.

[215] EUMETSAT (Organization). EUMETSTAT: The European Organisation for Meteorological Satellites. European Organisation for Meteorological Satellites; 1988.

[216] EUMETSAT. EUMETSAT SEVIRI 0 degree service. https://navigator.eumetsat.int/product/EO:EUM:DAT:MSG:HRSEVIRI, 2022.

[217] EUMETSAT. EUMETSAT SEVIRI Indian Ocean. https://navigator.eumetsat.int/product/EO:EUM:DAT:MSG:HRSEVIRI-IODC, 2022.

[218] Himawari. JMA Himawari-8. https://registry.opendata.aws/noaa-himawari/, 2022.

[219] Sahoo Doyen, Pham Quang, Lu Jing, Hoi Steven CH. Online deep learning: learning deep neural networks on the fly. https://doi.org/10.48550/arXiv.1711.03705, November 2017.

[220] Wilbert Stefan, Nouri Bijan, Kötter-Orthaus Norbert, Hanrieder Natalie, Prahl Christoph, Kuhn Pascal, et al. Irradiance maps from a shadow camera on a mountain range. AIP Conf Proc May 2022;2445(1):150006. https://doi.org/10.1063/5.0085723.

[221] Le Guen Vincent, Thome Nicolas. A deep physical model for solar irradiance forecasting with fisheye images. In: Proceedings of the IEEE/CVF conference on computer vision and pattern recognition workshops; 2020. p. 630–1.

[222] Siddiqui Talha, Bharadwaj Samarth. Future semantic segmentation of time-lapsed videos with large temporal displacement. arXiv:1812.10786 [cs], December 2018.

[223] Cheng Lilin, Zang Haixiang, Wei Zhinong, Ding Tao, Xu Ruiqi, Sun Guoqiang. Short-term solar power prediction learning directly from satellite images with regions of interest. IEEE Trans Sustain Energy January 2022;13(1):629–39. https://doi.org/10.1109/TSTE.2021.3123476.

[224] Kellerhals Samuel A, De Leeuw Fons, Rodriguez Rivero Cristian. Cloud nowcasting with structure-preserving convolutional gated recurrent units. Atmosphere October 2022;13(10):1632. https://doi.org/10.3390/atmos13101632.

[225] Liandrat Olivier, Braun Antonin, Cros Sylvain, Gomez Andre, Sas Reuniwatt, Caterpillar JA Delmas. Sky-imager forecasting for improved management of a hybrid photovoltaic-diesel system. In: International hybrid power systems workshop; 2018. p. 6.

[226] Besson Pierre. Integration of short-term PV forecasts in control strategies of PV-diesel systems. In: International workshop on the integration of solar power into power systems; 2018. p. 5.

[227] Morales Juan M, Conejo Antonio J, Madsen Henrik, Pinson Pierre, Zugno Marco. Integrating renewables in electricity markets: operational problems. Springer Science & Business Media. ISBN 978-1-4614-9411-9, December 2013.

[228] Hagolle Olivier, Huc Mireille, Villa Pascual David, Dedieu Gerard. A multi-temporal and multi-spectral method to estimate aerosol optical thickness over land, for the atmospheric correction of FormoSat-2, LandSat, VEN____S and Sentinel-2 images. Remote Sens 2015;7(3):2668–91. https://doi.org/10.3390/rs70302668.

[229] Sun Lin, Yang Xu, Jia Shangfeng, Jia Chen, Wang Quan, Liu Xinyan, et al. Satellite data cloud detection using deep learning supported by hyperspectral data. Int J Remote Sens February 2020;41(4):1349–71. https://doi.org/10.1080/01431161.2019.1667548.

[230] Yu Junchuan, Li Yichuan, Zheng Xiangxiang, Zhong Yufeng, He Peng. An effective cloud detection method for Gaofen-5 images via deep learning. Remote Sens January 2020;12(13):2106. https://doi.org/10.3390/rs12132106.

[231] Yang Dazhi, Li Weixing, Yagli Gokhan Mert, Srinivasan Dipti. Operational solar forecasting for grid integration: standards, challenges, and outlook. Sol Energy 2021;224:930–7. https://doi.org/10.1016/j.solener.2021.04.002.
[232] Bodin Svante. Very short-range forecasting: observations, methods, and systems. 1983.
[233] Bryce Richard, Buster Grant, Doubleday Kate, Feng Cong, Ring-Jarvi Ross, Rossol Michael, et al. Solar PV, wind generation, and load forecasting dataset for ERCOT 2018: performance-based energy resource feedback, optimization, and risk management (PERFORM). Technical report. Golden, CO (United States): National Renewable Energy Lab. (NREL); 2023.
[234] Tawn R, Browell J. A review of very short-term wind and solar power forecasting. Renew Sustain Energy Rev 2022;153:111758. https://doi.org/10.1016/j.rser.2021.111758.
[235] Bradbury Kyle, Saboo Raghav, Johnson Timothy L, Malof Jordan M, Devarajan Arjun, Zhang Wuming, et al. Distributed solar photovoltaic array location and extent dataset for remote sensing object identification. Sci Data 2016;3(1):1–9. https://doi.org/10.1038/sdata.2016.106.
[236] Yuan Jiangye, Yang Hsiu-Han Lexie, Omitaomu Olufemi A, Bhaduri Budhendra L. Large-scale solar panel mapping from aerial images using deep convolutional networks. In: 2016 IEEE international conference on big data (big data); December 2016. p. 2703–8.
[237] Gao Xiang, Munson Eric, Abousleman Glen P, Si Jennie. Automatic solar panel recognition and defect detection using infrared imaging. Automatic target recognition XXV, vol. 9476. SPIE; May 2015. p. 196–204.
[238] Bartler Alexander, Mauch Lukas, Yang Bin, Reuter Michael, Stoicescu Liviu. Automated detection of solar cell defects with deep learning. In: 2018 26th European signal processing conference (EUSIPCO); September 2018. p. 2035–9.
[239] Insaf IM, Wickramathilaka HMKD, Upendra MAN, Godaliyadda GMRI, Ekanayake MPB, Herath HMVR, et al. Global horizontal irradiance modeling from sky images using ResNet architectures. In: 2021 IEEE 16th international conference on industrial and information systems (ICIIS); December 2021. p. 239–44.
[240] Jiang Huaiguang, Gu Yi, Xie Yu, Yang Rui, Zhang Yingchen. Solar irradiance capturing in cloudy sky days–a convolutional neural network based image regression approach. IEEE Access 2020;8:22235–48. https://doi.org/10.1109/ACCESS.2020.2969549.
[241] Nie Yuhao, Sun Yuchi, Chen Yuanlei, Orsini Rachel, Brandt Adam. PV power output prediction from sky images using convolutional neural network: the comparison of sky-condition-specific sub-models and an end-to-end model. J Renew Sustain Energy Jul 2020;12(4):046101. https://doi.org/10.1063/5.0014016. http://aip.scitation.org/doi/10.1063/5.0014016.
[242] Cano Daniel, Monget Jean-Marie, Albuisson Michel, Guillard Hervé, Regas Nathalie, Wald Lucien. A method for the determination of the global solar radiation from meteorological satellite data. Sol Energy 1986;37(1):31–9. https://doi.org/10.1016/0038-092X(86)90104-0.
[243] Rigollier Christelle, Lefèvre Mireille, Wald Lucien. The method Heliosat-2 for deriving shortwave solar radiation from satellite images. Sol Energy 2004;77(2):159–69. https://doi.org/10.1016/j.solener.2004.04.017.
[244] Qu Zhipeng, Oumbe Armel, Blanc Philippe, Espinar Bella, Gesell Gerhard, Gschwind Benoît, et al. Fast radiative transfer parameterisation for assessing the surface solar irradiance: the Heliosat-4 method. Meteorol Z 2017;26(1):33. https://doi.org/10.1127/metz/2016/0781.
[245] Tournadre Benoît, Gschwind Benoît, Saint-Drenan Yves-Marie, Blanc Philippe. An improved cloud index for estimating downwelling surface solarirradiance from various satellite imagers in the framework of a Heliosat-V method. Preprint, others (wind, precipitation, temperature, etc.)/remote sensing/data processing and information retrieval, February 2021.
[246] Jiang Hou, Lu Ning, Huang Ling Yao Guanghui, Qin Jun, Liu Hengzi. Spatial scale effects on retrieval accuracy of surface solar radiation using satellite data. Appl Energy July 2020;270:115178. https://doi.org/10.1016/j.apenergy.2020.115178.
[247] Verbois Hadrien, Saint-Drenan Yves-Marie, Becquet Vadim, Gschwind Benoit, Blanc Philippe. Retrieval of surface solar irradiance from satellite using machine learning: pitfalls and perspectives. EGUsphere March 2023:1–26. https://doi.org/10.5194/egusphere-2023-243.
[248] Jurakuziev Dadajon, Jumaboev Sherozbek, Lee Malrey. A framework to estimate generating capacities of PV systems using satellite imagery segmentation. Eng Appl Artif Intell August 2023;123:106186. https://doi.org/10.1016/j.engappai.2023.106186.
[249] Yang Dazhi. A guideline to solar forecasting research practice: reproducible, operational, probabilistic or physically-based, ensemble, and skill (ROPES). J Renew Sustain Energy 2019;11(2). https://doi.org/10.1063/1.5087462. ISSN 19417012.
[250] Yang Dazhi. Choice of clear-sky model in solar forecasting. J Renew Sustain Energy 2020;12(2):026101. https://doi.org/10.1063/5.0003495.
[251] Kleissl Jan. Solar energy forecasting and resource assessment. Academic Press; 2013.
[252] Paletta Quentin, Lasenby Joan. Convolutional neural networks applied to sky images for short-term solar irradiance forecasting. In: EU PVSEC. ISBN 3-936338-73-6, 2020. p. 1834–7.
[253] Feng Cong, Zhang Jie, Zhang Wenqi, Hodge Bri Mathias. Convolutional neural networks for intra-hour solar forecasting based on sky image sequences. Appl Energy mar 2022;310:118438. https://doi.org/10.1016/J.APENERGY.2021.118438.
[254] Yu Dukhwan, Lee Seowoo, Lee Sangwon, Choi Wonik, Liu Ling. Forecasting photovoltaic power generation using satellite images. Energies 2020;13(24):6603. https://doi.org/10.3390/en13246603.
[255] Camiruaga Ignacio, Herrera Andres, Mozo Franco. DeepCloud: intra-day satellite prediction of cloudiness using deep learning strategies. PhD thesis. Universidad de la República - Facultad de Ingenieria; 2022.
[256] Yeom Jong-Min, Deo Ravinesh C, Adamowski Jan F, Park Seonyoung, Lee Chang-Suk. Spatial mapping of short-term solar radiation prediction incorporating geostationary satellite images coupled with deep convolutional LSTM networks for South Korea. Environ Res Lett 2020;15(9):094025. https://doi.org/10.1088/1748-9326/ab9467.
[257] Lorenz Elke, Kühnert Jan, Heinemann Detlev. Short term forecasting of solar irradiance by combining satellite data and numerical weather predictions. In: Proceedings of the 27th European PV solar energy conference (EU PVSEC), vol. 2428. 2012. p. 44014405.
[258] Gallo Raimondo, Castangia Marco, Macii Alberto, Macii Enrico, Patti Edoardo, Aliberti Alessandro. Solar radiation forecasting with deep learning techniques integrating geostationary satellite images. Eng Appl Artif Intell 2022;116:105493. https://doi.org/10.1016/j.engappai.2022.105493.
[259] Pothineni Dinesh, Oswald Martin R, Poland Jan, Kloudnet Marc Pollefeys. Deep learning for sky image analysis and irradiance forecasting. In: German conference on pattern recognition. Springer; 2018. p. 535–51.
[260] Abuella Mohamed, Chowdhury Badrul. Forecasting of solar power ramp events: a post-processing approach. Renew Energy 2019;133:1380–92. https://doi.org/10.1016/j.renene.2018.09.005.
[261] Leelaruji T, Short N Teerakawanich. Term prediction of solar irradiance fluctuation using image processing with ResNet. In: 2020 8th international electrical engineering congress (iEECON); March 2020. p. 1–4.
[262] Vallance Loïc, Charbonnier Bruno, Paul Nicolas, Dubost Stéphanie, Blanc Philippe. Towards a standardized procedure to assess solar forecast accuracy: a new ramp and time alignment metric. Sol Energy July 2017;150:408–22. https://doi.org/10.1016/J.SOLENER.2017.04.064.
[263] Liu Shuang, Zhang Linbo, Zhang Zhong, Wang Chunheng, Xiao Baihua. Automatic cloud detection for all-sky images using superpixel segmentation. IEEE Geosci Remote Sens Lett February 2015;12(2):354–8. https://doi.org/10.1109/LGRS.2014.2341291.
[264] Boykov Yuri, Kolmogorov Vladimir. An experimental comparison of min-cut/max-flow algorithms for energy minimization in vision. IEEE Trans Pattern Anal Mach Intell 2004;26(9):1124–37. https://doi.org/10.1109/TPAMI.2004.60.
[265] Boykov Yuri, Veksler Olga, Zabih Ramin. Fast approximate energy minimization via graph cuts. IEEE Trans Pattern Anal Mach Intell 2001;23(11):1222–39. https://doi.org/10.1109/34.969114.
[266] Dev Soumyabrata, Hui Lee Yee, Winkler Stefan. Systematic study of color spaces and components for the segmentation of sky/cloud images. In: 2014 IEEE international conference on image processing (ICIP). IEEE; 2014. p. 5102–6.
[267] Terrén-Serrano Guillermo, Martínez-Ramón Manel. Segmentation algorithms for ground-based infrared cloud images. In: 2021 IEEE PES innovative smart grid technologies Europe (ISGT Europe); 2021. p. 01–6.
[268] Terrén-Serrano Guillermo, Martínez-Ramón Manel. Explicit basis function kernel methods for cloud segmentation in infrared sky images. Energy Rep 2021;7:442–50. https://doi.org/10.1016/j.egyr.2021.08.020.
[269] Xie Wanyi, Liu Dong, Yang Ming, Chen Shaoqing, Wang Benge, Wang Zhenzhu, et al. A novel cloud image segmentation model using a deep convolutional neural network for ground-based all-sky-view camera observation. Atmos Meas Tech April 2020;13(4):1953–61. https://doi.org/10.5194/amt-13-1953-2020.
[270] Roy Roshan, R Ahan M, Soni Vaibhav, Chittora Ashish. Towards automatic transformer-based cloud classification and segmentation. In: NeurIPS 2021 workshop on tackling climate change with machine learning. Tackling climate change with machine learning, vol. 2021. December 2021. p. 60. https://hal.archives-ouvertes.fr/hal-03453957.
[271] Gupta Rachana, Nanda Satyasai Jagannath. Cloud detection in satellite images with classical and deep neural network approach: a review. Multimed Tools Appl September 2022;81(22):31847–80. https://doi.org/10.1007/s11042-022-12078-w.
[272] Pugazhenthi A, Kumar Lakshmi Sutha. Automatic cloud segmentation from INSAT-3D satellite image via IKM and IFCM clustering. IET Image Process 2019;14(7):1273–80. https://doi.org/10.1049/iet-ipr.2018.5271.
[273] Francis Alistair, Sidiropoulos Panagiotis, Muller Jan-Peter. CloudFCN: accurate and robust cloud detection for satellite imagery with deep learning. Remote Sens 2019;11(19):2312. https://doi.org/10.3390/rs11192312.
[274] Wieland Marc, Li Yu, Martinis Sandro. Multi-sensor cloud and cloud shadow segmentation with a convolutional neural network. Remote Sens Environ 2019;230:111203. https://doi.org/10.1016/j.rse.2019.05.022.
[275] Bahl Gaétan, Daniel Lionel, Moretti Matthieu, Lafarge Florent. Low-power neural networks for semantic segmentation of satellite images. In: Proceedings of the IEEE/CVF international conference on computer vision workshops; 0–0 2019.
[276] Malof Jordan M, Bradbury Kyle, Collins Leslie M, Newell Richard G. Automatic detection of solar photovoltaic arrays in high resolution aerial imagery. Appl Energy December 2016;183:229–40. https://doi.org/10.1016/j.apenergy.2016.08.191. ISSN 03062619.

[277] Mayer Kevin, Rausch Benjamin, Arlt Marie-Louise, Gust Gunther, Wang Zhecheng, Neumann Dirk, et al. 3D-PV-locator: large-scale detection of rooftop-mounted photovoltaic systems in 3D. Appl Energy March 2022;310:118469. https://doi.org/10.1016/j.apenergy.2021.118469. ISSN 03062619.
[278] Kasmi Gabriel, Dubus Laurent, Blanc Philippe, Saint-Drenan Yves-Marie. Towards unsupervised assessment with open-source data of the accuracy of deep learning-based distributed PV mapping. In: Workshop on machine learning for Earth observation (MACLEAN), in conjunction with the ECML/PKDD 2022; September 2022.
[279] Kasmi Gabriel, Saint-Drenan Yves-Marie, Trebosc David, Jolivet Raphaël, Leloux Jonathan, Sarr Babacar, et al. A crowdsourced dataset of aerial images with annotated solar photovoltaic arrays and installation metadata. Sci Data January 2023;10(1):59. https://doi.org/10.1038/s41597-023-01951-4.
[280] Yao Xudong, Guo Qing, Li An. Light-weight cloud detection network for optical remote sensing images with attention-based DeeplabV3+ architecture. Remote Sens 2021;13(18):3617.
[281] Ye Liang, Cao Zhiguo, Deepcloud Yang Xiao. Ground-based cloud image categorization using deep convolutional features. IEEE Trans Geosci Remote Sens 2017;55(10):5729–40. https://doi.org/10.1109/TGRS.2017.2712809.
[282] Zhang Jinglin, Liu Pu, Zhang Feng, Cloudnet Qianqian Song. Ground-based cloud classification with deep convolutional neural network. Geophys Res Lett 2018;45(16):8665–72. https://doi.org/10.1029/2018GL077787.
[283] Krizhevsky Alex, Sutskever Ilya, Hinton Geoffrey E. Imagenet classification with deep convolutional neural networks. Adv Neural Inf Process Syst 2012;25:1097–105. https://doi.org/10.1145/3065386.
[284] Wang Min, Zhou Shudao, Yang Zhong, Clouda Zhanhua Liu. A ground-based cloud classification method with a convolutional neural network. J Atmos Ocean Technol 2020;37(9):1661–8. https://doi.org/10.1175/JTECH-D-19-0189.1.
[285] Kong Weicong, Jia Youwei, Yang Dong Zhao, Meng Ke, Chai Songjian. Hybrid approaches based on deep whole-sky-image learning to photovoltaic generation forecasting. Appl Energy December 2020;280:115875. https://doi.org/10.1016/j.apenergy.2020.115875.
[286] Lu Zhiying, Zhou Zhiyi, Li Xin, Stanet Jianfeng Zhang. A novel predictive neural network for ground-based remote sensing cloud image sequence extrapolation. IEEE Trans Geosci Remote Sens 2023.
[287] Ravuri Suman, Lenc Karel, Willson Matthew, Kangin Dmitry, Lam Remi, Mirowski Piotr, et al. Skillful precipitation nowcasting using deep generative models of radar. Nature 2021;597:672–7. https://doi.org/10.1038/s41586-021-03854-z.
[288] Andrianakos G, Tsourounis D, Oikonomou S, Kastaniotis D, Economou G, Kazantzidis A. Sky image forecasting with generative adversarial networks for cloud coverage prediction. In: 2019 10th international conference on information, intelligence, systems and applications (IISA); July 2019. p. 1–7.
[289] Lotter William, Kreiman Gabriel, Cox David. Deep predictive coding networks for video prediction and unsupervised learning. arXiv:1605.08104 [cs, q-bio], February 2017.
[290] Crisosto Cristian, Luiz Eduardo W, Seckmeyer Gunther. Convolutional neural network for high-resolution cloud motion prediction from hemispheric sky images. Energies January 2021;14(3):753. https://doi.org/10.3390/en14030753.
[291] Kelly Jack, Dudfield Peter. Predict PV yield. https://github.com/openclimatefix/predict_pv_yield, 2022.
[292] Jaegle Andrew, Gimeno Felix, Brock Andrew, Zisserman Andrew, Vinyals Oriol, Perceiver Joao Carreira. General perception with iterative attention. https://arxiv.org/abs/2103.03206, 2021.
[293] Jaegle Andrew, Borgeaud Sebastian, Alayrac Jean-Baptiste, Doersch Carl, Ionescu Catalin, Ding David, et al. Perceiver IO: a general architecture for structured inputs & outputs. https://arxiv.org/abs/2107.14795, 2021.
[294] Pedro Hugo Carreira, Larson David, Coimbra Carlos. A comprehensive dataset for the accelerated development and benchmarking of solar forecasting methods. https://doi.org/10.5281/zenodo.2826939, June 2019.
[295] Koopman Cynthia. Forecasting solar energy. https://github.com/CynthiaKoopman/Forecasting-Solar-Energy, 2020.
[296] Sun Yuchi, Szűcs Gergely, Brandt Adam R. Solar PV output prediction from video streams using convolutional neural networks. Energy Environ Sci 2018;11:1811–8. https://doi.org/10.1039/C7EE03420B.
[297] IEA-PVPS. Solar resource for high penetration and large scale applications. https://iea-pvps.org/research-tasks/solar-resource-for-high-penetration-and-large-scale-applications/, 2022.
[298] Yang Dazhi, Alessandrini Stefano, Antonanzas Javier, Antonanzas-Torres Fernando, Badescu Viorel, Beyer Hans Georg, et al. Verification of deterministic solar forecasts. Sol Energy 2020;210:20–37. https://doi.org/10.1016/j.solener.2020.04.019.
[299] Lauret Philippe, David Mathieu, Pinson Pierre. Verification of solar irradiance probabilistic forecasts. Sol Energy 2019;194:254–71. https://doi.org/10.1016/j.solener.2019.10.041.
[300] Si Zhiyuan, Yu Yixiao, Yang Ming, Li Peng. Hybrid solar forecasting method using satellite visible images and modified convolutional neural networks. IEEE Trans Ind Appl 2020;57(1):5–16. https://doi.org/10.1109/TIA.2020.3028558.
[301] Hong Tao, Pinson Pierre, Fan Shu. Global energy forecasting competition 2012. Int J Forecasting 2014;30(2):357–63. https://doi.org/10.1016/j.ijforecast.2013.07.001.
[302] Aicardi Daniel, Musé Pablo, Alonso-Suárez Rodrigo. A comparison of satellite cloud motion vectors techniques to forecast intra-day hourly solar global horizontal irradiation. Sol Energy 2022;233:46–60. https://doi.org/10.1016/j.solener.2021.12.066.
[303] Feng Cong, Zhang Wenqi, Hodge Mathias-Hodge, Zhang Yingchen. Occlusion-perturbed deep learning for probabilistic solar forecasting via sky images. In: 2022 IEEE power & energy society general meeting. IEEE; 2022. p. 1–5.
[304] Zhen Zhao, Pang Shuaijie, Wang Fei, Li Kangping, Li Zhigang, Ren Hui, et al. Pattern classification and PSO optimal weights based sky images cloud motion speed calculation method for solar PV power forecasting. IEEE Trans Ind Appl 2019;55(4):3331–42. https://doi.org/10.1109/TIA.2019.2904927.
[305] Doubleday Kate, Van Scyoc Hernandez Vanessa, Hodge Bri-Mathias. Benchmark probabilistic solar forecasts: characteristics and recommendations. Sol Energy 2020;206:52–67. https://doi.org/10.1016/j.solener.2020.05.051.
[306] Murphy Allan H. What is a good forecast? An essay on the nature of goodness in weather forecasting. Weather Forecast 1993;8(2):281–93. https://doi.org/10.1175/1520-0434(1993)008<0281:WIAGFA>2.0.CO;2.
[307] Zhang Jie, Florita Anthony, Hodge Bri-Mathias, Lu Siyuan, Hamann Hendrik F, Banunarayanan Venkat, et al. A suite of metrics for assessing the performance of solar power forecasting. Sol Energy 2015;111:157–75. https://doi.org/10.1016/j.solener.2014.10.016.
[308] Ryu Anto, Ishii Hideo, Hayashi Yasuhiro. Battery smoothing control for photovoltaic system using short-term forecast with total sky images. Electr Power Syst Res 2021;190:106645. https://doi.org/10.1016/j.epsr.2020.106645.
[309] Saleh Mojtaba, Meek Lindsay, Masoum Mohammad AS, Abshar Masoud. Batteryless short-term smoothing of photovoltaic generation using sky camera. IEEE Trans Ind Inform 2017;14(2):403–14. https://doi.org/10.1109/TII.2017.2767038.
[310] Wen Haoran, Du Yang, Chen Xiaoyang, Lim Enggee, Wen Huiqing, Jiang Lin, et al. Deep learning based multistep solar forecasting for PV ramp-rate control using sky images. IEEE Trans Ind Inform 2020;17(2):1397–406. https://doi.org/10.1109/TII.2020.2987916.
[311] van der Meer Dennis. Comment on “Verification of deterministic solar forecasts”: verification of probabilistic solar forecasts. Sol Energy 2020;210:41–3. https://doi.org/10.1016/j.solener.2020.04.015.
[312] Winkler Robert L. A decision-theoretic approach to interval estimation. J Am Stat Assoc 1972;67(337):187–91. https://doi.org/10.2307/2284720.
[313] Hodge Bri-Mathias, Lew Debra, Milligan Michael. Short-term load forecast error distributions and implications for renewable integration studies. In: 2013 IEEE green technologies conference (GreenTech). IEEE; 2013. p. 435–42.
[314] Zhang Jie, Hodge Bri-Mathias, Florita Anthony. Investigating the correlation between wind and solar power forecast errors in the western interconnection, vol. 55515. American Society of Mechanical Engineers; 2013.
[315] Nuño Edgar, Koivisto Matti, Cutululis Nicolaos A, Sørensen Poul. On the simulation of aggregated solar PV forecast errors. IEEE Trans Sustain Energy 2018;9(4):1889–98. https://doi.org/10.1109/TSTE.2018.2818727.
[316] Lauret Philippe, David Mathieu, Pinson Pierre. Verification of solar irradiance probabilistic forecasts. Sol Energy December 2019;194:254–71. https://doi.org/10.1016/j.solener.2019.10.041.
[317] Liu Yu, Xia Jun, Shi Chun-Xiang, Hong Yang. An improved cloud classification algorithm for China’s FY-2C multi-channel images using artificial neural network. Sensors 2009;9(7):5558–79. https://doi.org/10.3390/s90705558.
[318] Zhang Wenqi, Kleiber William, Florita Anthony, Hodge Bri-Mathias, Mather Barry. A stochastic downscaling approach for generating high-frequency solar irradiance scenarios. Sol Energy 2018;176:370–9. https://doi.org/10.1016/j.solener.2018.10.019.
[319] Porter Kevin, Rogers J. Survey of variable generation forecasting in the West: August 2011-June 2012. Technical report. Golden, CO (United States): National Renewable Energy Lab. (NREL); 2012.
[320] Widiss R, Porter K. A review of variable generation forecasting in the West. Technical report. Golden, CO (United States): National Renewable Energy Lab. (NREL); 2014.
[321] Wang Qin, Wu Hongyu, Florita Anthony R, Brancucci Martinez-Anido Carlo, Hodge Bri-Mathias. The value of improved wind power forecasting: grid flexibility quantification, ramp capability analysis, and impacts of electricity market operation timescales. Appl Energy 2016;184:696–713. https://doi.org/10.1016/j.apenergy.2016.11.016.
[322] Hodge Bri-Mathias, Brancucci Martinez-Anido Carlo, Wang Qin, Chartan Erol, Florita Anthony, Kiviluoma Juha. The combined value of wind and solar power forecasting improvements and electricity storage. Appl Energy 2018;214:1–15. https://doi.org/10.1016/j.apenergy.2017.12.120.
[323] Ellen Haupt Sue, Garcia Casado Mayte, Davidson Michael, Dobschinski Jan, Du Pengwei, Lange Matthias, et al. The use of probabilistic forecasts: applying them in theory and practice. IEEE Power Energy Mag 2019;17(6):46–57. https://doi.org/10.1109/MPE.2019.2932639.
[324] Mahoney William P, Parks Keith, Wiener Gerry, Liu Yubao, Myers William L, Sun Juanzhen, et al. A wind power forecasting system to optimize grid integration. IEEE Trans Sustain Energy 2012;3(4):670–82. https://doi.org/10.1109/TSTE.2012.2201758.
[325] Orwig Kirsten D, Ahlstrom Mark L, Banunarayanan Venkat, Sharp Justin, Wilczak James M, Freedman Jeffrey, et al. Recent trends in variable genera-

tion forecasting and its value to the power system. IEEE Trans Sustain Energy 2015;6(3):924–33. https://doi.org/10.1109/TSTE.2014.2366118.
[326] Tuohy Aidan, Zack John, Ellen Haupt Sue, Sharp Justin, Ahlstrom Mark, Dise Skip, et al. Solar forecasting: methods, challenges, and performance. IEEE Power Energy Mag 2015;13(6):50–9. https://doi.org/10.1109/MPE.2015.2461351.
[327] Kakimoto Mitsuru, Endoh Yusuke, Shin Hiromasa, Ikeda Ryosaku, Kusaka Hiroyuki. Probabilistic solar irradiance forecasting by conditioning joint probability method and its application to electric power trading. IEEE Trans Sustain Energy 2019;10(2):983–93. https://doi.org/10.1109/TSTE.2018.2858777.
[328] Dominguez R, Baringo L, Conejo AJ. Optimal offering strategy for a concentrating solar power plant. Appl Energy 2012;98:316–25. https://doi.org/10.1016/j.apenergy.2012.03.043.
[329] He Guannan, Chen Qixin, Kang Chongqing, Xia Qing. Optimal offering strategy for concentrating solar power plants in joint energy, reserve and regulation markets. IEEE Trans Sustain Energy 2016;7(3):1245–54. https://doi.org/10.1109/TSTE.2016.2533637.
[330] Attarha Ahmad, Amjady Nima, Dehghan Shahab. Affinely adjustable robust bidding strategy for a solar plant paired with a battery storage. IEEE Trans Smart Grid 2019;10(3):2629–40. https://doi.org/10.1109/TSG.2018.2806403.
[331] Apostolopoulou Dimitra, De Grève Zacharie, McCulloch Malcolm. Robust optimization for hydroelectric system operation under uncertainty. IEEE Trans Power Syst 2018;33(3):3337–48. https://doi.org/10.1109/TPWRS.2018.2807794.
[332] Wang Jianxiao, Zhong Haiwang, Tang Wenyuan, Rajagopal Ram, Xia Qing, Kang Chongqing, et al. Optimal bidding strategy for microgrids in joint energy and ancillary service markets considering flexible ramping products. Appl Energy 2017;205:294–303. https://doi.org/10.1016/j.apenergy.2017.07.047.
[333] Wang Hao, Huang Jianwei. Joint investment and operation of microgrid. IEEE Trans Smart Grid 2017;8(2):833–45. https://doi.org/10.1109/TSG.2015.2501818.
[334] Law Edward W, Kay Merlinde, Taylor Robert A. Evaluating the benefits of using short-term direct normal irradiance forecasts to operate a concentrated solar thermal plant. Sol Energy 2016;140:93–108. https://doi.org/10.1016/j.solener.2016.10.037.
[335] Dersch Jürgen, Schroedter-Homscheidt Marion, Gairaa Kacem, Hanrieder Natalie, Landelius Tomas, Lindskog Magnus, et al. Impact of DNI nowcasting on annual revenues of CSP plants for a time of delivery based feed in tariff. Meteorol Z 2019;28(3):235–53. https://doi.org/10.1127/metz/2019/0925.
[336] Chang Jiaming, Du Yang, Gee Lim Eng, Wen Huiqing, Li Xingshuo, Jiang Lin. Coordinated frequency regulation using solar forecasting based virtual inertia control for islanded microgrids. IEEE Trans Sustain Energy 2021;12(4):2393–403. https://doi.org/10.1109/TSTE.2021.3095928.
[337] Habib Abdulelah H, Pecenak Zachary K, Disfani Vahid R, Kleissl Jan, de Callafon Raymond A. Reliability of dynamic load scheduling with solar forecast scenarios. In: 2016 annual IEEE systems conference (SysCon); 2016. p. 1–7.
[338] Sivaneasan Balakrishnan, Kumar Kandasamy Nandha, Lim May Lin, Ping Goh Kwang. A new demand response algorithm for solar PV intermittency management. Appl Energy 2018;218:36–45. https://doi.org/10.1016/j.apenergy.2018.02.147.
[339] Ma Jie, Ma Xiandong. Consensus-based hierachical demand side management in microgrid. In: 2019 25th international conference on automation and computing (ICAC); 2019. p. 1–6.
[340] Zhou Zhi, Levin Todd, Conzelmann Guenter. Survey of US ancillary services markets. Technical report. United States: Argonne National Lab. (ANL), Argonne, IL; 2016.
[341] Denholm Paul L, Sun Yinong, Mai Trieu T. An introduction to grid services: concepts, technical requirements, and provision from wind. Technical report. Golden, CO (United States): National Renewable Energy Lab. (NREL); 2019.
[342] Dranka Géremi Gilson, Ferreira Paula, Vaz A Ismael F. A review of co-optimization approaches for operational and planning problems in the energy sector. Appl Energy 2021;304:117703. https://doi.org/10.1016/j.apenergy.2021.117703.
[343] Wang Beibei, Hobbs Benjamin F. Real-time markets for flexiramp: a stochastic unit commitment-based analysis. IEEE Trans Power Syst 2016;31(2):846–60. https://doi.org/10.1109/TPWRS.2015.2411268.
[344] Ye Hongxing, Li Zuyi. Deliverable robust ramping products in real-time markets. IEEE Trans Power Syst 2018;33(1):5–18. https://doi.org/10.1109/TPWRS.2017.2688972.
[345] Wang Zhiwen, Shen Chen, Liu Feng, Wang Jianhui, Wu Xiangyu. An adjustable chance-constrained approach for flexible ramping capacity allocation. IEEE Trans Sustain Energy 2018;9(4):1798–811. https://doi.org/10.1109/TSTE.2018.2815651.
[346] Holttinen Hannele, Milligan Michael, Ela Erik, Menemenlis Nickie, Dobschinski Jan, Rawn Barry, et al. Methodologies to determine operating reserves due to increased wind power. IEEE Trans Sustain Energy 2012;3(4):713–23. https://doi.org/10.1109/TSTE.2012.2208207.
[347] Li Binghui, Feng Cong, Siebenschuh Carlo, Zhang Rui, Spyrou Evangelia, Krishnan Venkat, et al. Sizing ramping reserve using probabilistic solar forecasts: a data-driven method. Appl Energy 2022;313:118812. https://doi.org/10.1016/j.apenergy.2022.118812.
[348] Zhang Guangyuan, McCalley James D. Estimation of regulation reserve requirement based on control performance standard. IEEE Trans Power Syst 2018;33(2):1173–83. https://doi.org/10.1109/TPWRS.2017.2734654.
[349] Bruninx Kenneth, Delarue Erik. A statistical description of the error on wind power forecasts for probabilistic reserve sizing. IEEE Trans Sustain Energy 2014;5(3):995–1002. https://doi.org/10.1109/TSTE.2014.2320193.
[350] Bruninx Kenneth, Delarue Erik. Endogenous probabilistic reserve sizing and allocation in unit commitment models: cost-effective, reliable, and fast. IEEE Trans Power Syst 2017;32(4):2593–603. https://doi.org/10.1109/TPWRS.2016.2621261.
[351] Sreekumar Sreenu, Chand Sharma Kailash, Bhakar Rohit. Gumbel copula based multi interval ramp product for power system flexibility enhancement. Int J Electr Power Energy Syst 2019;112:417–27. https://doi.org/10.1016/j.ijepes.2019.05.018.
[352] Li Binghui, Zhang Jie, Hobbs Benjamin F. A copula enhanced convolution for uncertainty aggregation. In: 2020 IEEE power & energy society innovative smart grid technologies conference (ISGT); 2020. p. 1–5.
[353] Etingov P, Miller L, Hou Z, Makarov Y, Pennock K, Beaucage P, et al. Balancing needs assessment using advanced probabilistic forecasts. In: 2018 IEEE international conference on probabilistic methods applied to power systems (PMAPS); 2018. p. 1–6.
[354] Etingov P, Miller L, Hou Z, Makarov Y, Loutan C, Katzenstein W. Improving BA control performance through advanced regulation requirements prediction. In: 2018 IEEE power & energy society general meeting (PESGM); 2018. p. 1–5.
[355] Nonnenmacher Lukas, Kaur Amanpreet, Coimbra Carlos FM. Day-ahead resource forecasting for concentrated solar power integration. Renew Energy 2016;86:866–76. https://doi.org/10.1016/j.renene.2015.08.068.
[356] California Independent System Operator. Flexible ramping product refinements initiative Appendix C–quantile regression approach. http://www.caiso.com/InitiativeDocuments/AppendixC-QuantileRegressionApproach-FlexibleRampingProductRequirements.pdf, 2020. [Accessed 25 January 2022].
[357] Chu Yinghao, Pedro Hugo TC, Kaur Amanpreet, Kleissl Jan, Coimbra Carlos FM. Net load forecasts for solar-integrated operational grid feeders. Sol Energy 2017;158:236–46. https://doi.org/10.1016/j.solener.2017.09.052.
[358] Hobbs Benjamin F, Zhang Jie, Hamann Hendrik F, Siebenschuh Carlo, Zhang Rui, Li Binghui, et al. Using probabilistic solar power forecasts to inform flexible ramp product procurement for the California ISO. Sol Energy Adv 2022;2:100024. https://doi.org/10.1016/j.seja.2022.100024.
[359] Hobbs Benjamin F, Krishnan Venkat, Zhang Jie, Hamann Hendrik F, Siebenschuh Carlo, Zhang Rui, et al. How can probabilistic solar power forecasts be used to lower costs and improve reliability in power spot markets? A review and application to flexiramp requirements. IEEE Open Access J Power Energy 2022;9:437–50. https://doi.org/10.1109/OAJPE.2022.3217909.
[360] Sun Yuchi, Nelson James H, Stevens John C, Au Adrian H, Venugopal Vignesh, Gulian Charles, et al. Machine learning derived dynamic operating reserve requirements in high-renewable power systems. J Renew Sustain Energy 2022;14(3):036303. https://doi.org/10.1063/5.0087144.
[361] Costilla-Enriquez Napoleon, Ortega-Vazquez Miguel A, Tuohy Aidan, Motley Amber, Webb Rebecca. Operating dynamic reserve dimensioning using probabilistic forecasts. IEEE Trans Power Syst 2023;38(1):603–16. https://doi.org/10.1109/TPWRS.2022.3163106.
[362] Chen Xiaoyang, Du Yang, Wen Huiqing, Jiang Lin, Xiao Weidong. Forecasting-based power ramp-rate control strategies for utility-scale PV systems. IEEE Trans Ind Electron 2019;66(3):1862–71. https://doi.org/10.1109/TIE.2018.2840490.
[363] Chen Xiaoyang, Du Yang, Lim Enggee, Fang Lurui, Yan Ke. Towards the applicability of solar nowcasting: a practice on predictive PV power ramp-rate control. Renew Energy 2022;195:147–66. https://doi.org/10.1016/j.renene.2022.05.166.
[364] Wen H, Du Y, Chen X, Lim E, Wen H, Jiang L, et al. Deep learning based multistep solar forecasting for PV ramp-rate control using sky images. IEEE Trans Ind Inform February 2021;17(2):1397–406. https://doi.org/10.1109/TII.2020.2987916.
[365] Saleh Mojtaba, Meek Lindsay, Masoum Mohammad AS, Abshar Masoud. Batteryless short-term smoothing of photovoltaic generation using sky camera. IEEE Trans Ind Inform 2018;14(2):403–14. https://doi.org/10.1109/TII.2017.2767038.
[366] Makibar Aitor, Narvarte Luis, Lorenzo Eduardo. Contributions to the size reduction of a battery used for PV power ramp rate control. Sol Energy 2021;230:435–48. https://doi.org/10.1016/j.solener.2021.10.047.
[367] Gonzalez-Moreno Alejandro, Marcos J, de la Parra I, Marroyo L. A PV ramp-rate control strategy to extend battery lifespan using forecasting. Appl Energy 2022;323:119546. https://doi.org/10.1016/j.apenergy.2022.119546.
[368] Bergstra James, Bengio Yoshua. Random search for hyper-parameter optimization. J Mach Learn Res 2012;13(2).
[369] Nguyen Vu. Bayesian optimization for accelerating hyper-parameter tuning. In: 2019 IEEE second international conference on artificial intelligence and knowledge engineering (AIKE). IEEE; 2019. p. 302–5.
[370] Seeger Matthias. Gaussian processes for machine learning. Int J Neural Syst 2004;14(02):69–106. https://doi.org/10.7551/mitpress/3206.001.0001.
[371] Viana Felipe AC. A tutorial on Latin hypercube design of experiments. Qual Reliab Eng Int 2016;32(5):1975–85. https://doi.org/10.1002/qre.1924.
[372] Scaramuzza Davide, Martinelli Agostino, Siegwart Roland, Scaramuzza Davide, Martinelli Agostino, Siegwart Roland. A toolbox for easily calibrating omnidirectional cameras. Iros 2006.
[373] Bernecker David, Riess Christian, Angelopoulou Elli, Hornegger Joachim. Continuous short-term irradiance forecasts using sky images. Sol Energy December 2014;110:303–15. https://doi.org/10.1016/j.solener.2014.09.005.

[374] Paletta Quentin, Arbod Guillaume, Lasenby Joan. Cloud flow centring in sky and satellite images for deep solar forecasting. In: WCPEC-8; 2022. p. 5.
[375] Nie Yuhao, Zamzam Ahmed S, Brandt Adam. Resampling and data augmentation for short-term PV output prediction based on an imbalanced sky images dataset using convolutional neural networks. Sol Energy August 2021;224:341–54. https://doi.org/10.1016/j.solener.2021.05.095.
[376] Wu Ren, Yan Shengen, Shan Yi, Dang Qingqing, Sun Gang. Deep image: scaling up image recognition. Arxiv. https://doi.org/10.48550/arXiv.1501.02876, 2015.
[377] Chawla NV, Bowyer KW, Hall LO, Kegelmeyer WP. SMOTE: synthetic minority over-sampling technique. J Artif Intell Res June 2002;16:321–57. https://doi.org/10.1613/jair.953.
[378] Torgo Luís, Branco Paula, Ribeiro Rita P, Pfahringer Bernhard. Resampling strategies for regression. Expert Syst 2015;32(3):465–76. https://doi.org/10.1111/exsy.12081.
[379] Zhang Hongyi, Cisse Moustapha, Dauphin Yann N, Lopez-Paz David. mixup: beyond empirical risk minimization. https://doi.org/10.48550/arXiv.1710.09412, April 2018.
[380] Shi Cunzhao, Wang Chunheng, Wang Yu, Xiao Baihua. Deep convolutional activations-based features for ground-based cloud classification. IEEE Geosci Remote Sens Lett 2017;14(6):816–20. https://doi.org/10.1109/LGRS.2017.2681658.
[381] Phung Van Hiep, Rhee Eun Joo. A deep learning approach for classification of cloud image patches on small datasets. J Inf Commun Converg Eng 2018;16(3):173–8. https://doi.org/10.6109/jicce.2018.16.3.173.
[382] Pothineni Dinesh, Oswald Martin R, Poland Jan, KloudNet Marc Pollefeys. Deep learning for sky image analysis and irradiance forecasting. In: Brox Thomas, Bruhn Andrés, Fritz Mario, editors. Pattern recognition. Lecture notes in computer science. Cham: Springer International Publishing. ISBN 978-3-030-12939-2, 2019. p. 535–51.
[383] Fabel Yann, Nouri Bijan, Wilbert Stefan, Blum Niklas, Triebel Rudolph, Hasenbalg Marcel, et al. Applying self-supervised learning for semantic cloud segmentation of all-sky images. Atmos Meas Tech Discuss March 2021:1–20. https://doi.org/10.5194/amt-2021-1.
[384] Jha Atindra, Visaria Dhvaneel. Sky image-based photovoltaic output forecasting. Stanford report. https://doi.org/10.13140/RG.2.2.36473.75362, 2022.
[385] Kurtz Benjamin, Mejia Felipe, Kleissl Jan. A virtual sky imager testbed for solar energy forecasting. Sol Energy December 2017;158:753–9. https://doi.org/10.1016/j.solener.2017.10.036.
[386] Jain Mayank, Meegan Conor, Dev Soumyabrata. Using gans to augment data for cloud image segmentation task. In: 2021 IEEE international geoscience and remote sensing symposium IGARSS. IEEE; 2021. p. 3452–5.
[387] El Alani Omaima, Ghennioui Hicham, Ghennioui Abdellatif, Saint-Drenan Yves-Marie, Blanc Philippe, Hanrieder Natalie, et al. A visual support of standard procedures for solar radiation quality control. Int J Renew Energy Dev August 2021;10(3):401–14. https://doi.org/10.14710/ijred.2021.34806.
[388] Krinitskiy Mikhail, Aleksandrova Marina, Verezemskaya Polina, Gulev Sergey, Sinitsyn Alexey, Kovaleva Nadezhda, et al. On the generalization ability of data-driven models in the problem of total cloud cover retrieval. Remote Sens January 2021;13(2):326. https://doi.org/10.3390/rs13020326.
[389] Page JK. Proposed quality control procedures for the meteorological office data tapes relating to global solar radiation, diffuse solar radiation, sunshine and cloud in the UK. Report FCIBSE. 1997.
[390] Geiger M, Diabaté L, Ménard L, Wald L. A web service for controlling the quality of measurements of global solar irradiation. Sol Energy December 2002;73(6):475–80. https://doi.org/10.1016/S0038-092X(02)00121-4.
[391] Younes S, Claywell R, Muneer T. Quality control of solar radiation data: present status and proposed new approaches. Energy July 2005;30(9):1533–49. https://doi.org/10.1016/j.energy.2004.04.031.
[392] Ineichen Pierre. Solar radiation resource in Geneva: measurements, modeling, data quality control, format and accessibility. In: Archive ouverte UNIGE; 2013.
[393] Geuder N, Wolfertstetter F, Wilbert S, Schüler D, Affolter R, Kraas B, et al. Screening and flagging of solar irradiation and ancillary meteorological data. Energy Proc May 2015;69:1989–98. https://doi.org/10.1016/j.egypro.2015.03.205.
[394] Journée Michel, Bertrand Cédric. Quality control of solar radiation data within the RMIB solar measurements network. Sol Energy January 2011;85(1):72–86. https://doi.org/10.1016/j.solener.2010.10.021.
[395] Moradi Isaac. Quality control of global solar radiation using sunshine duration hours. Energy January 2009;34(1):1–6. https://doi.org/10.1016/j.energy.2008.09.006.
[396] Urraca Ruben, Gracia-Amillo Ana M, Huld Thomas, Martinez-de-Pison Francisco Javier, Trentmann Jörg, Lindfors Anders V, et al. Quality control of global solar radiation data with satellite-based products. Sol Energy December 2017;158:49–62. https://doi.org/10.1016/j.solener.2017.09.032.
[397] Moreno-Tejera S, Ramírez-Santigosa L, Silva-Pérez MA. A proposed methodology for quick assessment of timestamp and quality control results of solar radiation data. Renew Energy June 2015;78:531–7. https://doi.org/10.1016/j.renene.2015.01.031.
[398] Dubey Swapnil, Sarvaiya Jatin Narotam, Seshadri Bharath. Temperature dependent photovoltaic (PV) efficiency and its effect on PV production in the world – a review. Energy Proc January 2013;33:311–21. https://doi.org/10.1016/j.egypro.2013.05.072.
[399] Xu Danfei, Anguelov Dragomir, Pointfusion Ashesh Jain. Deep sensor fusion for 3d bounding box estimation. In: Proceedings of the IEEE conference on computer vision and pattern recognition; 2018. p. 244–53.
[400] Zhou Yilun, Hauser Kris. Incorporating side-channel information into convolutional neural networks for robotic tasks. In: 2017 IEEE international conference on robotics and automation (ICRA). IEEE; 2017. p. 2177–83.
[401] Venugopal Vignesh, Sun Yuchi, Brandt Adam R. Short-term solar PV forecasting using computer vision: the search for optimal CNN architectures for incorporating sky images and PV generation history. J Renew Sustain Energy 2019;11(6):066102. https://doi.org/10.1063/1.5122796.
[402] Huertas-Tato Javier, Galván Inés M, Aler Ricardo, Rodríguez-Benítez Francisco Javier, Pozo-Vázquez David. Using a multi-view convolutional neural network to monitor solar irradiance. Neural Comput Appl April 2021. https://doi.org/10.1007/s00521-021-05959-y.
[403] Blum Niklas Benedikt, Nouri Bijan, Wilbert Stefan, Schmidt Thomas, Lünsdorf Ontje, Stührenberg Jonas, et al. Cloud height measurement by a network of all-sky imagers. Atmos Meas Tech July 2021;14(7):5199–224. https://doi.org/10.5194/amt-14-5199-2021.
[404] Vallance Loïc. Synergie des mesures pyranométriques et des images hémisphériques in situ avec des images satellites météorologiques pour la prévision photovoltaïque. PhD thesis. MINES ParisTech; 2018.
[405] Alonso J, Batlles FJ. Short and medium-term cloudiness forecasting using remote sensing techniques and sky camera imagery. Energy August 2014;73:890–7. https://doi.org/10.1016/j.energy.2014.06.101.
[406] Rodríguez-Benítez Francisco J, López-Cuesta Miguel, Arbizu-Barrena Clara, Fernández-León María M, Pamos-Ureña Miguel Á, Tovar-Pescador Joaquín, et al. Assessment of new solar radiation nowcasting methods based on sky-camera and satellite imagery. Appl Energy June 2021;292:116838. https://doi.org/10.1016/j.apenergy.2021.116838.
[407] Zhuang Fuzhen, Qi Zhiyuan, Duan Keyu, Xi Dongbo, Zhu Yongchun, Zhu Hengshu, et al. A comprehensive survey on transfer learning. Proc IEEE January 2021;109(1):43–76. https://doi.org/10.1109/JPROC.2020.3004555.
[408] Nie Yuhao, Paletta Quentin, Scotta Andea, Pomares Luis Martin, Arbod Guillaume, Sgouridis Sgouris, et al. Sky image-based solar forecasting using deep learning with heterogeneous multi-location data: Dataset fusion versus transfer learning. https://doi.org/10.48550/arXiv.2211.02108, November 2022.
[409] Zhang Yu, Yang Qiang. An overview of multi-task learning. Nat Sci Rev January 2018;5(1):30–43. https://doi.org/10.1093/nsr/nwx105.
[410] Thung Kim-Han, Wee Chong-Yaw. A brief review on multi-task learning. Multimed Tools Appl 2018;77(22):29705–25. https://doi.org/10.1007/s11042-018-6463-x.
[411] Socher Richard, Lin Cliff C, Manning Chris, Ng Andrew Y. Parsing natural scenes and natural language with recursive neural networks. In: Proceedings of the 28th international conference on machine learning (ICML-11); 2011. p. 129–36.
[412] Qin Jun, Jiang Hou, Lu Ning, Yao Ling, Zhou Chenghu. Enhancing solar pv output forecast by integrating ground and satellite observations with deep learning. Renew Sustain Energy Rev 2022;167. https://doi.org/10.1016/j.rser.2022.112680:112680.
[413] Siddiqui Talha Ahmad, Bharadwaj Samarth, Kalyanaraman Shivkumar. A deep learning approach to solar-irradiance forecasting in sky-videos. In: 2019 IEEE winter conference on applications of computer vision (WACV). IEEE. ISBN 978-1-72811-975-5, January 2019. p. 2166–74.
[414] Ruder Sebastian. An overview of multi-task learning in deep neural networks. https://doi.org/10.48550/arXiv.1706.05098, June 2017.
[415] Gunning David, Stefik Mark, Choi Jaesik, Miller Timothy, Stumpf Simone, Yang Guang-Zhong. XAI—explainable artificial intelligence. Sci Robot December 2019;4(37):eaay7120. https://doi.org/10.1126/scirobotics.aay7120.
[416] Adadi Amina, Berrada Mohammed. Peeking inside the black-box: a survey on explainable artificial intelligence (XAI). IEEE Access 2018;6:52138–60. https://doi.org/10.1109/ACCESS.2018.2870052.
[417] Sengupta Manajit, Habte Aron, Wilbert Stefan, Gueymard Christian, Remund Jan. Best practices handbook for the collection and use of solar resource data for solar energy applications: third edition. Technical Report NREL/TP-5D00-77635, 1778700, MainId:29561. National Renewable Energy Lab; April 2021.
[418] Gao Huiyu, Liu Miaomiao. Short-term solar irradiance prediction from sky images with a clear sky model. In: Proceedings of the IEEE/CVF winter conference on applications of computer vision; 2022. p. 2475–83.
[419] Phung Van Hiep, Rhee Eun Joo. A high-accuracy model average ensemble of convolutional neural networks for classification of cloud image patches on small datasets. Appl Sci January 2019;9(21):4500. https://doi.org/10.3390/app9214500.
[420] Hariharan Bharath, Arbelaez Pablo, Girshick Ross, Malik Jitendra. Hypercolumns for object segmentation and fine-grained localization. In: Proceedings of the IEEE conference on computer vision and pattern recognition; 2015. p. 447–56.
[421] Wang Huaizhi, Liu Yangyang, Zhou Bin, Li Canbing, Cao Guangzhong, Voropai Nikolai, et al. Taxonomy research of artificial intelligence for deterministic solar power forecasting. Energy Convers Manag June 2020;214:112909. https://doi.org/10.1016/j.enconman.2020.112909.
[422] Li Binghui, Zhang Jie. A review on the integration of probabilistic solar forecasting in power systems. Sol Energy November 2020;210:68–86. https://doi.org/10.1016/j.solener.2020.07.066.

[423] Bahl Gaetan, Daniel Lionel, Moretti Matthieu, Lafarge Florent. Low-power neural networks for semantic segmentation of satellite images. In: Proceedings of the IEEE/CVF international conference on computer vision workshops; 0–0 2019.
[424] Dev Soumyabrata, Nautiyal Atul, Lee Yee Hui, Winkler Stefan. CloudSegNet: a deep network for nychthemeron cloud image segmentation. IEEE Geosci Remote Sens Lett December 2019;16(12):1814–8. https://doi.org/10.1109/LGRS.2019.2912140.
[425] Park Seongha, Kim Yongho, Ferrier Nicola J, Collis Scott M, Sankaran Rajesh, Beckman Pete H. Prediction of solar irradiance and photovoltaic solar energy product based on cloud coverage estimation using machine learning methods. Atmosphere March 2021;12(3):395. https://doi.org/10.3390/atmos12030395.
[426] Liu Shuang, Duan Linlin, Zhang Zhong, Cao Xiaozhong, Durrani Tariq S. Multimodal ground-based remote sensing cloud classification via learning heterogeneous deep features. IEEE Trans Geosci Remote Sens November 2020;58(11):7790–800. https://doi.org/10.1109/TGRS.2020.2984265.
[427] Zhu Tingting, Wei Liang, Guo Yiren. Cloud classification of ground-based cloud images based on convolutional neural network. J Phys Conf Ser September 2021;2035(1):012020. https://doi.org/10.1088/1742-6596/2035/1/012020.
[428] Wang Fei, Zhang Zhanyao, Chai Hua, Yu Yili, Lu Xiaoxing, Wang Tieqiang, et al. Deep learning based irradiance mapping model for solar PV power forecasting using sky image. In: 2019 IEEE industry applications society annual meeting; September 2019. p. 1–9.
[429] Xiang Mingjun, Cui Wenkang, Wan Can, Zhao Changfei. A sky image-based hybrid deep learning model for nonparametric probabilistic forecasting of solar irradiance. In: 2021 international conference on power system technology (POWERCON); December 2021. p. 946–52.
[430] Terrén-Serrano Guillermo, Bashir Adnan, Estrada Trilce, Martínez-Ramón Manel. Girasol, a sky imaging and global solar irradiance dataset. Data Brief 2021;35:106914. https://doi.org/10.1016/j.dib.2021.106914.
[431] Nie Yuhao, Zelikman Eric, Scott Andea, Paletta Quentin, SkyGPT Adam Brandt. Probabilistic short-term solar forecasting using synthetic sky videos from physics-constrained VideoGPT. https://doi.org/10.48550/arXiv.2306.11682, June 2023.
[432] Ludkovski Mike, Swindle Glen, Grannan Eric. Large scale probabilistic simulation of renewables production. arXiv preprint. arXiv:2205.04736, 2022.
[433] Nonnenmacher Lukas, Coimbra Carlos FM. Streamline-based method for intra-day solar forecasting through remote sensing. Sol Energy 2014;108:447–59. https://doi.org/10.1016/j.solener.2014.07.026.
[434] San Martín Felipe I, Perez Claudio A, Tapia Juan E, Virani Shahzad, Holzinger Marcus J. Automatic space object detection on all-sky images from a synoptic survey synthetic telescope array. Adv Space Res 2020;65(1):337–50. https://doi.org/10.1016/j.asr.2019.09.037.
[435] Sirko Wojciech, Kashubin Sergii, Ritter Marvin, Annkah Abigail, Salah Eddine Bouchareb Yasser, Dauphin Yann, et al. Continental-scale building detection from high resolution satellite imagery. https://doi.org/10.48550/arXiv.2107.12283, July 2021.
[436] Jochem Andreas, Höfle Bernhard, Rutzinger Martin, Pfeifer Norbert. Automatic roof plane detection and analysis in airborne lidar point clouds for solar potential assessment. Sensors July 2009;9(7):5241–62. https://doi.org/10.3390/s90705241.
[437] López-Fernández Luis, Lagüela Susana, Fernández Jesús, González-Aguilera Diego. Automatic evaluation of photovoltaic power stations from high-density RGB-T 3D point clouds. Remote Sens 2017;9(6):631. https://doi.org/10.3390/rs9060631.
[438] Goodess CM, Troccoli A, Acton C, Añel JA, Bett PE, Brayshaw DJ, et al. Advancing climate services for the European renewable energy sector through capacity building and user engagement. Clim Serv December 2019;16:100139. https://doi.org/10.1016/j.cliser.2019.100139.